EVALUATION OF CONSTRUCTION WORKERS' PHYSICAL DEMANDS THROUGH COMPUTER VISION-BASED KINEMATIC DATA COLLECTION AND ANALYSIS

by

JoonOh Seo

A dissertation submitted in partial fulfillment
of the requirements for the degree of
Doctor of Philosophy
(Civil Engineering)
in the University of Michigan
2016

Doctoral Committee:

Associate Professor SangHyun Lee, Chair
Professor Thomas J. Armstrong
Professor Vineet R. Kamat
Assistant Professor Carol C. Menassa

DEDICATION

To my family

ACKNOWLEDGEMENTS

Firstly, I would like to thank my advisor, Dr. SangHyun Lee, for all his help and guidance that he has given me during my PhD study over the past four years, and I would like to thank my PhD committee members, Dr. Thomas J. Armstrong , Dr. Vineet R. Kamat, and Dr. Carol Menassa, for their thoughtful advice for my dissertation. I would also like to thank the scholars who have directly influenced my PhD, Dr. Carl T. Haas, Dr. Hyungkwan Kim, and Dr. Jongwon Seo. I have been very fortunate to have been able to discuss my research with these great scholars.

Next, I would like to thank my colleagues and friends. My colleagues who I spent countless hours with at the University of Michigan discussing our research in general: Dr. Seungjun Ahn, Dr. Kyle Anderson, Dr. Sungjoo Hwang, Meiyin Liu, Byunjoo Choi, Houtan Jebelli, Juhyeong Ryu, Kaiqi Yin, and Richmond Starbuck. Their assistance, cooperation, and experience were essential for the completion of my PhD study.

Last but not least, I would like to thank my family for their unwavering support and patience. This dissertation would not have been completed without their support.

TABLE OF CONTENTS

LIST OF TABLES

LIST OF FIGURES

ABSTRACT

EVALUATION OF CONSTRUCTION WORKERS' PHYSICAL DEMANDS THROUGH COMPUTER VISION-BASED KINEMATIC DATA COLLECTION AND ANALYSIS

by

JoonOh Seo

Construction workers are frequently exposed to considerable physical demands as construction tasks largely rely on manual handling tasks. Excessive physical demands beyond one's capabilities may lead to productivity, safety, and health issues in construction. Assessing physical demands from work helps not only to identify the fundamental cause of the gap between physical demands and capabilities, but also to find an appropriate method of intervention to eliminate the gap. Although many researchers have worked on methods for evaluating physical demands, the use of these methods in construction is limited due to the difficulty in collecting reliable kinematic data with the required level of detail according to evaluation methods. In addition, a discussion on how excessive physical demands affect workers' time and cost performance in construction is sparse.

With this background, the overarching goal of this dissertation is twofold: 1) to enable practitioners to evaluate construction workers' physical demands on sites in a timely manner without technical sophistication or skill, and 2) to enhance our understanding of the impact of excessive physical demands on construction operations. Specifically, computer vision-based approaches are proposed to non-invasively collect kinematic data by recording and processing

video sequences. This data can be used to quantify and evaluate physical demands through postural ergonomic risk assessment and biomechanical analysis. Also, worker-oriented modeling and simulation of construction operations is proposed to capture the interactive effects between excessive physical demands and construction operations by combining a Discrete Event Simulation (DES) model with biomechanical and fatigue models. This approach enables us to evaluate workers' fatigue from operations in the early design stages, and then to quantify the impact of fatigue on workers' time and cost performance. The proposed approaches have been tested through a series of laboratory tests and case studies, proving their feasibility and applicability under real conditions at construction sites. Ultimately, continuous evaluation and monitoring of physical demands during construction tasks using the proposed approaches will enhance the understanding of the gap between physical work demands and workers' capability, and offer a firm foundation for the improvement of workers' health (e.g., reducing WMSDs), as well as productivity in construction.

CHAPTER 1

INTRODUCTION

1.1 BACKGROUND

The construction industry is labor intensive, and relies largely on manual handling tasks. Despite recent advancements in construction technologies, a large portion of construction work is still performed by manual workers due to low-level of automation and mechanization (Khoshnevis 2004; Ardiny et al. 2015). As a result, construction labor costs are one of the largest cost components in the project budget, accounting for 33-50% of total costs (Hanna 2001).

Combined with non-standardized operations in unstructured environments, high labor intensiveness in construction has had adversary impacts on construction performance in terms of productivity, safety, and health. Labor productivity in construction has been stagnant or even decreased while other industries such as manufacturing have shown a sustained increase in labor productivity, resulting in 25% of higher productivity (Rojas and Aramvareekul 2003; Teicholz 2013). The construction industry showed the largest number of fatal occupational injuries, and the fourth-highest non-fatal injury rate (i.e., cases per 10,000 full-time workers) in 2014 (BLS 2015a; BLS 2015b). Also, construction workers are frequently exposed to forceful and repetitive exertions with awkward postures, which leads to work-related musculoskeletal disorders (WMSDs) such as strains, tendonitis, back and wrist injuries (Everett 1999; Boschman et al. 2012). As a result, in construction, WMSDs account for 31% of nonfatal occupational injuries and illnesses involving days away from work (BLS 2015b).

Previous research efforts have tried to address worker-related issues by identifying causes, and eliminating them. One of the well-established theories used to explain the fundamental causes

of those issues is a demand-capability model in Figure 1.1 (Armstrong et al. 2001; Karwowsky 2001; Mitropoulos et al. 2009). The basic premise of this model is that human performance is affected by human─system interactions (Salvendy 2012). In order to achieve the goals of the given system, the system assigns jobs to humans, who create specific task demands. However, as workers have limited capabilities, a mismatch between the task demands and worker capabilities could occur under the given system. According to Karwowsky (2001), *"the gap between the demands and capabilities can lead to human errors and accidents, characteristics of a sub-optimal, unsafe situation in which the final product is low in quantity and poor in quality."* The task demands range from physical demands to cognitive demands (Grandjean 1989). Considering that over 70% of the construction workforce is engaged in physical activities involving heavy load lifting and awkward postures (U.S. Census Bureau 2012; Mitropoulos and Memarian 2012), identifying and eliminating the gap between physical demands and capabilities is crucial to establishing an efficient and safe working environment.

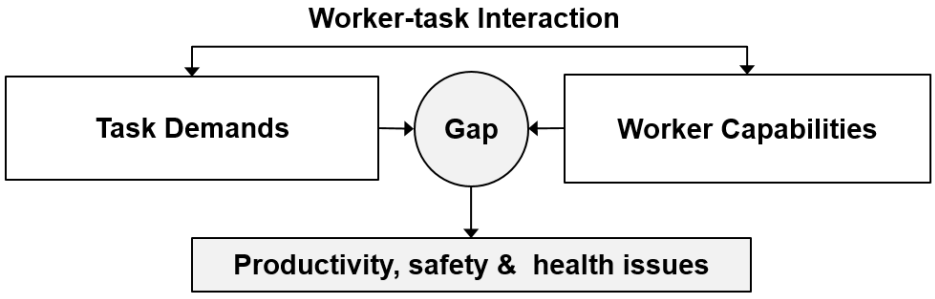

Figure 1.1: Demand-Capability Model (adapted from Armstrong et al. (2001))

From an ergonomics perspective, identifying the gap between physical demands and worker capabilities starts from assessing: 1) worker or population physical capabilities; and 2) physical demands from the job, equipment, and environment (Armstrong et al. 2001). As all human being have different capabilities, quantitative information about worker capabilities should be provided on both an individual and population basis (Chaffin et al. 2006). Previous research efforts have investigated the various physical capabilities of specific populations such as anthropometry, range of motion or muscle strength and endurance, and human variability according gender and age through self-reports or objective measurements at field or laboratory conditions (Chaffin et al. 2006; Cooper et al. 2010). For assessing physical demands, extensive information on both what

and how the worker does should be obtained directly from the job through discussions with workers and supervisors, worker observation, and the measurement of work layout or assessment of various stresses using instrumentation (Armstrong et al. 2001).

Assessing physical capabilities and demands from the job enables us to not only identify the fundamental cause of the gap between them, but also to find an appropriate form of intervention to eliminate the gap. Armstrong et al. (2001) proposed two complementary means to match job demands and worker capabilities: 1) the use of assistive devices (e.g., gloves to relieve tool pressure points, special glasses for reading a computer screen) to improve worker capabilities; and 2) the design of the job, equipment, and environments to reduce job demands, and thus to accommodate a variety of worker capabilities. In the ergonomic perspective that aims to design the job to fit the worker, the latter approach is preferred because designing for all workers is the only way to fundamentally eliminate the gap (Armstrong et al. 2001; Chaffin et al. 2006).

According to Bernold and AbouRizk (2010), *"one of the prime beneficiaries of ergonomics is the construction industry, with its physically demanding work."* However, despite an increasing need for applying ergonomic approaches in construction, both research and practice have focused exclusively on providing general ergonomic guidelines for working postures or material handling without an in-depth understanding of physical demands from construction tasks under real conditions. Generally, several iterations are required to obtain more detailed descriptions on the job such as actions, movements, and forces (Armstrong et al. 2001). Unlike manufacturing, construction is characterized as unique design according to projects, non-standardized work procedures, and unstructured and continuously changing work environments. Unique characteristics of the construction industry may hinder iterative job analyses, making it challenging to quantify and assess physical demands at construction sites.

1.2 CURENT APPROACHES TO ASSESS PHYSICAL DEMANDS

Physical demands are determined not only by external loads in the physical work environment, but also by a worker's response to these external loads (Radwin et al. 2001). The external loads are affected by the geometry of the workplace, the type of tools used, and the work objects (e.g., materials) and environmental conditions (Armstrong et al. 1993). However, under

the same working conditions, the way a worker performs a task (e.g., working postures) could vary depending on an individual's preference, experience and techniques, leading to variations on postures, motions and force exertions. According to Radwin et al. (2001), *"these external loads are transmitted to through the biomechanics of the body to create internal loads on tissues and anatomical structures."* The internal loads are stresses that disturb the internal state of the individual mechanically, physiologically, and psychologically, resulting in cascading responses on the preceding internal stress (Armstrong et al. 1993). For example, biomechanical stresses refer to tissue forces (e.g., muscle forces) at each body part that are produced as a result of force exertion and movement of the body. Creating muscle forces on the human body leads to physiological disturbances on the human body such as energy consumptions, production of metabolic substrates or by-products, and localized or whole body fatigue. If the biomechanical or physiological responses exceed the individual's tolerance, one may experience discomfort and pain that may lead to anxiety about the workload.

Previous research efforts have developed diverse approaches to evaluate physical demands by measuring external or internal stresses through self-reports, observations or instrumentation (Janowitz et al. 2006). External stresses include repetitive motions, sustained postures, and external forces (Radwin et al. 2001). These external stresses can be directly measured using instrumentation, for example, motion capture systems, goniometers, and force gauges in both laboratory and occupational settings (Chaffin et al. 2006). In occupational settings, due to their ease of learning, repeatability, and application, postural ergonomic risk assessments through human observations have been widely used, enabling rapid assessments of occupational tasks (Karhu et al. 1981; Kivi and Mattila 1991; Kee and Karwowski 2007). Those include, but are not limited to, Ovako Working Posture Analysing System (OWAS) (Karhu et al. 1977, Karhu et al. 1981), postural targeting (Corlett et al. 1979), Rapid Upper Limb Assessment (RULA) (McAtamney and Corlett 1993), Posture, Activity, Tools and Handling (PATH) (Buchholz et al. 1996), and Rapid Entire Body Assessment (REBA) (Hignett and McAtamney 2000). These methods aims to capture postures (some include hand loads) through human observations using checklists, and provide overall indices or scores to determine the degree of risk of exposure (David 2005). Videotaping is often used to supplement human observation.

Internal stresses are generally evaluated by using physiological or psychophysical measures. For example, to quantify biomechanical stresses (e.g., muscle forces), indirect electrophysiological measures such as amplitude changes in integrated electromyograms and frequency shifts in electromyogram spectra are commonly used (Radwin et al. 2001). It has been found that there is a quantitative relationship between a processed electromyographic signal and the corresponding force produced by skeletal muscle (Perry and Bekey 1980). Other physiological measures used to evaluate internal stresses include heart rate, oxygen consumption, substrate consumption and metabolite production (Radwin et al. 2001). However, most of above measures can be obtained only under laboratory conditions due to the need for complex instrumentation. Alternatively, model-based approaches have provided an in-depth understanding of internal responses of the human body to external loads (Armstrong et al. 1993). Previous research efforts have found a strong relationship between external loads and internal responses to the loads, and thus biomechanical and physiological mathematical models have been developed to quantitatively describe some of these relationships (Radwin et al. 2001). These models help to quantitatively estimate internal loads under given external stress factors. The psychophysical methods rely on an individual's subjective evaluation to estimate magnitudes of internal stresses or to assess the severity of body part discomfort as a result of a task (Olendorf and Drury 2001). Those include Rated Perceived Exertion (Borg 1981), and Body Part Discomfort Scale (Corllett and Bishop 1976).

1.3 PROBLEM STATEMENTS

Although many researchers have worked on methods for evaluating physical demands, the use of these methods in occupational settings, especially in construction is limited due to the difficulty in collecting reliable data on working postures and motions with the required level of detail according to evaluation methods. For example, postural ergonomic assessment methods are best used for initial assessments to screen risky tasks that need ergonomic interventions (Janowitz et al. 2006). However, as these methods rely on human observations to record postures, issues with the reliability and practicability of these methods—due to a lack of precision, and time-consuming procedures—have been reported (Burdorf et al. 1992). The disadvantages and limitations of observational methods are magnified in construction tasks that involve dynamic work situations

such as complex and non-repetitive work patterns in relatively large work spaces, resulting in the limited use of observational methods. Also, the need for well-trained analysts may hinder the evaluation of real tasks in construction where the few practitioners responsible for health and safety at construction sites have little ergonomic expertise.

For more in-depth analysis of physical demands, collecting kinematics (motion) data is needed, which is challenging in construction. Body kinematics—a description of a person's postures or movements—is not only necessary in the analysis of external stresses from the job, but also useful for estimating internal stresses using biomechanical models (Radwin et al. 2001). Also, kinematics data provides contextual information on the fundamental causes of physical demands as a worker's behavior is affected by physical work environmental factors (e.g., geometry of the workplaces, types of tools), as well as individual factors (e.g., anthropometry, preferred working techniques). Current approaches to measure body kinematics rely on complex motion capture systems that need instruments (e.g., goniometers), sensors (e.g., accelerometers) or markers (e.g., optical motion capture systems). Due to the possibility of interfering with on-going work, however, these approaches can work better in laboratory settings by simulating tasks in a controlled environment. The representation of the tasks in data collection is generally based on extensive field or video observations to reflect general working methods and styles (Kim et al. 2011). However, it is difficult to reflect all possible variations in diverse construction sites and workers' working styles in the laboratory.

In addition, despite the increasing attention paid to the adversary effects of excessive physical demands, discussion on how excessive physical demands affect workers' time and cost performance in construction is sparse. Construction is one of the most human-oriented industrial sectors (Loosemore et al. 2003), and thus human performance is a critical factor in construction projects' success. As most work activities involve interaction between humans and systems (e.g., including tasks, equipment, tools, and software), how to maximize human performance (e.g., productivity) without causing detrimental results on workers' health under the given interactions is extremely important (Salvendy 2012). However, current approaches to evaluate physical demands mainly focus on identification of potential health issues such as the risk of WMSDs. A lack of a tool with which we can understand the potential impact of excessive physical demands on construction operations prohibits us from using knowledge on human aspects (e.g., workers'

response to work) in our planning and control decisions to improve work performance (e.g., productivity) and well-being.

1.4 RESEARCH OBJECTIVES AND APPROACHES

With this background, the overarching goal of this research is twofold: 1) to enable practitioners to evaluate construction workers' physical demands on sites in a timely manner without technical sophistication or skill; and 2) to enhance our understanding of the impact of excessive physical demands on construction operations. Specific objectives in this research are listed below.

1. **To enable an automated initial assessment of postural stresses to compare different jobs or tasks within a job to determine a prioritization of ergonomics efforts**: The major obstacle for the use of postural ergonomic assessment methods is manual procedures to collect postural information at construction sites through human observations. An automated and easily applicable means for postural ergonomic evaluation is necessary to identify risk tasks that need further in-depth analysis and timely interventions.

2. **To enable non-invasive kinematics measurements required for in-depth analysis of physical demands at construction sites**: Postural requirements and workers' movements in the workplace vary greatly according to types of tasks and individuals. Non-invasive kinematics measurements that

3.

4. do not require the introduction of any instruments into the body enable us to not only identify the severity of postures (e.g., body angles), but also to understand variability on how workers perform tasks (e.g., movement patterns, range of motions etc.) under real conditions without interfering with on-going work.

5. **To test the feasibility of on-site biomechanical analysis using the kinematics data obtained from sites for quantifying musculoskeletal stresses on different body parts**: Even though postural and kinematics analysis provides an understanding of the external factors that lead to excessive physical demands, internal stresses such as musculoskeletal stresses can rarely be measured directly. A slightly different posture, combined with the

external forces and body weight, can create potentially hazardous loading conditions on certain musculoskeletal tissues (Chaffin et al. 2006). Through on-site biomechanical analysis that estimate musculoskeletal stresses at each body part using kinematics data directly obtained from sites, we can identify when and in which body parts workers are exposed to internal stresses under given external factors, which can contribute to the development of interventions to effectively reduce physical demands.

6. **To develop a means to model interactions between human aspects (i.e., muscle fatigue) and tasks and to evaluate the impact of excessive physical demands on construction operations**: Biomechanical analysis using the kinematic data reflecting possible operational scenarios can estimate physical demands from construction operations, enabling us to evaluate their impacts on workers' performance (e.g., productivity). When workers are exposed to excessive physical demands without proper rest time, they suffer from a significant level of physical fatigue that could generate diverse detrimental impacts on the project performance. A systematic understanding and management of workers' fatigue in planned operations of which activities and resources are determined prior to work can greatly contribute to workers' productivity, safety, and health—all by taking proper actions before severe fatigue takes place.

To achieve these research objectives, an inter-disciplinary approach is used in this research. The first approach taken in this research is computer vision-based posture classification that enables an automated initial assessment of postural stresses by automatically recognizing and evaluating workers' postures on video sequences (Research Objective #1). The central hypothesis of this approach is that different postures on images create distinguishable image pixel patterns, allowing classification algorithms to learn the patterns and differentiate the postures on images with a higher accuracy than human observations. The substantial novelty of the proposed research is the development of virtual human modeling to create training datasets without a significant effort to manually collect massive datasets. Because computer vision-based classification relies heavily on machine learning techniques, one of its key challenges is to reflect variations caused by viewpoints or anthropometric differences (Poppe 2010). Since viewpoints and anthropometry of a virtual human model can be easily adjusted to match diverse viewpoints and anthropometries

prevalent in real construction sites, virtually created training datasets can be universally applicable to classify postures for any real-world images, and thus, can minimize the efforts to manually collect massive and extensive datasets.

Another approach used in this research is vision-based motion capture to non-invasively collect kinematics information while performing construction tasks at sites (Research Objective #2). Vision-based motion capture is considered an attractive solution to the limitations on existing motion capture approaches (Corazza et al. 2006). The main advantage of the vision-based motion capture is that it does not require any markers or sensors attached to the subject during motion capture, and allows researchers to generate human-skeleton–based motion data. As will be introduced in Chapter 3, kinematics measurement directly from sites will open the door toward analyzing diverse in-depth analysis of physical demands based on workers' postures and movements.

Another approach taken in this research is motion-data driven on-site biomechanical analysis using vision-based motion data (Research Objective #3). The implementation of on-site biomechanical analysis may broadly involve two technical challenges. One is to collect accurate motion data without interfering with on-going works in construction sites; the other is to process the motion data to make it compatible with existing computerized biomechanical analysis tools. While the vision-based motion capture approaches described above can be used to collect motion data required for biomechanical analysis, the compatibility issue still remains. Also, it should be further investigated whether the vision-based motion data can provide acceptable accuracy for biomechanical analysis. As will be introduced in Chapter 4, a semi-automated process to convert the motion data into available data and represent motions in biomechanical analysis tools is proposed to address the compatibility issue. Additionally, through sensitivity analysis of musculoskeletal stresses on motion data errors, whether vision-based motion data is viable for biomechanical analysis is discussed.

The final approach taken in this research is worker-oriented modeling and simulation of construction operations by combining a Discrete Event Simulation (DES) model with biomechanical and fatigue models to capture the interactive effects between excessive demands, muscle fatigue and construction operations (Research Objective #4). Specifically, when combined with DES simulations, biomechanical analysis using the kinematic data (Research Objective #3)

enables us to estimate physical demands from possible operational scenarios. Then, the proposed dynamic fatigue models estimate the level of muscle fatigue of each worker as a function of the estimated physical demands. Workers' strategies to mitigate muscle fatigue, such as taking voluntary rests, are, in turn, modeled in the DES to understand how muscle fatigue affects time and cost performance of the planned operation. A clear identification and quantification of the dynamics underlying construction operations through this approach can have tremendous potential to improve how the construction workforce is working as well as how workplaces and processes are designed.

1.5 THE STRUCTURE OF THE DISSERTATION

This dissertation is a compilation of the studies used to achieve the proposed research objectives. This dissertation is composed of 6 Chapters, and Chapters 2 – 5 introduce each of the studies that corresponds to a research objective. Following is the list of the Chapters.

Chapter 1: Introduction. This chapter covers the background, problem statements, and objectives and approaches of the proposed research.

Chapter 2: Automated Postural Ergonomic Risk Assessment Using Vision-based Posture Classification. This chapter introduces a study to classify working postures on video sequences through vision-based posture classification algorithms, and validate, aiming at automating current observation methods. Additionally, this chapter also introduces the results of laboratory testing to test the feasibility of the proposed approach.

Chapter 3: Three Dimensional Body Kinematics Measurement Using Vision-based Motion Capture Approaches. This chapter introduces vision-based motion capture approaches that invasively collect kinematics information while performing construction tasks at sites, and the comparison of motion data accuracy through laboratory tests. This chapter also discusses the potential applications of the motion data for in-depth analysis of physical demands.

Chapter 4: Motion Data-Driven Biomechanical Analysis Using Vision-based Motion Data. This chapter introduces a motion-data–driven biomechanical analysis on construction manual tasks using motion data obtained from vision-based motion capture approaches. A case

study on lifting tasks is also introduced to see the feasibility of on-site biomechanical analysis using the motion data.

Chapter 5: Simulation-based Assessment of Workers' Muscle Fatigue and Its Impact on Construction Operation. This chapter introduces a simulation-based framework to estimate physical demands and corresponding muscle fatigue from the planned operation, and then evaluate the impact of muscle fatigue on construction operations. In addition, a case study on masonry work is described to demonstrate how the proposed framework can be applied to the actual construction operation.

Chapter 6: Conclusions and Recommendations. This chapter provides a summary of the conclusions that can be drawn from the research. Several recommendations for future work stemming from this research are also provided.

CHAPTER 2

AUTOMATED POSTURAL ERGONOMIC RISK ASSESSMENT USING VISION-BASED POSTURE CLASSIFICATION

2.1 INTRODUCTION

Workers perform diverse tasks in workplaces that have different levels of risks associated with physical demands. Practitioners must identify problematic tasks and activities in order to establish priorities across a range of tasks, and to allocate appropriate levels of resources toward the improvement of in-depth job analyses and workplace interventions (Li and Buckle 1999). Among various types of methods for the assessment of physical exposure, postural ergonomic assessment methods have been commonly used for initial screening assessments due to the advantages of being quick and easy to use (Janowitz et al. 2006). Postural ergonomic risk assessment methods aim to systematically record exposure to risky postures through human observations, and then determine overall indices or scores that indicate relative levels of physical exposure.

Even though observation-based postural ergonomic risk assessment methods appear to be best matched to the needs of occupational safety and health practitioners, these methods have not been widely applied in construction due to their manual procedures and need for trained analysts. In contrast to manufacturing, working conditions are continuously changing as the work progresses, and equivalent tasks are performed differently depending on projects. As a result, safety and health practitioners may need more frequent assessments to reflect changing conditions, which is a great burden to them. Also, despite the severity of ergonomic injuries, safety and health practitioners in construction do not generally possess the requisite ergonomic expertise to use these methods, and thus just focus on providing simple ergonomic training to workers. As a result, an effective and

easily accessible means for postural ergonomic risk assessment is required to assess physical exposure during construction tasks.

Computer vision can provide one alternative for an automated, non-invasive, and cost-effective means to facilitate the use of postural ergonomic evaluation methods in construction. Vision-based action recognition has been especially successful when applied to capture changes in postures (i.e., motions) from images (Weinland et al. 2011), suggesting its potential to classify postures at a specific moment. However, one of the key challenges is that massive and comprehensive training datasets are essential to reflect variations according to viewpoints or anthropometric differences because it heavily relies on machine learning techniques (Poppe 2010). Thus, persistent challenges in obtaining such training datasets must be overcome (Golparvar-Fard et al. 2013). In addition, intra- and inter-class variations due to dynamic environments (e.g., lighting conditions) and human variability (e.g., clothing, anthropometry etc.) in construction should be also addressed. In this regard, to achieve high postural classification performance, it is important to select image features that have the capacity to not only differentiate diverse postures on real-world images, but also to generalize over these variations.

To address this issue, this study proposes vision-based posture classification algorithms using training datasets obtained by modeling human motions in a virtual environment. Because viewpoints and anthropometry of a virtual human model can be easily adjusted to match real conditions, virtually created training datasets are universally applicable to classify postures from any real-world image, and thus can minimize the efforts to collect extensive datasets. In addition, features from body silhouettes are extracted to represent images for minimizing differences in color and texture between virtual and real-world images, as well as capturing local variations due to moving body parts. The algorithms are tested on a set of video images containing different simulated postures by eight subjects that are collected at the laboratory. Based on the results, potential issues and future studies are discussed.

2.2 LITERATURE REVIEW

2.2.1 Current Approaches for Postural Ergonomic Risk Assessment

Awkward postures that are combined with external forces (e.g., hand loads) can create excessive musculoskeletal stresses beyond the internal tolerances of tissues, leading to WMSDs (Radwin et al. 2001). Therefore, the majority of current techniques for measuring and evaluating workers' exposure to the risk factors of WMSDs focus on postural stresses, providing overall indices or scores to determine the degree of risk of each posture (David 2005). Since the advent of the Posturegram, the first systematic postural recording method developed by Priel (1974), a number of observational postural ergonomic evaluation methods have been developed for systematically recording exposure to postural stresses (David 2005). Those include, but are not limited to, Ovako Working Posture Analysing System (OWAS) (Karhu et al. 1977, Karhu et al. 1981), postural targeting (Corlett et al. 1979), Rapid Upper Limb Assessment (RULA) (McAtamney and Corlett 1993), PATH (Buchholz et al. 1996), and Rapid Entire Body Assessment (REBA) (Hignett and McAtamney 2000).

Generally, these methods evaluate whole body postures that are defined by combining different postures at specific body parts (Karwowski and Marras 1998). For example, OWAS defines postures at three body parts such as a back (e.g., standing, twisting, bending etc.), arms (e.g., arms below or above the shoulder level) and legs (e.g., standing on both straight legs, squatting, kneeling, walking, sitting etc.) respectively according to pre-defined postural codes as shown in Figure 2.1(a). Other methods such as REBA also have similar postural classifications with OWAS as they are developed based on OWAS, even though details of posture classifications are different each other (See Figure 2.1(b)). Once observations and corresponding posture classifications are made, the posture combinations are classified into four action categories that are evaluation indices to determine postural stresses (e.g., '1' with minimum risks to '4' with a very harmful effect on the musculoskeletal system).

A. OWAS

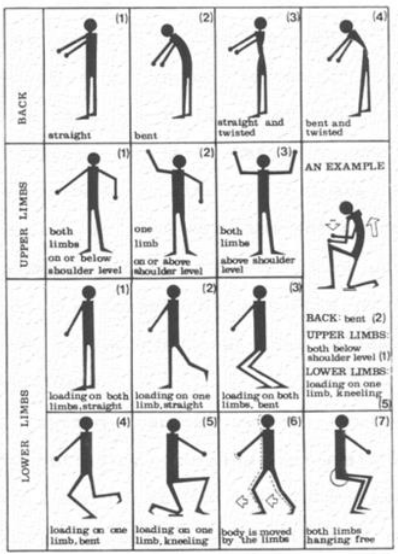

B. REBA

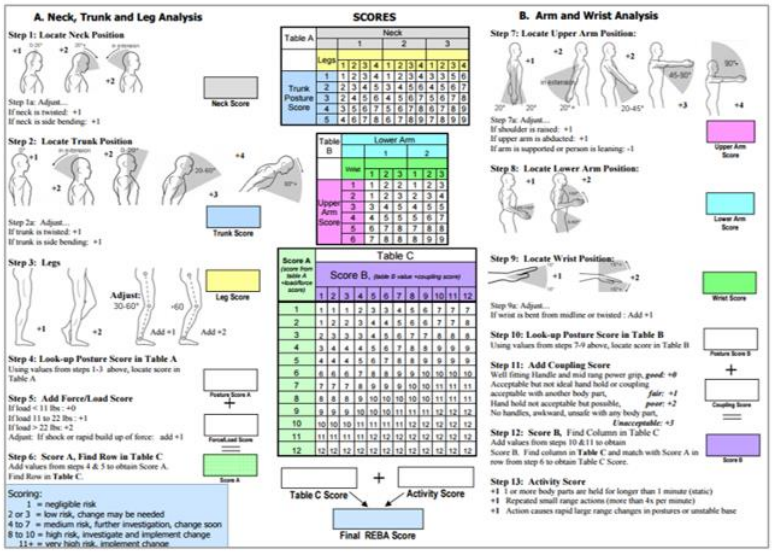

Figure 2.1: Examples of Postural Classification in OWAS and REBA

Among these methods, work-sampling based approaches such as OWAS are recommended for the construction tasks that are non-cyclical and irregular (Buchholz et al. 1996). OWAS has been tested in diverse physically demanding tasks in construction such as hammering, scaffolding, and laying bricks etc. (Kivi and Mattila 1991; Mattila et al. 1993; Li and Lee 1999; Saurin and de Macedo Guimarães 2008). From these studies, the OWAS method proved to be well suited for analyzing working postures in construction, providing opportunities to identify tasks involving a large portion of poor postures, and thus to improve working postures (Kivi and Mattila 1991).

2.2.2 Computer Vision-based Posture Classification

Computer vision-based action recognition has drawn attention for automated monitoring of workers in construction (Seo et al. 2015a). This approach aims to recognize actions by: 1) collecting 2D or 3D training images; 2) extracting human features from the images; 3) training classifiers; and 4) classifying diverse actions from an individual or a sequence of image frames (i.e., testing images) (Poppe 2010). It has been studied for several applications in construction, including productivity analysis (Gong et al. 2011), safety monitoring (Han and Lee 2013), and ergonomics training (Ray and Teizer 2012). These studies have proved the applicability of vision-based action recognition in construction, indicating the potential for vision-based posture

classification needed to automate existing postural ergonomic evaluation procedures only by collecting video or time-lapse images on sites.

Despite its potential, significant challenges still exist in the application of computer vision techniques for posture classification. For example, there are large variations of postures on images according to viewpoints. The same postures, observed from different viewpoints, can lead to very different image observations, which may result in classification errors (Poppe 2010). Therefore, collecting multi-view images from a set of cameras for training and matching an observation to recorded views have been suggested to alleviate viewpoint issues (Weinland et al. 2011; Ogale et al. 2004; Rogez et al. 2006; Ogale et al. 2007). However, it is difficult to collect training images for construction workers from all possible viewpoints that would exist in real conditions, which severely limits its applicability.

In addition, human variability in anthropometry (e.g., weight and height) can create large variations in posture (Poppe 2010). Differences in body length and mass could result in differences in silhouettes of postures, which may lead to intra-class variations. Wearing safety equipment or a waist tool bag could also cause variations in silhouettes. In particular, posture classification for workers holding materials or hand tools may require pre-processing on images to detect materials or tools and distinguish them from silhouettes of postures, which is challenging as well.

Further, vision-based posture classification has to detect more details based on less information from images than action recognition, which is also very challenging. Unlike action recognition that is based on whole body motions from a sequence of image frames, posture classification needs to detect different postures according to body parts. Computer vision algorithms for posture classification, as a result, should be sensitive to localized variations. A range of combinations of postures that exist in real worlds makes it more challenging to classify postures on back, upper, or lower limbs respectively. In addition, the temporal structure of motion features in a sequence of images commonly used for action recognition would be not effective for posture classification problems because a posture is a configuration of a person's body in space at a specific moment (Haslegrave 1994).

2.3 METHOD

This study aims to classify postures defined by existing postural ergonomic evaluation methods from video or time-lapse images. Figure 2.2 shows the overall research procedure of the proposed approach. The underlying mechanism of the developed approach is that different postures on images create distinguishable image pixel patterns (i.e., image features), allowing classification algorithms to learn the patterns from training images and differentiate the postures on testing images. As discussed earlier, one of the key challenges of vision-based approaches is the creation of comprehensive training images that reflect variations in real conditions (e.g., viewpoints or workers' anthropometry). To address this issue, a novel approach to create training datasets by using virtual human modeling is introduced. In addition, this study proposes an algorithm for vision-based posture classification based on image features from body silhouettes that are obtained through a background subtraction. As a result, posture classification algorithms make a classifier learn diverse postures using silhouettes-based features from virtual training images, and then to classify postures on real-world images by using the learned classifier

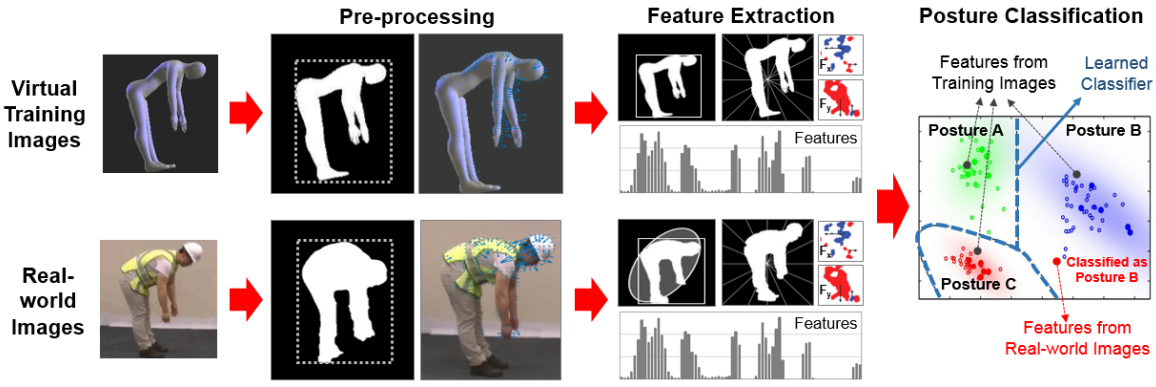

Figure 2.2: Overall Procedure for Vision-based Posture Classification

2.3.1 Virtual Training Datasets

Training images for diverse postures are obtained by using virtual human modeling that is an emerging technology for motion simulation in a virtual environment (VE), which helps to study human-system interactions in workplaces (Demirel and Duffy 2007). A virtual human model with

specific population attributes (e.g., height and weight), which is inserted and animated according to human motion capture data in a 3D virtual space will be used to generate virtual training image datasets as shown in Figure 2.3.

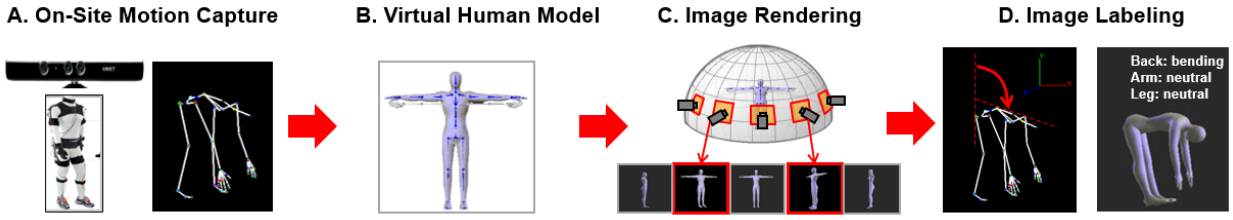

Figure 2.3: Procedure for Virtual Training Datasets

First, the motion data from actual workers at construction sites is collected by using motion capture systems such as a RGB-D sensor and an Inertial Measurement Unit (IMU)-based motion capture system (A in Figure 2.3). The use of a virtual human model allows us to manipulate any posture from any viewpoint of workers with substantial anthropometric variability without collecting real workers' motion data. However, this study intends to collect real workers' motion data because our own manual manipulation of postures may miss important postures given non-standardized and complex construction work. Thus, the purpose of collecting real workers' motion data in this step is to encompass as diverse a range of workers' postures as possible. Collecting real workers' motion data also preserves time and energy because it eliminates the need to collect additional training datasets even though there are new data to be analyzed. Existing computer vision-based action recognition approaches, by contrast, require massive training datasets that have to be continuously collected (Poppe 2010). Further, if there is any missing posture, a virtual human model enables us to create that posture by simply modifying existing postures without collecting that real posture, making it possible to easily update the training datasets.

Once motion data are obtained, a virtual human model is constructed and simulated based on the motion data in the VE (B in Figure 2.3). Specifically, as body shapes (i.e., silhouettes on images) are significantly influenced by anthropometry, virtual human models that represent diverse weight and height distributions among a specific population need to be created by varying a virtual human model's shape. Then, the scene of the human model is projected onto an image sphere, creating a sequence of images containing human postures. By changing the virtual camera

positions, virtual video sequences from all possible viewpoints that would exist in real conditions can be created (C in Figure 2.3).

Each video image should then be labeled according to body postures to be used as training datasets. Existing postural ergonomic assessment methods define whole body postures by combining different postures at specific body parts (Karwowski and Marras 1998). For example, OWAS defines postures at three body parts such as a back (e.g., standing, twisting, and bending), arms (e.g., arms below or above the shoulder level) and legs (e.g., standing on both straight legs, squatting, kneeling, walking, and sitting) respectively, according to pre-defined postural codes. Other methods such as RULA or REBA also have similar postural classifications with OWAS as they are developed based on OWAS, even though details of posture classifications are different each other. Postures on each video image can be automatically identified by using corresponding motion data where three-dimensional joint positions and body angles are available (D in Figure 2.3). The use of 3D skeleton data enables not only accurate and instant postural labeling for training datasets, but also extension of this approach to any types of postural ergonomic assessment methods only by changing the criteria to define postures of interest.

2.3.2 Background Subtraction

By using silhouettes, the proposed approach is color invariant, which allows to avoid possible confusion caused by workers' different color clothes and lighting conditions. As a result, the proposed approach can be universally applicable to diverse environments in construction. As the proposed approach relies on silhouette images for posture classification, it is important to extract clear body silhouettes. This study applies background subtraction and noise removal algorithms to obtain silhouette images from video sequences, and then detect the Region of Interest (ROI) with a bounding box containing a body silhouette as shown in Figure 2.4.

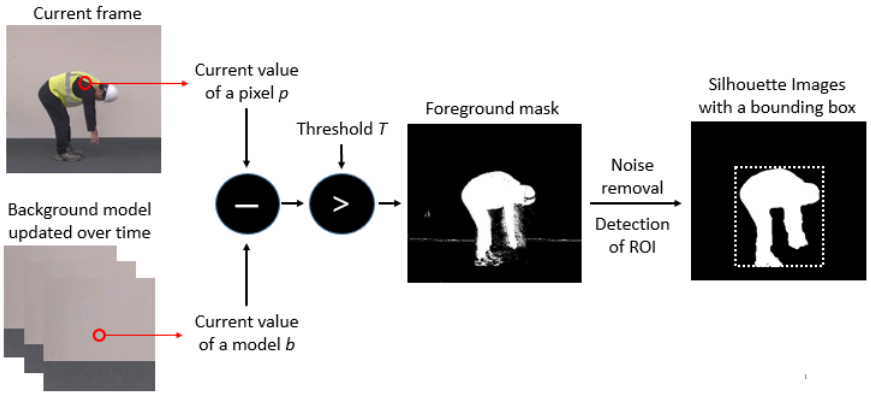

Figure 2.4. Procedures for Background Subtraction and Detection of ROI

Background subtraction is a widely used approach for detecting moving objects in videos from static cameras (Piccardi 2004). Generally, background subtraction techniques detect the foreground region (e.g., moving objects) by comparing the current frame with the background model. For example, when the difference between the current value of a pixel p and the value of model b is higher than the threshold T, the current pixel can be defined as a foreground. This study applies one of the state-of-the-art background subtraction algorithms, ViBe, that is robust to lighting changes and appearance of new objects in the scene by updating the background model over time (Barnich and Droogenbroeck 2011). Also, Vibe enables real-time processing of images. This algorithm considers the problem of background subtraction as a classification problem. It classifies a new pixel value ($v(x)$, the value of the pixel located at x in the image) by comparing the value with its corresponding background model, $\mathcal{M}(x)$ (Equation 2.1) taken in the N previous frames. Specifically, if the number of background pixel samples that are closed to the new pixel value in a Euclidean color space is higher than a given threshold, the new pixel is classified as background.

$$\mathcal{M}(x) = \{v_1, v_2, \dots, v_N\} \text{ where } v_i \text{ is a background pixel samples} \quad (2.1)$$

However, the foreground mask after subtracting background could have some noisy pixels in the background. As shown in Figure 2.4, for example, shadows on a wall and high contrast edges result in the false detection of background regions (Elgammal et al. 2000). To remove the noisy pixels in the background, several noise removal algorithms are implemented. For example, objects containing fewer than 50 pixels are removed, and then a median-based filter replaces the

noisy pixels ($f(x,y)$, a pixel value at the position of (x,y)) by median values ($g(x,y), a\ median\ filtered\ pixel$) in a 5×5 pixel window as shown in Equation 2.2 (Dong and Xu 2007). This study used the MATLAB function 'medfilt2' for median filtering.

$$g(x,y) = median\ (\sum_{i=-2}^{2}\sum_{j=-2}^{2} f(x-i, y-j)) \quad (2.2)$$

In addition, a morphological closing is applied to fill in the thin gulfs and small holes on body silhouettes by using the MATLAB function 'strel' and 'imclose' (Maragos 2005). Once a clear silhouette is generated, a bounding box is placed around the silhouettes, serving as a ROI for feature extraction.

2.3.3 Silhouette-based Feature Extraction

Once a clear silhouette is generated, image features that represent body postures are extracted based on shapes and radial histograms of the silhouette within the bounding box as shown in Figure 2.5. The fundamental idea behind the use of shape- and radial histogram-based features is that a human body has a specific range of joint motion that creates unique characteristics of body silhouettes. As a result, each body posture can be encoded using these features that represent the variability of body silhouettes according to various postures.

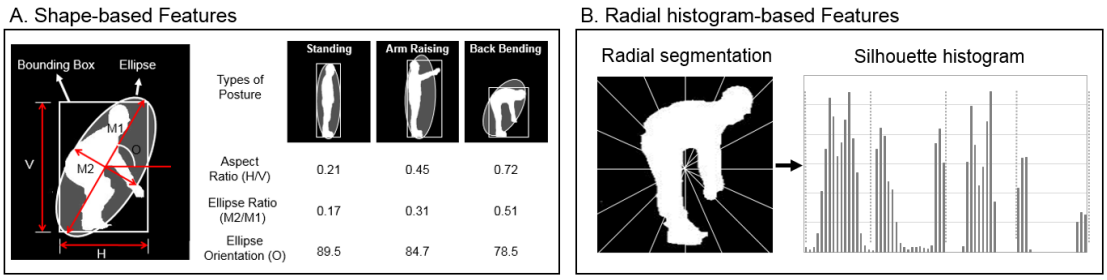

Figure 2.5: Feature Extraction from Body Silhouette

This study developed shape-based features such as: 1) the aspect ratio of the bounding box (horizontal length of the bounding box / vertical length of the bounding box); 2) the ratio of the minor to the major axis of the ellipse that is fit to the silhouette (length of the minor axis / length of the major axis of the ellipse); and 3) the orientation of the ellipse. Bounding boxes and ellipses

that fit body silhouettes were obtained using the MATLAP function 'regionprops'. Figure 2.5A shows that different postures create distinct values of these features. To extract more detailed shape-based features, the bounding box is further divided into 2×1 (2 subsets) and 2×2 (4 subsets) sub-windows, and the features are extracted from each sub-window.

To extract radial histograms of the silhouette, the bounding box is normalized as a square of which length is the bigger side of the bounding box (Tran and Sorokin 2005). Then, the silhouette's center of gravity ((x_c, y_c)) was calculated by using the following equations.

$$x_c = \frac{1}{N_C}\sum_{i=1}^{N_C} x_i\,,\ y_c = \frac{1}{N_C}\sum_{i=1}^{N_C} y_i \tag{2.3}$$

The normalized bounding box of which center is the silhouette's center of gravity is divided into 8, 12, 16 and 20 slices respectively, and the ratio of black versus white pixels in each slice is histogrammed as shown in Figure 2.5B.

2.3.4 Classification Algorithm

Once image features are constructed, a classifier needs to learn the features from training datasets for classifying postures in new testing images. As a classifier, Support Vector Machines (SVMs) are applied. SVMs are discriminative classifiers that have been widely used for action recognition (Poppe 2010). Basically, the SVM classification aims to separate the set of training vectors belonging to two separate classes,

$$\mathcal{D} = \{(x^1, y^1), \ldots, (x^l, y^l)\},\ x \in R^n, y \in \{-1, 1\}, \tag{2.4}$$

with a hyperplane,

$$< w, x > + b = 0 \tag{2.5}$$

where the parameters *w*, b are constrained by

$$min_i \left|\langle w, x^i\rangle + b\right| = 1. \tag{2.6}$$

The set of vectors is said to be optimally separated by the hyperplane if it is separated without error and the distance between the closest vector to the hyperplane is maximal. Even though the SVM classifier was originally developed for two-class classification, it can be extended

to multi-class classification by combining a number of two-class classification SVMs to form a multi-class classifier (Hsu and Lin 2002). This study implemented the one-against-one method that constructs k(k-1)/2 classifiers (k is the number of classes) where each one is trained on data from two classes, and predict the class of a testing vector based on majority voting (Kreßel 1999).

2.3.5 Post-processing for Noise Removal

The proposed algorithms perform posture classification based on frame-by-frame processing, which means that each frame is classified independently. Under real conditions, workers perform tasks by changing their postures from one to another, and a specific posture is maintained for a certain period. As a result, if the classification results show variations in a short period of consecutive frames, they could be incorrectly classified postures. To remove this noise, classified postures that do not continue for more than 10 consecutive image frames are labeled as dominantly classified postures near the frames as shown in Figure 2.6.

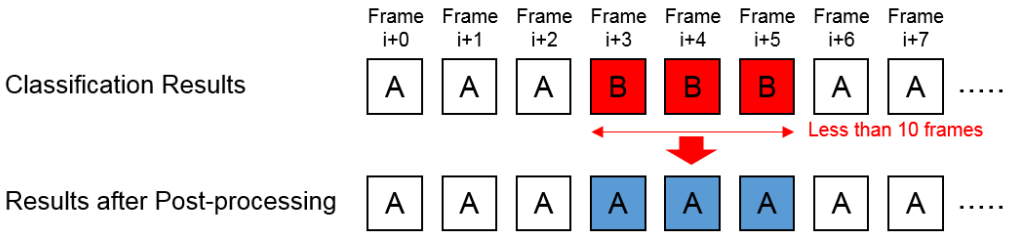

Figure 2.6: Post-processing on Classification Results

2.4 LABORATORY TESTING

To test the feasibility of the proposed approach, laboratory-based tests were conducted. The primary purpose of the tests is to examine whether training images from a virtual environment independent of testing conditions (i.e., real-world environment) are applicable for classifying workers' postures on real-world images with a higher accuracy than human observations. Previous research efforts found that trained analysts showed more than 10% of errors in classifying postures (Burt and Punnett 1999; Paquet et al. 2001; Spielholz et al. 2001; Lowe 2004; Weir et al. 2011). Also, this study also investigates the effect of the anthropometry and viewpoint on classification performance.

2.4.1 Testing Postures

For this test, three representative postures according to different body parts such as back-bending for back posture, arm-raising for arm posture, and knee-bending for leg posture were selected as shown in Figure 2.7. Each posture is defined based on the OWAS criteria. For example, in OWAS, when the upper body is bent forward or backward 20° or more, the posture is considered back-bending. An arm-raising means both arms at or above should level, and a squat posture is when both knees are bent on a 150° or smaller angle.

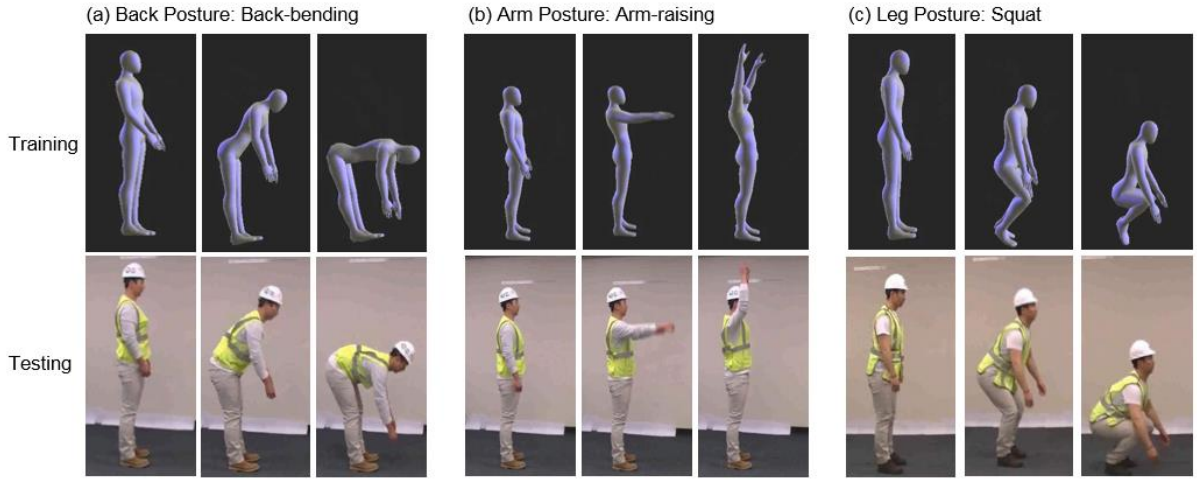

Figure 2.7: Examples of postures in training and testing images

2.4.2 Data Collection

The tests were performed at the Construction Laboratory at the University of Michigan. Eight male subjects who have different anthropometries such as height (ranges from 4.1th to 95.9th percentile, (CDC 2012)) and Body Mass Index (BMI) (ranges from 5th to 75th percentile, (Flegal et al. 2012)) were recruited to consider human variability in silhouettes as shown in Table 2.1.

Table 2.1: Subjects' Heights and BMIs

	#1	#2	#3	#4	#5	#6	#7	#8	Average
Height	163cm (4.1 %tile)	173cm (34.4 %tile)	175cm (44.7 %tile)	175cm (44.7 %tile)	180cm (70.4 %tile)	180cm (70.4 %tile)	181cm (74.8 %tile)	189cm (95.9 %tile)	177cm
BMI	25.6 (normal)	18.5 (under)	24.4 (normal)	25.2 (normal)	23.5 (normal)	29.3 (over)	26.3 (over)	25.8 (over)	24.9

Note: under (underweight, < 18.5 BMI), normal (normal weight, 18.5 – 24.9 BMI) and over (overweight, 25.0 – 29.9 BMI)

The subjects were asked to simulate each posture 10 times repeatedly. For example, the subjects stood straight at the beginning, and then: 1) bent their back up to 90°; 2) raised their arms to the top of their head; or 3) bent their knees like squatting, followed by a standing posture again. They were provided several practices to simulate the postures identically.

While simulating each posture, videos were recorded from three viewpoints (left, back left diagonal, and back views) as shown in Figure 2.8. These views were chosen after considering that front views are not easily available in construction sites where workers generally face workspace such as walls.

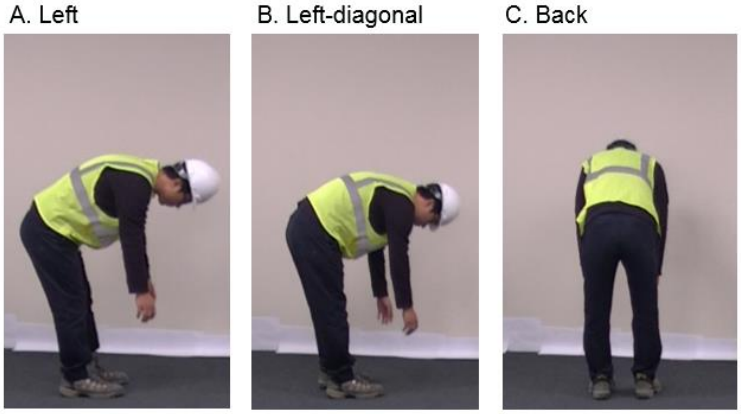

Figure 2.8: Testing Images from Three (left, left-diagonal and back) Views

From videos (30 frames per second), 60,091 image frames in total (averagely 7,500 image frames per subject) were extracted as testing images as shown in Table 2.2. Also, motion data for each subject was collected using a RGB-D sensor (i.e., Microsoft Kinect^{TM}) to identify postures

on corresponding images as ground truth. For training data, nine different virtual human models that respectively represent 15^{th}, 50^{th} and 85^{th} percentile males for height and Body Mass Index (BMI) were created, and simulated in a virtual environment using the motion data from one of the subjects. Next, image sequences from the same viewpoints with testing images were extracted. Both training and testing images were processed to obtain body silhouettes, and then to extract image features using MATLAB.

Table 2.2: Numbers of Testing Images of Each posture according to Viewpoints

Postures	Viewpoints			
	Left	Left-diagonal	Back	Sub-total
Standing	9,616	7,676	9,906	27,198
Back-bending	3,829	3,070	3,937	10,836
Arm-raising	4,823	3,355	3,862	12,040
Knee-bending	3,640	3,122	3,255	10,017
Sub-total	21,908	17,223	20,960	**Total: 60,091**

2.4.3 Testing Conditions and Measures

Testing the proposed algorithms has three purposes: 1) testing overall classification performance according to three views of testing images without considering selection of optimal training images (Test #1); 2) investigating the effect of viewpoints on classification performance (Test #2); and 3) investigating the effect of anthropometry of virtual models on classification performance (Test #3).

For Test #1, each viewpoint of training and testing images are selected, and tested respectively. Also, all training images (from nine virtual models, and from three views) are used to learn the SVM classifier. As measures of classification performance (Test #1), the accuracy, precision and recall are calculated in a confusion matrix that is used to describe the performance of a classification model as shown in Figure 2.9.

		Predicted Postures		
		Positive	Negative	
Actual Postures	Positive	True Positive	False Negative	Recall = ∑ True Positive / (∑ True Positive + ∑ False Negative)
	Negative	False Positive	True Negative	-
		Precision = ∑ True Positive / (∑ True Positive + ∑ False Positive)	-	Accuracy = (∑ True Positive + ∑ True Negative) / ∑ Total

- True Positive = the number of images correctly classified as belonging to the positive class of a posture
- True Negative = the number of images correctly classified as belonging to the negative class of a posture
- False Positive = the number of images incorrectly classified as belonging to the positive class of a posture
- False Negative = the number of images incorrectly classified as belonging to the negative class of a posture

Figure 2.9: Measures of Classification Performance

Test #2 is to test the hypothesis that selection of training images from the same viewpoint with testing images would increase the classification performance. For this test, two sets of training images were selected: 1) one is from a left view and 2) the other is from a left diagonal view. Testing images from a same view (i.e., a left view) of the first set of training images were selected. Then, each subject's posture classification was performed using both two sets of training images, respectively. The classification accuracy when selecting the same view of training images was compared with the accuracy when selecting the other view of training images using a paired t-test.

Test #3 is to test the hypothesis that selection of training images from a virtual model that has similar anthropometry with the subject would increase the classification accuracy. For this test, nine sets of training images according to anthropometry of virtual models (3 (short, average, tall) × 3 (underweight, medium, overweight)) were selected, and using each set of training images, each subject's postures were classified. The classification accuracy when selecting a virtual model that has similar anthropometry with the subject (See Table 2.1) was compared

with the average accuracy when selecting other virtual models. For this comparison, a paired t-test was used.

2.4.4 Testing Results

A. Testing Images from a Left View

Confusion Matrix		Predicted				Recall
		1	2	3	4	
Actual	1	**8,075**	819	719	3	84.0%
	2	265	**3,564**	0	0	93.0%
	3	12	0	**4,811**	0	99.7%
	4	669	0	0	**2,971**	81.5%
Precision		89.5%	81.3%	87.0%	99.8%	Accuracy = **88.6%**

B. Testing Images from a Left-diagonal View

Confusion Matrix		Predicted				Recall
		1	2	3	4	
Actual	1	**6,558**	538	509	71	85.4%
	2	221	**2,849**	0	0	92.7%
	3	8	0	**3,323**	24	99.0%
	4	1,104	0	0	**2,018**	64.6%
Precision		83.1%	84.1%	86.6%	95.3%	Accuracy = **85.6%**

C. Testing Images from a Back View

Confusion Matrix		Predicted				Recall
		1	2	3	4	
Actual	1	**8,305**	1,402	75	124	83.8%
	2	862	**3,075**	0	0	78.1%
	3	904	197	**2,692**	69	69.7%
	4	895	0	0	**2,360**	72.4%
Precision		75.7%	65.8%	97.2%	92.3%	Accuracy = **78.4%**

Notes: 1. Standing, 2. Back-bending, 3. Arm-raising, and 4. Knee-bending

Figure 2.10: Confusion Matrices for Classification Results

Figure 2.10 shows overall classification performance using confusion matrices that contain information about actual and predicted posture classifications for testing images from each view (left, left-diagonal and back views) (Test #1). This result indicates that the proposed algorithms performed better for images from a left view (88.6%) than images from left-diagonal (85.6%) or back (78.4%) views. This result indicates that a side view of images is recommended to obtain the best classification results. One notable thing is that there is almost no confusion between back-

bending, arm-raising, and knee-bending postures when using left and left-diagonal views. This is because these three postures create clearly differentiable body silhouettes on images from left and left-diagonal views. Most classification errors occurred due to confusion between standing postures and the other postures. Further investigation revealed that the cause of errors was due to similarity of postures in transitions between standing and other postures, which will be described in detail in the discussion section.

The results from Test #2 show the importance of selecting a viewpoint of training images. As shown in Table 2.3, the mean accuracy when using same views for both training and testing images was 88.7% while it dropped to 80.8% if the different view was used for training images (P = 0.004, paired t-test). A slightly different view of images can produce large variations on body silhouettes, and thus views between training and testing images should match each other to obtain better classification results.

Table 2.3: Classification Accuracy According to Selection of Views for Training Images

Subjects	Classification Accuracy	
	Training: Left View Testing: Left View	Training: Left-diagonal View Testing: Left View
#1	90.7%	87.5%
#2	81.6%	83.0%
#3	84.1%	81.6%
#4	89.0%	82.6%
#5	85.5%	83.7%
#6	89.3%	72.4%
#7	94.7%	70.0%
#8	94.2%	85.8%
Mean	**88.7%**	**80.8%**
Standard Deviation	**4.3%**	**5.9%**

Note: P = 0.004, paired t-test

Table 2.4 shows the classification accuracy according to selection of virtual models for training images (Test #3). Training images from virtual models that have similar anthropometry

with the subjects showed statistically higher accuracies (mean: 85.8%, standard deviation: 2.4%) than the ones (mean: 83.0%, standard deviation: 3.7%) when using other virtual models (P-value=0.004, paired t-test). This result indicates that the shape of body silhouettes could vary according one's anthropometry (e.g., height, BMI), affecting classification performance. As a result, posture classification algorithms should consider inter-subject variability on height and body mass.

Table 2.4: Classification Accuracy According to Selection of Virtual Models for Training Images

Subjects	Classification Accuracy	
	Similar Anthropometry*	Different Anthropometry
#1	85.6%	81.7%
#2	84.2%	82.0%
#3	83.9%	77.4%
#4	89.4%	89.1%
#5	81.9%	79.6%
#6	85.1%	81.3%
#7	87.3%	85.9%
#8	89.0%	86.6%
Mean	**85.8%**	**83.0%**
Standard Deviation	**2.4%**	**3.7%**

Note: P-value = 0.004, paired t-test
* Classification accuracy when using training images from a virtual model that has similar anthropometry (i.e., height and BMI) with a subject

The mean accuracy (85.8%) when using training images from a specific virtual model was slightly lower than 88.6% of the overall accuracy that was obtained using all virtual models. This implies that, in each subject's body silhouettes, there are some variations that training images from a single virtual model with specific anthropometry could not fully reflect. So, combined training images from virtual models with all possible anthropometry can result in better classification performance by addressing issues due to intra-subject variability on height and body mass.

2.5 DISCUSSION

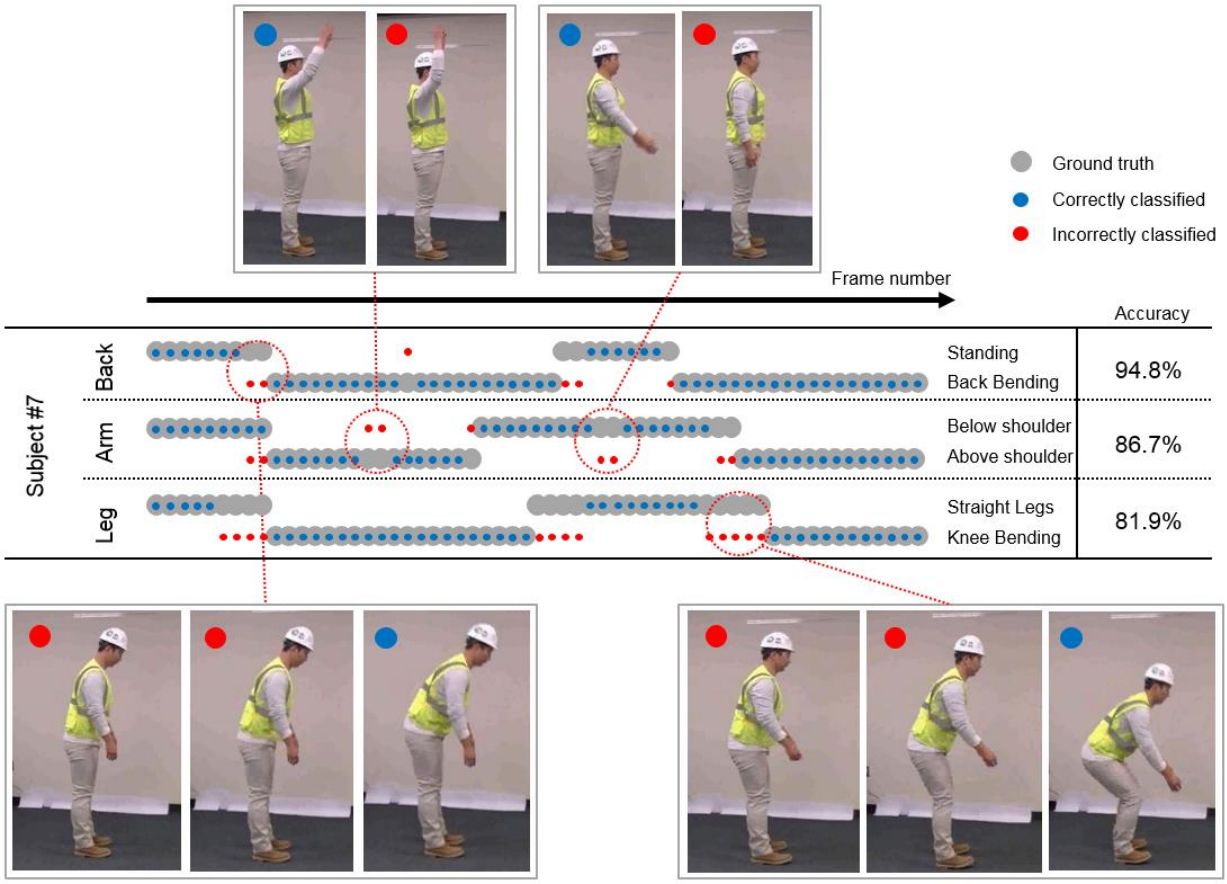

Figure 2.11: Classification Result for Two Cycles of Each Posture.

The results from the tests in the previous section show 88.6% of classification accuracy when selecting optical training images. To investigate where errors came from, classification results (two cycles of each posture) before post-processing were visualized in Figure 2.11. In this figure, gray dots denote the ground truth postures for consecutive frames (one frame: 1/30 second) while blue and red dots are correctly and incorrectly classified frames respectively. By observing incorrectly classified image frames, errors within a few of consecutive images were found, but those can be removed through the proposed post processing. As noted in the subject 4.4.4, most errors occurred in transitional postures that mean postures near the frame in transition between

standing and other postures (i.e., back-bending, arm-raising, knee-bending). As this study defined each posture based on body angles (e.g., 20° of back bending angles, 150° of knee angles), postures with body angles close to the criteria show similar body silhouettes that result in classification errors. By excluding three frames before and after the frame in transition, the overall accuracy was increased to 92.6%. If 10 frames were removed, almost over 98% of accuracy can be achieved. Although this testing is based on all image frames, observations for postural ergonomic risk assessment methods such as OWAS are generally made at fixed intervals of usually 45 or 60 seconds (Buchholz et al. 1996). Also, these transitional postures could amount to only a small portion of total working postures in practice. As a result, the possibility that the transitional frames are selected could be relatively low. Therefore, errors due to transitional postures can be alleviated in real situations, and over 90% of the accuracy is expected. However, for further improvement, algorithmic solutions to deal with transitional postures are required. Chalamala and ALP (2016) found that probabilistic classifiers are a better choice than deterministic approaches such as SVMs for continuous actions with random changes of classes. They proposed a probabilistic model based on both transition probabilities (between walking and running) and occurrence probabilities (walking or running), resulting in better performance than deterministic approaches. Even though further studies are required to test the feasibility of the probabilistic approach, this approach can be one of the viable solutions to reduce errors due to transitional postures.

When considering more than 10 % of observational errors for observation-based postural recording (Lowe 2004), achieving about 90% of posture classification accuracy can be acceptable. Despite significant differences in color and texture between virtual training and real-world testing images, the proposed approach shows robust performance, suggesting great potential for automated postural ergonomic risk assessment. In addition, the testing results imply that the use of virtual human models similar to real workers and the selection of same viewpoints with real-world views are important to increase accuracy. Adjustability of these factors when creating virtual training datasets enables us to achieve the best performance for classifying testing images.

Despite the potential of the proposed vision-based posture classification algorithm, several obstacles still remain to apply it under real conditions. First of all, the test for this algorithm was made only for single postures according to body parts. However, under real conditions, combinations of postures (e.g., back-bending + knee-bending, knee-bending + arm-raising) are

frequently observed. As a result, the proposed approach needs to be further validated for more complex postures involving combinations of different postures at each body part. Also, relatively large hand tools and materials workers are holding can significantly affect the shape of body silhouettes extracted from background subtraction, which may lead to classification errors. To address this issue, more sophisticated post processing algorithms such as detecting an object and recovering clear body silhouettes are required. In addition, as workers are continuously moving at the workplace, the views of workers that a video camera captures are continuously changing. Even though selection of same views for training images is the most significant factor to improve classification accuracy, it is required to determine which views of training images should be selected for moving workers. Automated object orientation detection that identifies rotation angles of an object based on statistical pattern recognition techniques can be a solution to determine which orientation the target worker is facing on images (Vailaya et al. 2002).

2.6 CONCLUSIONS

In this chapter, this study proposed vision-based posture classification based on machine-learning algorithms to automate existing postural ergonomic evaluations methods. Specifically, a novel method to create training datasets for diverse postures in a virtual environment was proposed. The method can create training images using virtual human models of which body mass and viewpoints can be adjusted as needed. In addition, this study designed new features to reflect local variations in postures on images by dividing the ROI into small patches, and learned different classifiers. To test the feasibility of the proposed approach, laboratory–based tests were conducted with eight male subjects who have different anthropometry. From the testing results, it was found that the proposed algorithm can provide robust posture classification with 88.6% of accuracy, when testing the algorithm on testing images from a left view. This result indicates the potential of virtual training datasets for posture classification from real-world images that have variations in viewpoints and workers' anthropometry. From the results, potential issues to be addressed to improve accuracy were found, such as sampling images in specific time intervals.

Even though the proposed approach needs to be further validated for more complex postures at construction sites and refined to address remaining obstacles such as automated viewpoint

detection, vision-based posture classification has great potential to automate current observational ergonomic evaluation methods. The proposed approach will enable practitioners to perform postural ergonomic evaluation in a practical manner without technical sophistication or skill, only by taking videos at a fixed location. Vision-based ergonomic evaluation can quickly evaluate all tasks in the workplace, and then identify risky tasks that need immediate interventions, enabling more effective use of resources to improve construction tasks.

CHAPTER 3

THREE DIMENSIONAL BODY KINEMATICS MEASUREMENT USING VISION-BASED MOTION CAPTURE APPROACHES

3.1 INTRODUCTION

In-depth analysis of physical demands begins with measuring body kinematics, which refers to body position, displacement, velocity and acceleration (Zatsiorski 2002). Human motion not only impacts the involved musculoskeletal system (e.g., muscles, tendons)—either on its own or combined with external forces—but also serves an important accompanying role by transmitting forces generated from a body (i.e., active muscle contraction) to the external environment (Radwin et al. 2001). Even though the level of detail in required kinematic descriptions varies according to the evaluation to be made, three-dimensional (3D) measurement of motion data is generally necessary to understand complex motion produced by a human (Chaffin et al. 2006).

One of the challenging issues for body kinematics measurement and analysis for occupational tasks is the lack of an effective and non-invasive means for data collection at workplaces. At present, optical motion capture systems are the most popular solution to obtain 3D full-body motion data, and have been widely used for diverse applications including clinical motion analysis and biomechanical studies. However despite their precision and reliability, their applications in practice have been hindered by the need for complex laboratory settings, the high cost of devices, and the time consuming procedure for data collection (Aminian and Najafi 2004). Alternatively, motion capture approaches using lightweight and potable kinematic sensors (e.g., acceleration and angular rate sensors) have provided effective solutions for in-field motion measurement. Combined with wireless data transmission techniques, these approaches enable us to obtain real-time motion data without any sophistication. However, the possibility of interfering

with on-going work due to the need to wear a full-body suit equipped with sensors should be overcome for occupational application.

Recently, vision-based motion capture approaches have gained increasing interest. These approaches appear to be very promising as in-field motion data collection methods by addressing some of the major challenges that exist with optical and sensor-based motion capture systems. For example, as these approaches obtain body kinematics data by processing 2D or 3D images directly collected from real conditions, they don't need complex laboratory settings or sensors attached to a human body. Also, 2D or 3D images can be collected using any type of existing ordinary video cameras or low-cost 3D image sensing devices (e.g., RGB-D sensors, stereovision cameras). For their ease of use, non-invasiveness, and cost-effectiveness vision-based approaches can broaden the spectrum of their applications for job analysis under real conditions. Despite these advantages, however, several challenges such as sensitivity to occlusions (errors due to occluded body parts), computationally expensive algorithms (requires lots of processing time), and limited operating ranges of 3D image sensors (e.g., RGB-D sensors) still remain (Han and Lee 2013; Han et al. 2013a; Starbuck et al. 2014; Liu et al. 2016). Given the strengths and limitations of each approach, understanding the performance and potential applications of vision-based motion capture approaches will lead to more appropriate uses of these approaches in construction.

With this background, this chapter evaluates the accuracy of motion data from vision-based motion capture approaches through an experimental study. Specifically, three emerging vision-based approaches for collecting motion data during construction tasks are selected. Those are: 1) multiple camera-based (Han and Lee 2013; Liu et al. 2016); 2) RGB-D sensor-based (Han et al. 2013a); and 3) stereo-vision camera-based (Starbuck et al. 2014) approaches. Also, a marker-based motion capture system (Optotrak^{TM}, Northern Digital, Inc., Waterloo, Canada) is used as the ground truth of motion data. To compare the accuracy of motion data, selected joint angles from vision-based approaches are compared with the ones from Optotrak^{TM} during performing several dynamic tasks.

The rest of this chapter is organized as follows. Literature review section (Section 3.2) provides technical aspects and procedures of vision-based approaches to be evaluated. The next section (Section 3.3) demonstrates experimental comparison of vision-based motion capture approaches with results. Then, performance of vision-based approaches and their potential

application areas for analyzing construction tasks are discussed (Section 3.4). Finally, the conclusion section (Section 3.5) summarizes the findings of this study.

3.2 LITERATURE REVIEW ON VISION-BASED MOTION CAPTURE APPROACHES

This section describes technical aspects and procedures of three vision-based motion capture approaches. Additionally, by reviewing previous work on vision-based motion capture approaches, the pros and cons of each approach are summarized.

3.2.1 Multiple Camera-based Motion Capture Approach

A multiple camera-based motion capture approach aims to estimate the 3D locations of body joints by processing 2D images from two different views using multiple video cameras or a 3D camcorder that has two lenses in one camera (Han and Lee 2013). Han and Lee (2013) proposed a motion capture process that consists of: 1) 2D pose estimation from one view of images; 2) correspondence matching of body joints on the other view of images; and 3) 3D reconstruction of body joints using the corresponding joint locations identified. However, this approach suffered from the need for extensive training images to detect joint locations on testing images, and significant computation time for 2D pose estimation. To address this issue, Liu et al. (2016) modified Han and Lee (2013)'s approach by proposing body joint tracking that accelerates the 2D pose estimation process without the prior knowledge (training images for joint detection). Figure 3.1 shows an overview of the modified approach.

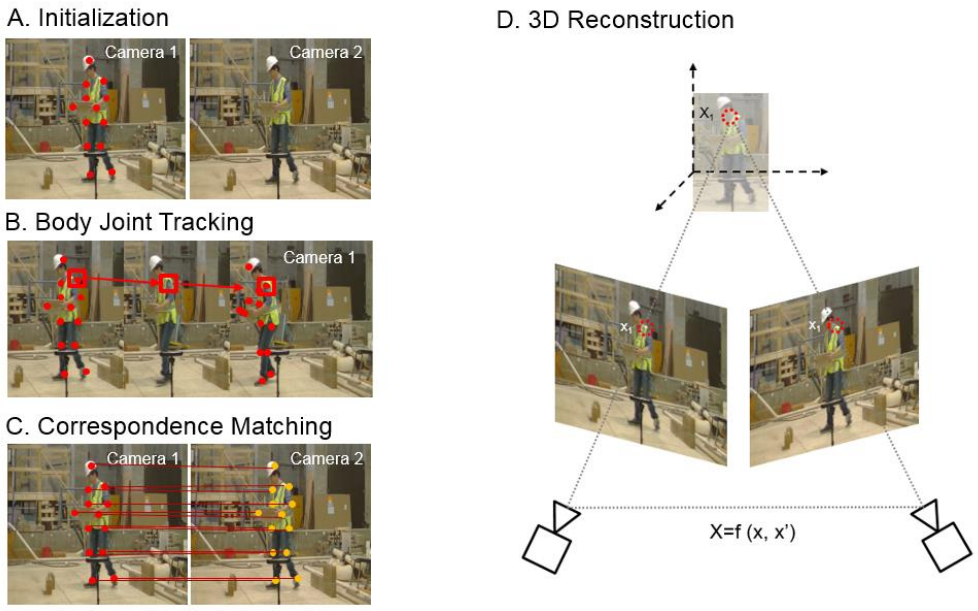

Figure 3.1: An Overview of a Multiple Camera-based Motion Capture Approach

The main idea of 2D joint tracking is that continuous tracking of body joints on consecutive image frames enables the fast estimation of 2D skeletons (Liu et al. 2016). To do this, the locations of body joints of interest should be initialized on the first image frame (A in Figure 3.1). Then, the algorithm tracks the joints in consecutive images by detecting the image patch with the most similar color histogram with that of the initialized target (B in Figure 3.1). A modified particle filter tracker was used to specify a number of reliable candidates for the targets in the subsequent frames, which can reduce computation time (Shan et al. 2007). The tracking of different body joints is performed independently, resulting in a 2D skeleton model.

The next process is to identify the corresponding body joints on the image from the other viewpoint (C in Figure 3.1). Several feature descriptors such as SIFT (Scale-Invariant Feature Transform) (Liu et al., 2011) and SURF (Speeded Up Robust Features) (Uijlings et al., 2010; Bay et al., 2008) are used for this step. Specifically, by comparing the features of a pixel with the feature descriptors, conjugate pairs of body joints can be found (Han and Lee 2013). Also, to obtain more reliable corresponding locations of body joints, the search pace is constrained by epipolar geometry (Hartley and Zisserman 2003), considering that the corresponding joints on the other view of images should lie on the epipolar line between two views of images (Han and Lee 2013).

In addition to epipolar geometry, the homography, which refers to a projective transformation that maps one plane to the other, is computed based on matched features and applied to minimize the search space for correspondence matching (Han and Lee 2013).

Once pairs of corresponding body joints are detected from two different viewpoints of images, a 3D reconstruction algorithm detects the 3D positions of each joints through triangulation, resulting in 3D full-body skeleton-based motion data. As shown in D of Figure 3.1, the position of a 3D position of each body joint can be found as the intersection of the two projection rays. If we know the optical center of two cameras and camera parameters (e.g., relative positions between cameras), the joint positions can be reconstructed in a 3D space. The most widely used technique to calculate the camera parameters is Zhang (2000)'s method. This method requires a planar checkerboard grid to be placed at different orientations (more than 2) in front of the camera, and then compute a projective transformation between the image points by using the extracted corner points of the checkerboard pattern. Then, the camera's intrinsic and extrinsic parameters are recovered using a closed-form solution. Given the camera's information, the linear triangulation method using Singular Value Decomposition (SVD) (Hartley and Zisserman 2003) computes the depth of each body joints in a 3D space, resulting in a 3D skeleton (Han and Lee 2013).

The strength of a multiple camera-based motion capture approach is that it enables researchers to use ordinary video cameras to obtain motion data. Not only do we benefit from its cost effectiveness, but also benefit from zoom lenses that collect video images from a distance. Even though environmental conditions such as illuminations may affect the performance of 3D skeleton extraction, post image processing enables us to obtain clear images even in a noisy environment. From previous studies that investigated the accuracy of this approach, about ± 10 cm of errors in body length (Han and Lee 2013) and up to 20 degrees of errors (Liu et al. 2016) in joint rotation angles have been reported. These errors came from either incorrectly detected joint locations or inaccurate camera calibration process. Especially, the performance of this approach was significantly affected by frequent self-occlusions of forearms (e.g., elbows and hands), which led to larger errors (Han and Lee 2013; Liu et al. 2016).

3.2.2 RGB-D Sensor-based Approach

While a multiple camera-based approach requires complicating image processing, the use of RGB-D images (i.e., 2D images plus depth information) collected from RGB-D sensors (e.g., Kinect™) has simplified the process for vision-based motion capture algorithms (Shotton et al. 2013). Several computer vision algorithms have been developed to estimate human poses by detecting the 3D positions of body joints directly from RGB-D images (Lee and Cohen 2006; Plagemann et al. 2010; Siddiqui and Medioni 2010; Shotton et al. 2013). Recently, motion capture solutions such as iPi Desktop Motion Capture (www.ipisoft.com) and OpenNI (http://www.openni.org) that use a Microsoft Kinect sensor have provided effective solutions for extracting skeleton-based motion data from RGB-D images obtained by RGB-D sensors.

The Kinect sensor that was initially developed for video gaming is capable of providing both depth and color information at the resolution of 640×480, and the rate of 30 frames per second (Rafibakhsh et al. 2012). This sensor is equipped with the infrared (IR) projector, the color camera and the IR camera. Using the projected structured IR lights, it measures the depth, reconstructing 3D scenes with point cloud (Zhang 2012). Combined with the 3D sensing feature of the Kinect, the iPi Desktop Motion Capture software provides a marker-less solution for collecting full-body motion data. Figure 3.2 shows an example of an RGB-D image with a pre-defined body model, and the corresponding motion data. Basically, the algorithm in this software is model-based, which means that motion data can be tracked by matching the surface of a pre-defined body model with a depth image (A in Figure 3.2). Then, the tracked motion data can be exported into any type of motion data format, such as the Biovision Hierarchy (BVH) motion data (B in Figure 3.2). This software also provides several post-processing algorithms to refine tracking and filtering algorithms for noise removal and smoothing.

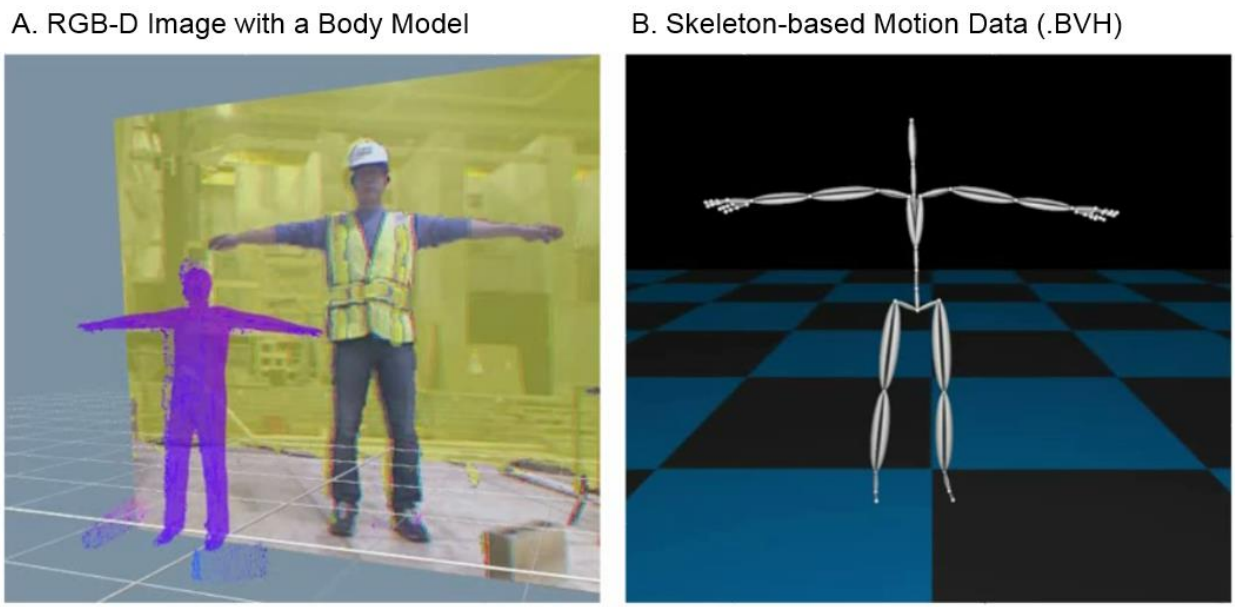

Figure 3.2: RGB-D (i.e., Kinect™) Sensor-based Motion Capture

The following are advantages of an RGB-D sensor-based motion capture approach: 1) no need for markers or sensors attached to human body, which allows for motion capture without interfering with on-going work; 2) low cost (e.g., approximately 150 – 250 USD); 3) an easy-to-use and easy-to-carry means for in-field motion data collection (Han et al. 2013a). Technically, this approach is robust to self-occlusions because the iPi software provides an inverse kinematics algorithm that can adjust incorrectly tracked body parts due to occlusions. However, as the Kinect use IR light, the use of this approach is limited only in an indoor environment due to its sensitivity to sunlight. Also, the short operating range of the Kinect sensor (within 4 m) is one of the disadvantages of this approach.

3.2.3 Stereovision Camera-based Motion Capture Approach

A stereovision system is designed to extract 3D information from a stereo image pair (Jin et al. 2010). Stereo vision works in a similar way to 3D sensing in human vision. It begins with identifying image pixels that correspond to the same point in a physical scene observed by multiple cameras. The 3D position of a point can then be established by triangulation using a ray from each camera. The more corresponding pixels identified, the more 3D points that can be determined with a single set of images. Correlation stereo methods attempt to obtain correspondences for every pixel in the stereo image, resulting in tens of thousands of 3D values generated with every stereo

image. A Bumblebee XB3^{TM} manufactured by Point Grey Technologies (www.ptgrey.com) is one of the widely used stereovision camera system. The stereo cameras employed measure line-of-sight distance using two lenses with a narrow baseline in a self-contained unit. This allows for both optical and depth data to be collected with few environmental restrictions (e.g. outdoor environments) and limited field-of-view.

Starbuck et al. (2014) proposed a stereovision camera-based motion capture approach that addressed the short operating range of an RGB-D sensor. The 3D point cloud data collected from the stereovision camera was converted into a format used by an existing kinematic modeling software solution (i.e., iPi Motion Capture software) designed for use with RGB-D sensors. The iPi software was not intended for use with stereovision cameras and provides no built-in framework for modifying the system such that alternative data sources can be utilized. In order to implement the proposed approach, a stand-alone program was developed for generating disparity maps in the same uncompressed AVI format that is available in the iPi software. Then, using the same algorithm described in the subsecsion 3.2.2, skeleton-based motion data was extracted. Through a laboratory test, the proposed method was proved to be comparable to the traditional RGB-D sensor-based approach.

A stereovision camera-based approach provides additional advantages, beyond the benefits from the RGB-D sensor-based approach. For example, the use of this approach do not suffer from environmental conditions, allowing both indoor and outdoor applications. Also, the operating range of the stereovision camera is flexible according to lens field-of-view, lens separation, and image size (Woodfill et al. 2004). However, as computing depth information from two images is a computationally intensive task, the frame rate relies on the performance of hardware (Woodfill et al. 2004).

3.3 EXPERIMENTAL COMPARISN OF VISION-BASED MOTION CAPTURE APPROACHES

The section describes an experimental test to assess the accuracy of three vision-based motion capture approaches: 1) a multiple camera-based approach; 2) an RGB-D sensor-based approach; and 3) a stereovision camera-based approach.

3.3.1 Testing Conditions

For this test, one male subject was recruited. Figure 3.3 shows experimental conditions for the comparison. Three image sensors were located in front of the subject to collect 2D or 3D images from a front view. The Kinect™ (640×480 resolution with 30 frames per second), Bumblebee XB3™ stereovision camera (320×240 resolution with about 10 frames per second) and 3D camcorder (1920×1080 resolution with 29 frames per second) were positioned 4, 6 and 8 meters away from the subject, respectively. The positions of the Kinect™ and Bumblebee XB3™ were determined based on the optimal operating distance proposed by the manufacturer. As the 3D camcorder has zoom lenses, its position was selected to obtain a clear view of the subject's whole body.

The Optotrak™ system uses active markers attached on body joints to track body motions. As a result, if the markers are captured by at least one of cameras, the system can provide accurate 3D positions of the markers with an accuracy of up to 0.1 mm. The markers were attached to the subject's center and left body joints, including neck, low back, shoulder, elbow, wrist, hip, knee and ankle joints. Two Optotrak cameras were positioned to the left side of the subject to prevent possible data loss due to occlusions of the markers.

In the experiment, human motion was simultaneously recorded with these devices. For the synchronization of motion data, the subject was asked to do a T-pose (i.e., a pose where the legs are straight and the arms are pointing sideways in a T shape) at the beginning of the recording. Data synchronization was manually performed by identifying the same frame for the T-pose.

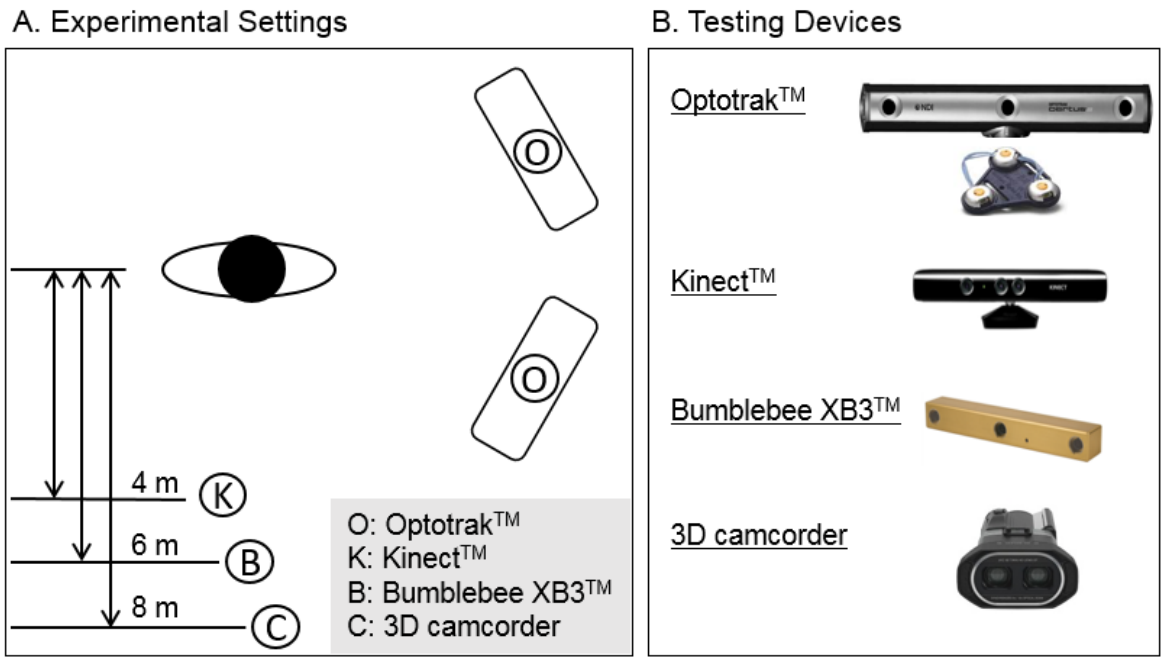

Figure 3.3: Experimental Settings and Testing Devices

3.3.2 Testing Tasks

To compare the accuracy of motion data for diverse tasks, one male subject simulated three types of tasks: 1) basic tasks with movements of specific body parts; 2) lifting; and 3) walking as shown in Figure 3.4. The basic tasks are to test the accuracy of simple motions that involve movements of specific body parts. Those include arm-raising to the front and the side, elbow-bending, back-bending, back-twisting and knee-bending. For more dynamic motions with whole body movements, a lifting and placing task was selected. Specifically, the subject was asked to simulate the lifting task by pretending to lift an object from the bottom, and placing it to the side. Also, a walking task was intended to reflect rapid repetitive movements. The subject repeatedly performed each task five times.

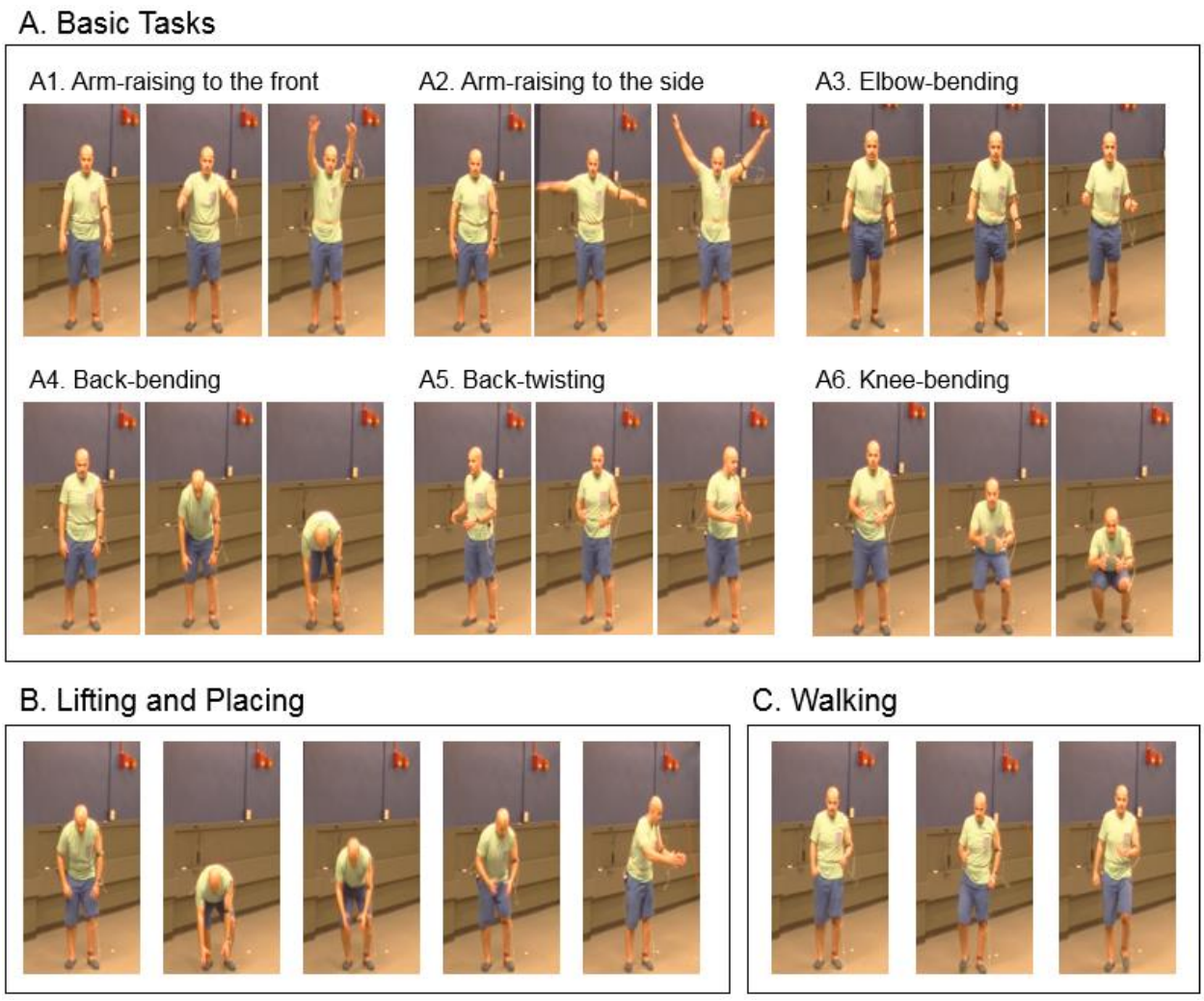

Figure 3.4: Testing Tasks

3.3.3 Measures for Accuracy Comparison

Previous studies have used 3D positions of body joints, body link lengths or joint rotation angles as measures of motion data accuracy (Han and Lee 2013; Han et al. 2013a; Starbuck et al. 2014; Liu et al. 2016). However, due to the difference in body models used in each vision-based approach, the use of these measures may lead to unexpected biases that obstruct the accuracy of the comparison. For example, joint locations and corresponding body link lengths from a multiple camera-based approach can be calculated based on the joint locations of the subject. Instead, as RGB-D sensor- and stereovision camera-based approaches use pre-defined body models that have fixed body lengths, joint locations and corresponding body link lengths are affected by the anthropometry of the body models. Also, while both RGB-D sensor- and stereovision camera-

based approaches provide motion data in a BVH file format that defines body postures using joint rotational angles, these rotational angles are not available in multiple camera-based motion data.

To address this issue, this study defined new body angles that are available from all approaches as shown in Figure 3.5. Specifically, the body angles at each body part were basically defined by angles between the vector of the body segments and the vertical vector. For example, the vector of the upper arm is obtained using 3D shoulder and elbow locations, and the angle between the vector of the upper arm and the vertical vector (y axis) is calculated as an upper arm (i.e. shoulder) angle. The other body angles such as lower arm (i.e., elbow), trunk flexion, upper leg (i.e., hip) and lower leg (i.e., knee) angles are calculated using the same way. However, the trunk axial rotation angle that indicates how much the back is twisted was computed by using shoulder and hip vectors that were projected onto x-y plane.

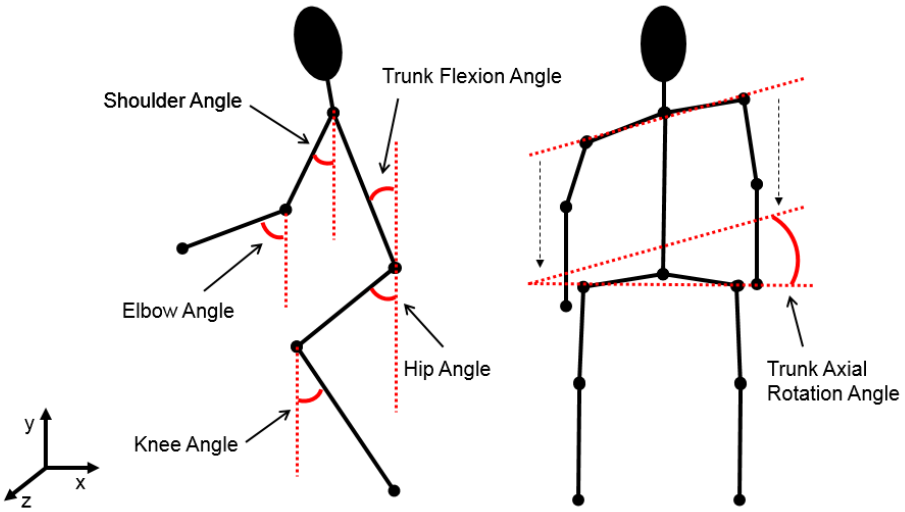

Figure 3.5: Body Angles to be Compared

As the markers for Optotrak™ were attached to the skin near the joints, the joint locations from the ground truth motion data may slightly differ from the locations from vision-based approaches. To adjust possible discrepancies due to this difference, the body angles were calibrated using the angles from a T-pose. Also, the body angles from each approach were smoothed using a Savitzky–Golay filter (Savitzky and Golay 1964) that has been widely used for post processing of motion data (Esser et al. 2009).

3.3.4 Results

Figure 3.6 shows plots of body angles from three vision-based motion capture approaches and an Optotrak™ during diverse basic tasks. Through the visual investigation, it was found that overall body angles from vision-based approaches were closely matched with body angles from an Optotrak™, while back (flexion and rotation) and upper leg angles from a multiple camera-based approach in particular showed some discrepancies during the middle of the tasks.

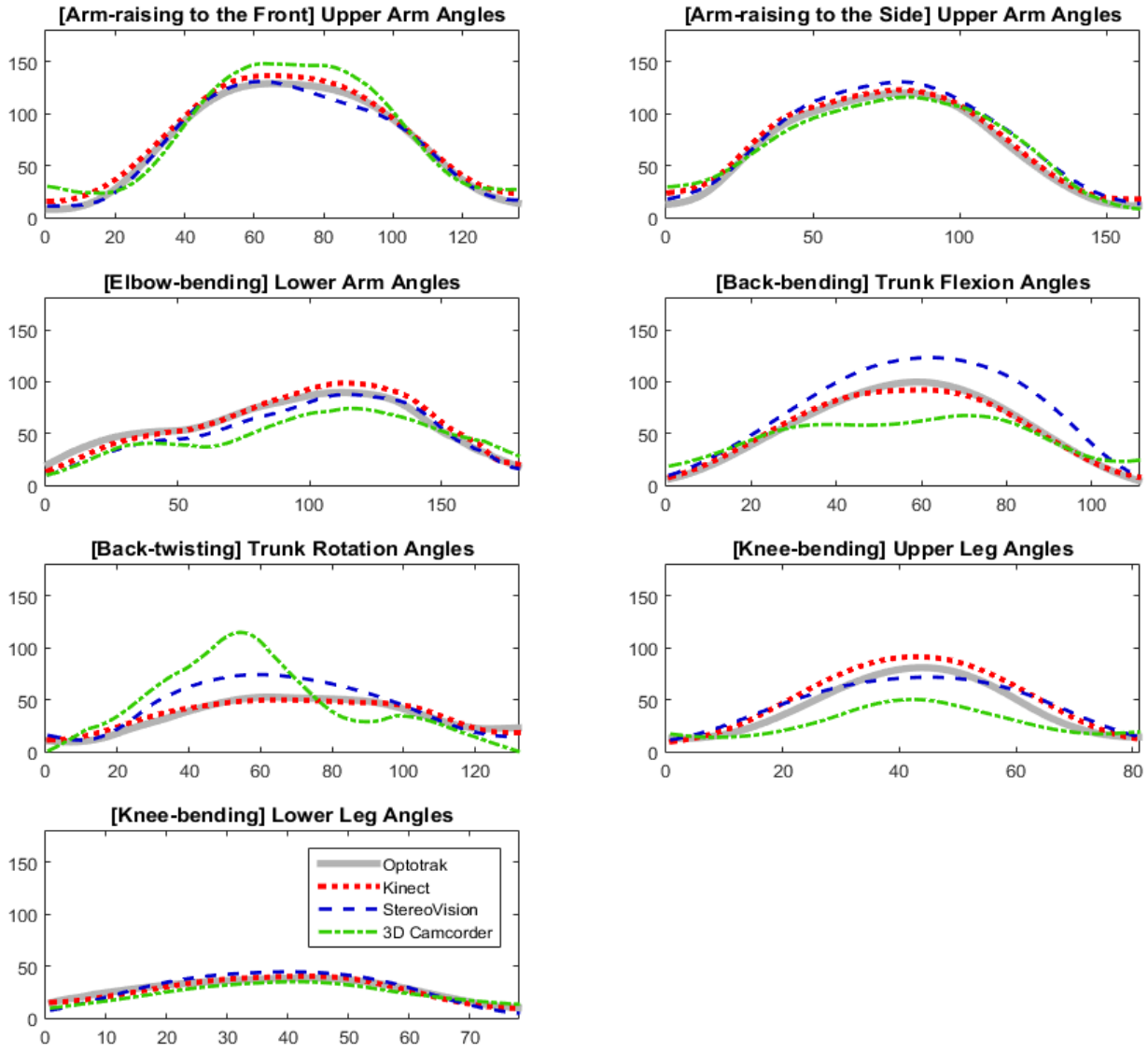

Figure 3.6: Comparison of Body Angles between Vision-based Motion Capture Approaches and an Optotrak™ during Basic Tasks

For the quantitative assessment during these tasks, mean and standard deviation of absolute errors (MAEs and S.D. of AEs), and maximum and minimum errors (MAX and MIN) in body angles between three vision-based approaches and an Optotrak™ were calculated as shown in Table 3.1.

Table 3.1: Accuracy of Vision-based Motion Capture Approaches during Basic Tasks

(Unit: degrees)

Body Angles	**Metrics**	**RGB-D Sensor (Kinect™)**	**Stereovision Camera (Bumblebee XB3™)**	**Multiple Camera (3D Camcorder)**
1. Arm-raising to the front				
Upper Arm	MAE	5.9	3.0	11.3
	S.D. of AE	2.5	2.6	6.8
	MAX	-0.6	9.9	12.0
	MIN	-9.9	-3.2	-22.0
2. Arm-raising to the side				
Upper Arm	MAE	4.7	8.2	7.6
	S.D. of AE	2.3	3.8	4.2
	MAX	-1.9	-0.3	7.6
	MIN	-11.1	-14.3	-16.8
3. Elbow-bending				
Lower Arm	MAE	4.9	8.1	16.2
	S.D. of AE	3.4	4.0	4.2
	MAX	8.6	14.0	24.5
	MIN	-9.8	-2.7	10.1
4. Back-bending				
Back Flexion	MAE	2.5	15.5	12.5
	S.D. of AE	2.1	11.2	12.5
	MAX	7.6	0.0	39.0
	MIN	-3.9	-34.3	-19.7
5. Back-twisting				
Back Axial Rotation	MAE	3.1	11.0	21.9
	S.D. of AE	1.9	8.6	18.5
	MAX	4.6	8.6	22.5
	MIN	-6.5	-23.8	-64.5
6. Knee-bending				
Upper Leg	MAE	5.4	4.3	9.8
	S.D. of AE	5.5	4.6	12.0
	MAX	3.3	9.3	32.4
	MIN	-13.7	-14.0	-4.9
Lower Leg	MAE	1.0	2.4	2.7
	S.D. of AE	1.1	2.6	2.8
	MAX	4.1	7.6	8.1
	MIN	-1.7	-6.5	-3.3
Average MAE		**4.2**	**6.2**	**11.6**
Average S.D		**2.8**	**4.4**	**8.1**

Notes: MAE (Mean Absolute Error), AE (Absolute Error), S.D. (Standard Deviation), MAX (Maximum Value of Errors), MIN (Minimum Value of Errors)

Average MAEs of three approaches during basic tasks were 4.2 (RGB-D sensor-based), 6.2 (stereovision camera-based) and 11.6 (multiple camera-based) degrees, respectively. One of the reasons for the least accurate results from a multiple camera-based approach is that it showed relatively larger errors in lower arm (16.2 degrees of MAE), truck flexion (12.5 degrees of MAE) and trunk rotation (21.9 degrees of MAE) angles than other body angles. As shown in A3 (elbow-bending), A4 (back-bending) and A5 (back-twisting) tasks in Figure 3.4, an elbow or a hip was occluded by a lower arm or a torso, which may lead to incorrect detections of these joints in a multiple camera-based approach. Excluding these body angles, a multiple camera-based approach showed 7.9 degrees of average MAEs.

RGB-D sensor- and stereovision camera-based approaches provided robust results even in the presence of self-occlusions as they rely on data-rich 3D information (i.e., 3D point clouds). An RGB-D sensor-based approach showed the most accurate (4.2 degrees of average MAE) and reliable (2.8 degrees of average S.D.) results for all body angles. A stereovision camera-based approach also provided relatively accurate motion data, resulting in 6.2 degrees of MAE, but showed higher S.D. (4.2 degrees) than RGB-D sensor-based approaches. These two approaches use same methods to extract motion data from 3D point clouds. Thus, one possible cause of different accuracies between them is that a Kinect™ has higher resolutions and frame rates than Bumblebee XB3™.

Figure 3.7 shows body angles during a lifting and placing task. Even for a complex task that involves simultaneous whole body movements, all three vision-based approaches provided robust results for all body parts. Unlike basic tasks, any severe discrepancies in body angles from a multiple camera-based approach were not observed.

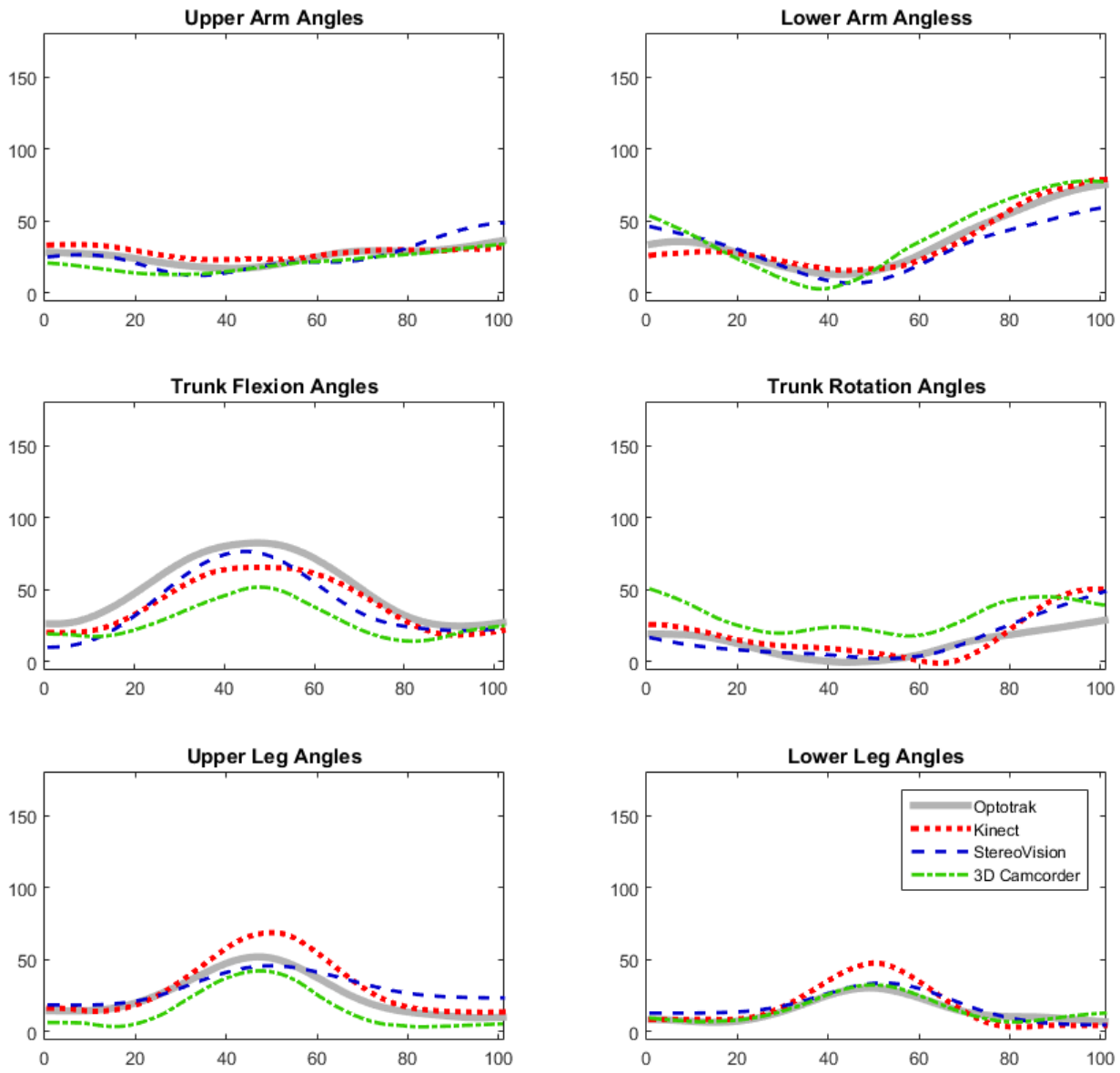

Figure 3.7: Comparison of Body Angles between Vision-based Motion Capture Approaches and an Optotrak™ during a Lifting and Placing Task

Average MAEs of three approaches during a lifting and placing task were 6.5 (RGB-D sensor-based), 6.6 (stereovision camera-based) and 10.9 (multiple camera-based) degrees, showing similar errors in body angles during basic tasks (Table 3.2). Again, in motion data from a multiple camera-based approach, larger errors in back (torso flexion and rotation) angles were observed while upper arm angles were relatively accurate because of no severe occlusion of an elbow. Both RGB-D sensor- and stereovision camera-based approaches showed robust results in

this task, even though errors in body angles in a RGB-D sensor-based approach were slightly increased.

Table 3.2: Accuracy of Vision-based Motion Capture Approaches during a Lifting and Placing Task

(Unit: degrees)

Body Angles	Metrics	RGB-D Sensor (Kinect™)	Stereovision Camera (Bumblebee XB3™)	Multiple Camera (3D Camcorder)
Upper Arm	MAE	3.5	4.6	4.4
	S.D. of AE	2.4	3.8	3.3
	MAX	4.4	6.5	10.4
	MIN	-6.3	-13.1	0.3
Lower Arm	MAE	3.6	7.6	7.5
	S.D. of AE	1.9	4.7	3.6
	MAX	8.3	16.2	11.1
	MIN	-4.9	-12.1	-19.3
Back Flexion	MAE	10.3	11.0	22.7
	S.D. of AE	5.1	5.2	11.2
	MAX	16.9	18.4	35.5
	MIN	2.9	3.1	2.2
Back Axial Rotation	MAE	8.4	5.5	18.8
	S.D. of AE	6.2	5.2	4.8
	MAX	11.3	7.2	-10.5
	MIN	-23.4	-20.0	-31.1
Upper Leg	MAE	6.9	7.1	10.3
	S.D. of AE	6.2	4.7	2.7
	MAX	1.5	7.0	14.9
	MIN	-19.4	-13.9	4.6
Lower Leg	MAE	6.0	4.0	1.5
	S.D. of AE	5.0	1.8	1.4
	MAX	7.2	4.0	3.7
	MIN	-17.5	-6.7	-6.1
Average MAE		**6.5**	**6.6**	**10.9**
Average S.D.		**4.5**	**4.2**	**4.5**

Notes: MAE (Mean Absolute Error), AE (Absolute Error), S.D. (Standard Deviation), MAX (Maximum Value of Errors), MIN (Minimum Value of Errors)

On the other hand, a walking task showed larger discrepancies in the patterns of body angles from all three vision-based approaches as shown in Figure 3.8. A multiple camera-based approach showed similar average MAEs (11.0 degrees) with other tasks (Table 3.3). However, considering that variations of body angels during walking are relatively smaller (less than 50 degrees, except lower arm angles) than other tasks, this error is quite significant. Also, in motion data from both

RGB-D sensor- and stereovision camera-based approaches, the largest errors were observed among three tasks, showing 7.1 and 12.6 degrees of average MAEs (Table 3.3). Considering that a walking task involves more rapid movements than other tasks, these approaches seem to be affected by the speed of movements. In particular, a stereovision camera-based approach significantly suffers from rapid movements due to a low frame rate.

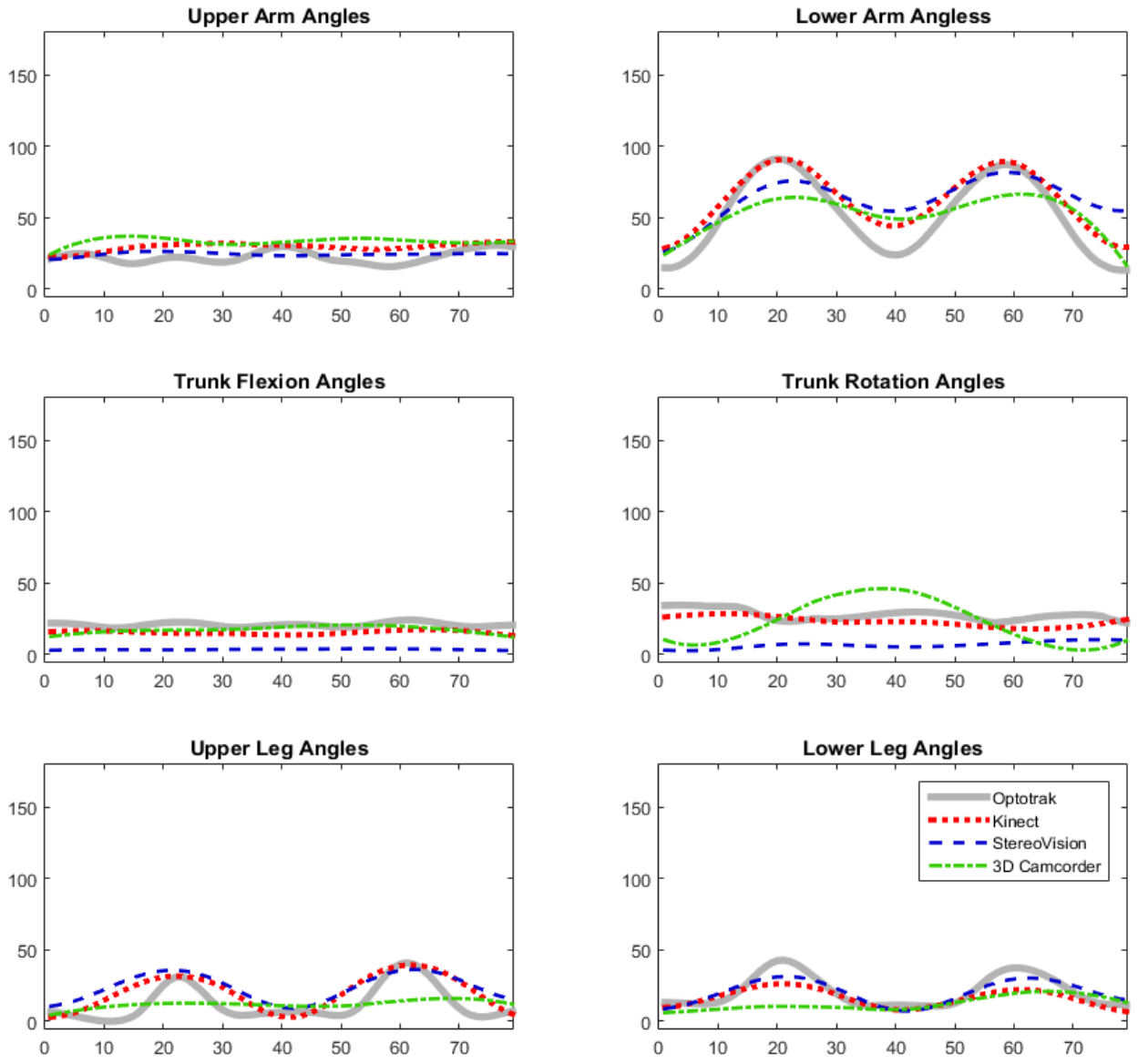

Figure 3.8: Comparison of Body Angles between Vision-based Motion Capture Approaches and an Optotrak™ during a Walking Task

Table 3.3: Accuracy of Vision-based Motion Capture Approaches during a Walking Task

(Unit: degrees)

Body Angles	Metrics	RGB-D Sensor (Kinect™)	Stereovision Camera (Bumblebee XB3™)	Multiple Camera (3D Camcorder)
Upper Arm	MAE	7.1	4.5	10.9
	S.D. of AE	4.0	2.3	5.5
	MAX	1.8	6.5	-2.0
	MIN	-13.3	-8.7	-19.3
Lower Arm	MAE	10.7	15.9	15.0
	S.D. of AE	6.3	11.6	7.7
	MAX	1.1	17.1	28.0
	MIN	-20.6	-41.8	-25.4
Back Flexion	MAE	5.4	17.3	3.5
	S.D. of AE	1.5	1.4	2.2
	MAX	7.9	20.4	9.4
	MIN	2.3	15.0	-1.7
Back Axial Rotation	MAE	4.8	21.3	15.3
	S.D. of AE	4.8	5.3	8.1
	MAX	8.8	32.0	27.9
	MIN	-24.4	14.6	-18.6
Upper Leg	MAE	8.8	12.1	11.6
	S.D. of AE	6.6	7.2	5.5
	MAX	3.8	4.9	23.1
	MIN	-21.2	-27.3	-18.9
Lower Leg	MAE	5.6	4.2	9.7
	S.D. of AE	5.1	2.7	8.9
	MAX	16.6	11.6	32.5
	MIN	-4.3	-6.9	-5.0
Average MAE		**7.1**	**12.6**	**11.0**
Average S.D.		**4.7**	**5.9**	**6.3**

Notes: MAE (Mean Absolute Error), AE (Absolute Error), S.D. (Standard Deviation), MAX (Maximum Value of Errors), MIN (Minimum Value of Errors)

3.4 DISCUSSION

3.4.1 Performance of Vision-based Motion Capture Approaches

Specifications and accuracies of three vision-based motion capture approaches are summarized in Table 3.4. The experimental tests in the previous section presented 5.9, 8.5 and 11.2 degrees of average MAEs for RGD-D sensor-based, stereovision camera-based and multiple camera-based approaches, respectively.

Table 3.4: Comparison of Specifications and Accuracies of Vision-based Motion Capture Approaches

Performance		**RGB-D Sensor (Kinect™)**	**Stereovision Camera (Bumblebee XB3™)**	**Multiple Camera (3D Camcorder)**
Specifications	Raw Data	3D images	3D images	2D images
	Operating Range	Less than 4m	Less than 10 m (unlimited, with zoom lenses)	Unlimited with zoom lenses
	Resolution	640×480	320×240	1920×1080
	Frame Rate	30 fps	About 10 fps	29 fps
	Processing Time per frame*	About 2 seconds	About 2 seconds	About 2 seconds
Accuracy (MAEs)	Basic Tasks	4.2°	6.2°	11.6°
	Lifting and Placing	6.5°	6.6°	10.9°
	Walking	7.1°	12.6°	11.0°
	Average	**5.9°**	**8.5°**	**11.2°**

* Total time required to process one raw image frame, varies depending on computing power

A multiple camera-based approach that uses 2D images showed larger errors in body angles than the other two approaches that are based on 3D images (RGD-D sensor-based and stereovision camera-based approaches). However, considering that 2D images contain less information (e.g., RGB pixel values) than 3D images (e.g., RGB pixel values + depth information) and occlusions are critical to track body joints, about 10 degrees of average MAEs in a multiple camera-based

approach are promising. Despite relatively larger errors, a multiple camera-based approach has several competitive advantages from a practical point of view, compared with the other two approaches. For example, as all types of ordinary cameras can be used to collect 2D images, additional investments on devices are not required. Due to the use of zoom lenses, its operating range is theoretically unlimited. Less sensitivity to rapid movements is another strength of this approach. In addition, there is room for further improvement if occlusion issues are handled. In these tests, a 3D camcorder was used to obtain two images from different views. However, as the distance between two lenses is very short (3.5 cm), both images are affected by self-occlusions. If two independent cameras are positioned away from each other, possibly, it could be possible to obtain at least one clear view of images, reducing errors due to self-occlusions.

A RGB-D sensor-based approach showed the most accurate and reliable results for all three tasks as it uses data-rich 3D images and has a high resolution and frame rate. Despite robust performance of this approach, the short operating range (less than 4m) and sensitivity to sunlight of a RGB-D sensor may limit its application to confined and indoor areas. Alternatively, a stereovision camera-based approach can be a practical solution by taking an advantage of its ability to collect 3D images at both indoor and outdoor conditions and longer operating range. As the quality of 3D point clouds from Bumblebee XB3^{TM} is significantly affected by the distance from the scene, it is recommended to set a stereovision camera within 10m. However, a binocular stereovision system theoretically works with any types of two 2D cameras that are separated by a short distance, and are mounted parallel to one another. As a result, this approach is flexible in terms of operating ranges if zoom lenses are used. Recently, a stereovision system with adjustable zoom lens control has been introduced (Kim et al. 2014), enabling more practical application of this approach. Also, the use of an advanced 3D reconstruction algorithm and a high performance computer can achieve a higher frame rate that was revealed as a critical factor to reduce errors in a stereovision camera-based approach.

3.4.2 Potential Application Areas of Vision-based Motion Capture Approaches in Construction

Three vision-based approaches tested in this study are considered practical means to collect motion data under real conditions, even though about 5-10 degrees of errors in body angles exist. Despite environmental constraints, a RGB-D sensor-based approach can provide accurate and

reliable motion data with about 5 degrees of errors in body angles. While stereovision camera-based and multiple camera-based approaches show a little bit higher errors, the use of these approaches is not limited by environmental conditions. In construction, tasks are performed in unstructured and varying environments, and thus work methods and postures are changing over time. Collecting motion data using these non-invasive and cost effective approaches enable us to understand how workers interact with the environment at construction sites, providing in-depth analysis of physical demands, specifically when accuracies would not significantly matter.

For example, vision-based motion capture data can be used to specify the severity of working postures. As described in Chapter 2, existing postural ergonomic risk assessment methods determine the level of ergonomic risks based on classified postures through human observation. Some methods such as RULA or REBA require detailed segmentations of body postures according to body angles. For example, in RULA, trunk postures are categorized into four groups according to trunk flexion angles (0°, 0°-20°, 20°-60° and over 60°). Even though vision-based posture classification can determine whether a back is bent or not, it may not accurately classify more specific back postures as defined in RULA. In this case, the use of vision-based motion capture approaches enables more detailed analysis of body postures, providing accurate posture classification results.

Also, as the continuous measurement of workers' motions during performing tasks is enabled using vision-based motion capture approaches, diverse in-depth motion analysis for understanding physical demands can be facilitated. Traditionally, pre-determined-motion-time-systems have been widely used to identify workloads during occupational tasks (Laurig et al. 1985). As these systems rely on human observations to describe workers' manual activities, significant human effort is generally required. However, by using a time series motion data from vision-based approaches, it is possible to accurately and automatically quantify motion-time values for these systems. Also, trajectory analysis using vision-based motion data helps to evaluate work efficiency, as well as the risk of ergonomic injuries. For example, shorter trajectories of body movements may imply more efficient movements of a human body, indicating smaller physical demands. Previous studies on movement patterns during occupational tasks found that a more 'dynamic' pattern of movements is believed to be associated with a lower incidence of WMSD development (Kilbom

and Persson 1987, Kilbom 1994). Analysis of motion patterns and trajectories using vision-based motion data can broaden our understanding on the job from an ergonomic perspective.

Another application area is evaluation of musculoskeletal stresses through biomechanical analysis. It has been found that external load factors such motions and musculoskeletal stresses have significant correlations each other, and thus by understanding the relationships, internal forces can be estimated using mathematical models. One of the examples of the models is a biomechanical model. Motion data is one of the important inputs for biomechanical models. Motion data collected from vision-based approaches helps to perform biomechanical analysis under real conditions. This topic will be further described in Chapter 4.

3.5 CONCLUSIONS

The chapter describes the potential of vision-based motion capture approaches as a means of measuring workers' motions. Three emerging vision-based motion capture approaches for construction tasks are compared through a laboratory test while performing three different tasks. The accuracy of these approaches was computed by comparing body angles from each approach and a marker-based motion capture. The comparison results indicated that the overall errors in body angles are about more or less 10 degrees, which is promising.

From a practical perspective, vision-based motion capture approaches have great potential as non-invasive motion data collection methods at construction sites. Even though several obstacles such a limited operating range (RGB-D sensor-based), low frame rates (stereovision camera) and occlusions (multiple camera-based) still remain to obtain more accurate data from these approaches, further algorithm refinements and hardware developments are expected to address these issues.

As the tests of vision-based approaches were made in a laboratory setting, further investigation of the accuracy of vision-based motion data is required for construction tasks performed at real sites. Despite some errors that exist in motion data, vision-based motion data can be used for diverse in-depth analysis without sacrificing its reliability to better understand workers' physical demands during occupational tasks including construction.

CHAPTER 4

MOTION DATA-DRIVEN BIOMECHANICAL ANALYSIS USING VISION-BASED MOTION CAPTURE APPROACHES[1]

4.1 INTRODUCTION

The previous chapters highlighted vision-based approaches that enable us to analyze and evaluate workers' postures and motions while performing tasks at construction sites. Although kinematics information is useful to understand external factors that result in excessive physical demands, it may be not enough to predict potentially hazardous loading conditions on specific musculoskeletal tissues (Chaffin et al. 2006). As described in Chapter 1, external physical loads such as voluntary motions and external forces (e.g., hand loads) are transmitted to the human body, creating internal forces such as muscle forces (Armstrong et al. 1993). A slightly different posture, combined with the external forces and body weight, can create potentially excessive internal loads on musculoskeletal tissues that could lead to tissue damage, pain or discomfort and even disability (Chaffin et al. 2006). In this regard, understanding of how external loads (i.e., motions and force exertions) result in internal forces acting on the human body is necessary to prevent WMSDs.

Unlike external stresses, internal stresses on the musculoskeletal system can rarely be measured directly. To address this issue, previous research efforts have developed mathematical models (i.e., biomechanical models) that quantify the relationship between external loads and corresponding musculoskeletal stresses, and thus estimate the internal forces (Radwin et al. 2001). However, biomechanical models and analyses have been applied in only limited or controlled

[1] This chapter is partially adapted from Seo, J., Starbuck, R., Han, S., Lee, S., and Armstrong, T. (2014). "Motion-Data–driven Biomechanical Analysis during Construction Tasks on Sites" *Journal of Computing in Civil Engineering*, ASCE, 29(4).

environments due to the difficulty of collecting and analyzing the motion data required for biomechanical models. Compared to other industries such as manufacturing where work methods and processes are usually fixed when designing workplaces, construction takes place in unstructured and varying environments, and thus work methods and postures are changing over time. Further, task requirements in construction vary depending on project-specific context (Mitropoulos and Memarian 2012), which results in different levels of physical exertion by workers' musculoskeletal systems. As a result, an effective and easily accessible means for on-site biomechanical analysis is required to assess risk factors (e.g., awkward postures, forceful exertions) that may cause excessive musculoskeletal stresses beyond human capability during construction tasks under real conditions.

In the previous chapter (Chapter 3), vision-based motion capture approaches were proposed to invasively collect motion data under real conditions. The vision-based approaches also have immense potential to replace complex motion capture systems that previous biomechanical studies have relied on to collect motion data, and thus to enable on-site biomechanical analysis at construction sites. However, two research challenges still remain unanswered. First, due to the differences on how to define postures and motions between vision-based approaches and existing biomechanical analysis tools, the vision-based motion data is not directly applicable in the existing tools. Second, as described in Chapter 3, approximately 5°-15° of errors in body angles exist in the vision-based motion data, which may lead to significant inaccuracies in estimated internal loads from biomechanical analysis. For example, Chaffin and Erig (1991) reported that an error of ±10 degrees in the joint angles could cause the biomechanical analysis results to vary up to ±30% at specific body joints (e.g., knees and angles).

Therefore in this chapter, this study tests the feasibility of on-site biomechanical analysis using the vision-based motion data for quantifying musculoskeletal stresses on different body parts. Specifically, this study aims to answer the following questions: 1) how to process the vision-based motion data for existing computerized biomechanical analysis tools; and 2) whether the accuracy of the vision-based motion data is acceptable for biomechanical analysis.

This chapter will proceed with an overview of biomechanical analysis for assessing musculoskeletal stresses. This is followed by detailed descriptions on the proposed motion data conversion methods to enable biomechanical analysis using vision-based motion data. Finally, this

study investigates the sensitivity of the estimated joint moments from biomechanical analysis to errors in the joint angles from vision-based motion data.

4.2 BIOMECHANICAL ANALYSIS FOR ASSESSING MUSCULOSKELETAL STRESSES

4.2.1 Biomechanical Models and Analysis

Biomechanical models have helped to understand how external factors create musculoskeletal stresses such as joint moments or muscle forces that can rarely be measure directly (Chaffin et al. 2006). Based on the assumption that the actions of the human body follow the laws of Newtonian mechanics, the biomechanical models estimate musculoskeletal loads during occupational tasks as a function of external exposure data, like motions and external forces (Chaffin et al. 2006). As a result, biomechanical models help one to identify hazardous loading conditions with excessive musculoskeletal stresses that may contribute to the development of WMSDs during occupational tasks (Marras and Radwin 2005).

Biomechanical models have been widely used to understand physical demands for diverse construction tasks. Hsiao and Stanevich (1996) found that the techniques used to handle end frames for scaffolding tasks varied among construction workers. Through biomechanical analyses on different lifting and carrying strategies, they found that construction workers are exposed to significant biomechanical stresses at the shoulders, elbows, and torso due to the heavy weight and bulky size of scaffold planks, and the restricted work space inherent during erection and dismantling of scaffolds (Hsiao and Stanevich 1996). Pan and Chiou (1999) analyzed different drywall installation techniques using biomechanical models by simulating the tasks at the laboratory, and found that considerable biomechanical stresses at the workers' shoulders, torsos, and hips were produced due to awkward working postures (e.g., twisted and asymmetric postures) adopted by the workers. Golabchi et al. (2015) used 3D SSPP^{TM} to identify risky tasks taking place in a construction prefabrication shop, and recommend an ergonomically safe workplace design. These studies indicate that construction workers are exposed to excessive physical demands by both working postures and workplace design, and biomechanical analysis during construction

tasks can be used not only to provide feedback to workers on their working postures, but also to ergonomically design workplaces.

4.2.2 Data Collection for Biomechanical Analysis

Collecting motion and external force data for biomechanical analysis requires complex instrumentation such as marker-based motion capture systems or force measurement devices. As a result, previous biomechanical studies have relied on laboratory experiments to collect these data by simulating tasks in a controlled environment. While vision-based motion capture approaches enable the collection of motion data without interfering with on-going work (See Chapter 3), external force measurement under real conditions is still challenging.

External forces that act against the human body (e.g., hand and foot forces) are generally produced during the manual handling of loads and materials (e.g., lifting, lowering, carrying, pushing and pulling, climbing) (Frings-Dresen et al. 2000). Figure 4.1 shows conceptual diagrams of external forces according to types of tasks. During lifting tasks (including lowering and carrying), hand forces are determined by the weight of an object or material, and foot forces are the sum of hand forces and the bodyweight when ignoring acceleration effects. Hand and foot forces during pushing or pulling tasks are more complex to understand as ground conditions (e.g., coefficient of friction) and postures (e.g., direction of exertion) are also important factors to determine hand and foot forces (Al-Eisawi et al. 1999; Lee et al. 1991; De Looze et al. 2000). Climbing activities such as ladder climbing requires pulling on hands and pushing on feet to lift up the bodyweight. There are ample evidences on specific movement patterns while climbing, which may determine body mass distribution through a ladder (McIntyre 1983; Lee et al. 1994; Armstrong et al. 2008).

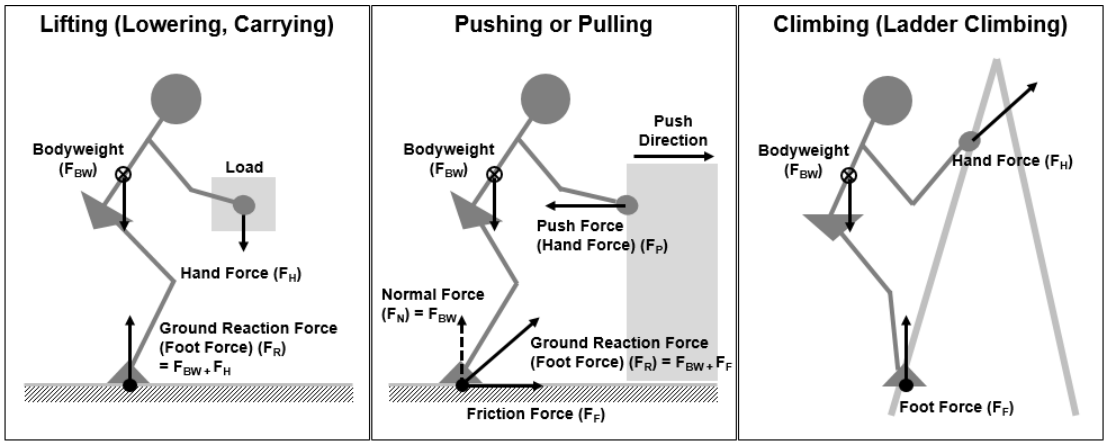

Figure 4.1: External Forces During Diverse Tasks

While it is relatively easy to estimate external forces (e.g., weight of an object) for lifting tasks, measurement of these forces for pushing or pulling, and ladder climbing generally replies on instrumentation in laboratory setting. To estimate hand and foot forces under real conditions, especially during pushing/pulling and ladder climbing, previous research efforts have developed non-invasive approaches such as mathematical models (Al-Eisawi et al. 1999; Seo et al. 2013) or minimally invasive approaches that use light-weight and low-cost sensors (Frings-Dresen et al. 2000; Hoozemans et al. 2001; Jacobs and Ferris 2015). For example, Al-Eisawi et al. (1999) developed multiple regression models that estimate horizontal and vertical hand loads during cart pushing and pulling tasks as a function of the minimum required force and handle height. Seo et al. (2013) proposed hand and foot force prediction models for ladder climbing activities by fitting polynomial lines to experimental data. In construction, a hand-held digital gauge has been used to measure pushing and pulling forces during diverse tasks at site (Frings-Dresen et al. 2000; Hoozemans et al. 2001). Also, Jacobs and Ferris (2015) have explored the feasibility of low-cost sensors such as pressure sensors on shoe insole as a means of estimating ground reaction forces. Even though further studies are required to improve accuracy and reliability, these are viable approaches to collect external force data at construction sites.

4.2.3 Computerized Biomechanical Analysis Tools

Because an estimation of internal loads requires tedious computations with three-dimensional whole-body biomechanical models, several computerized software packages such as

3D SSPP™ (Three-Dimensional Static Strength Prediction Program) and OpenSim have provided practical solutions to study musculoskeletal stresses.

3D SSPP™ is quasi-static biomechanical analysis software developed by the Center of Ergonomics at the University of Michigan (Chaffin et al. 2006). With posture data, anthropometry data, and force parameters, workers' motions can be simulated in a virtual 3D environment. Based on the biomechanical simulation, static strength requirements (e.g. joint moments) for certain tasks are predicted, including the spinal compression force using the static biomechanical model (Center for Ergonomics, University of Michigan 2011) that assumes the effects of acceleration and momentum are negligible (i.e., quasi-static postures). Importantly, based on the analysis results of postures, the body parts that endure forceful exertion can be found as compared with the relevant human capacity such as the National Institute for Occupational Safety and Health (NIOSH)-recommended limits for percent capables (i.e., the percentage of the population with the strength capability to generate a moment larger than the resultant moment) (Center for Ergonomics, University of Michigan 2011). For example, Figure 4.2(a) shows an example of the biomechanical analysis result in 3D SSPP™. The left three images in Figure 4.2(a) are the same pose from different viewpoints, and the right image in Figure 4.2(a) shows the analysis result. The limits in the bar graphs—green to yellow transition, and yellow to red transition—correspond to the NIOSH Action Limit (AL) and Maximum Permissible Limit (MPL) (NIOSH 1981) that were substantiated epidemiologically and biomechanically (Jäger and Luttmann 1999). The joint moments below the AL can be achieved by 99% of men and 75% of women, which means almost every type of worker can perform the task. On the other hand, the joint moments beyond the MPL can be exerted only by 25% of men and 1% of women, and thus should not be permitted to prevent musculoskeletal injuries. For back compression forces, the AL is set to 3,400N, and the MPL is set to 6,400N. As a result, if the bar that represents joint moments and back compression forces in certain postures is in the red zone, the body segments have a high risk of getting injured.

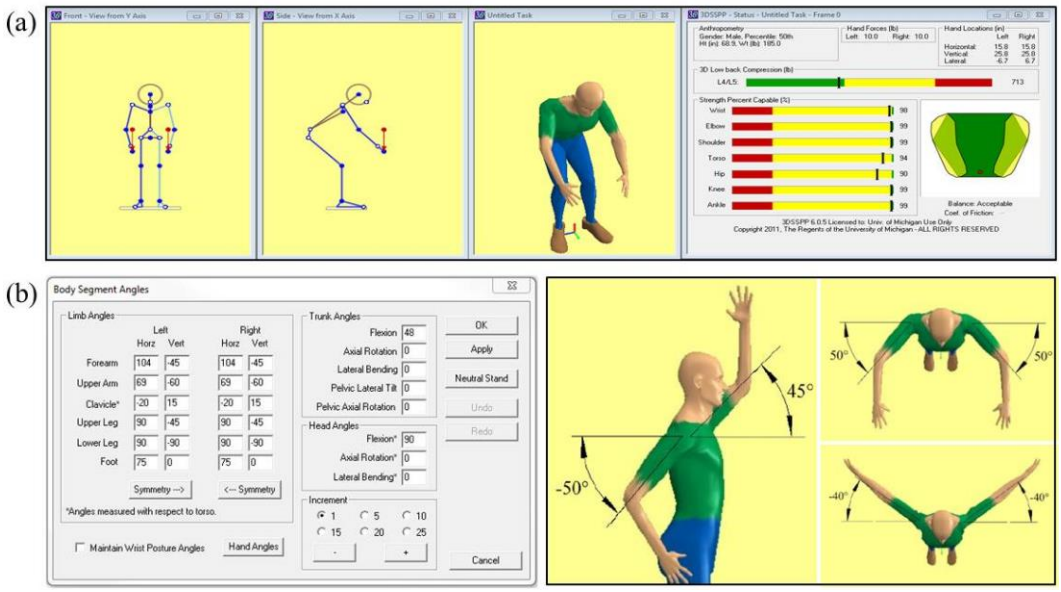

Figure 4.2: 3D SSPP^{TM}: (a) User Interface, (b) Angular Configurations of a Human Model

Generally, a biomechanical model requires three types of input data: 1) anthropometric factors (body lengths, masses, and centers of mass of body segments), 2) force parameters (external forces exerted on hands and feet), and 3) body angles at each body joint. In 3D SSPP^{TM}, anthropometric factors are set as default values for a US industrial population, and can be adjusted based on the subject's height and weight. Force parameters referring to hand forces during lifting, pushing, and pulling—foot forces are determined by summing body weight and hand force vectors—specify external forces during tasks. While anthropometric factors and force parameters can be included by simply inputting the subject's height and weight, and hand forces in 3D SSPP^{TM}, postural angles should be determined from motion data. The body model in 3D SSPP^{TM} defines a posture as body segment angles with 3 degrees of freedom, and thus can be manipulated by inputting the angles for each frame, as shown in Figure 4.2(b).

OpenSim (Delp et al. 2007) is a freely available software package that estimates biomechanical stresses including inertial forces exerted on human body joints due to changes in the velocity and direction of the motion (Anderson et al. 2012). Given the motion and external force data, OpenSim performs inverse dynamics analysis with a multibody musculoskeletal system that has rigid skeletal bones with virtual markers, as shown in Figure 4.3, to calculate joint moments (Symeonidis et al. 2010). OpenSim is designed to conduct biomechanical simulation

with experimental data, such as marker positions and kinematics obtained from marker-based motion capture systems. For this reason, the Track Row Column (TRC) file format that contains markers' geometric information from optical motion capture systems such as VICON™ is the only motion data format available in the current version of OpenSim.

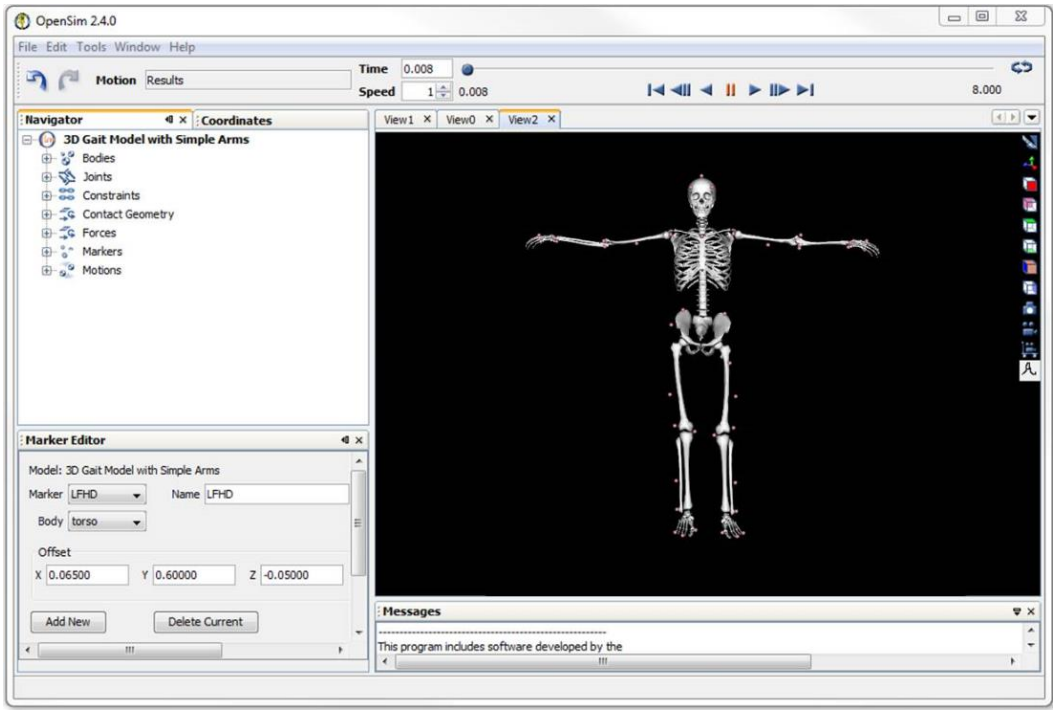

Figure 4.3: A Screenshot of OpenSim Window and a Multibody Model with Virtual Markers

Figure 4.4 shows Input and Output for 3DSSPP™ and OpenSim. While 3DSSPP™ simulate postures by inputting body angles at specific instances, OpenSim requires time-series motion data in the .trc file format. However, the motion data extracted from vision-based approaches are not readily applicable to these biomechanical analysis tools because of compatibility issues in body models of the motion data and these tools.

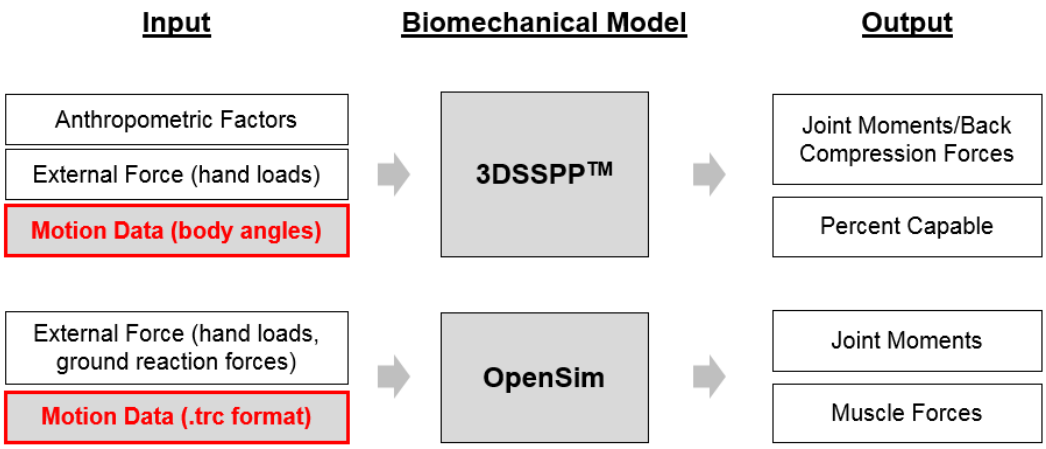

Figure 4.4: Input and Output for 3DSSPP™ and OpenSim

Figure 4.5 shows 3D skeleton models from vision-based motion capture approaches (Han et al. 2012; Han et al. 2013b). Vision-based motion capture data generally characterizes motions using Euler rotation angles at a body joint in a local coordinate system (i.e., defined for each body joint), for example, as in the Biovision Hierarchical (BVH) format—one of the most widely used motion data formats (Meredith and Maddock 2001)—which is different from the process used to define motions in 3D SSPP™ and OpenSim. Specifically, 3D SSPP™ defines a human posture with horizontal and vertical angles in a global coordinate system (i.e., defined for a full body). OpenSim simulates motions using marker-based motion data that contains positions of markers rather than body joints (i.e., more than one markers generally attached to one body joint). In this regard, a motion data reconfiguration that converts vision-based motion capture data into the proper form for ergonomic analysis tools is the key to the successful implementation of on-site biomechanical analysis.

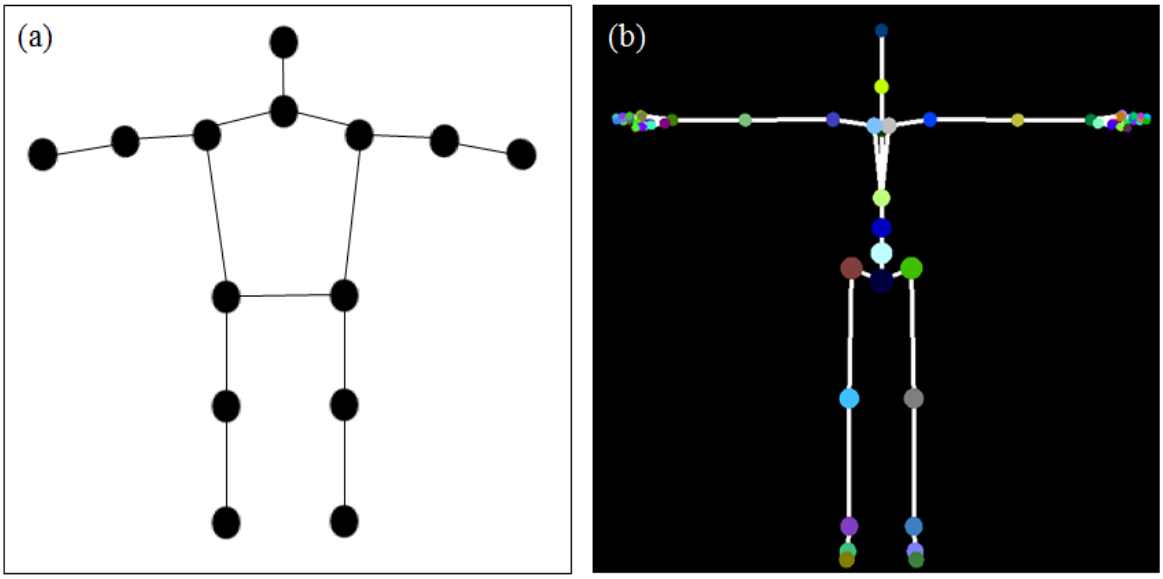

Figure 4.5: Skeleton-based Motion Data: (a) 3D Skeletons from Han et al. (2012; 2013b), (b) an Example of Skeleton Model in BVH Motion Data

4.3 MOTION DATA–DRIVEN BIOMECHANICAL ANALYSIS

This section provides the details on the processes that automatically convert the BVH motion data from vision-based motion capture approaches into available file formats in existing biomechanical analysis tools, 3D SSPP™ and OpenSim, thus allowing us to perform biomechanical analysis using the motion data without any time-consuming data processing. The feasibility of the proposed data processing was experimentally tested by conducting an experiment on lifting tasks.

4.3.1 Automated Motion Data Processing for Static Biomechanical Analysis in 3D SSPP™

An automated process was proposed to convert the BVH motion data into postural angles defined in 3D SSPP™, and then to run biomechanical analysis, given the BVH motion data as shown in Figure 4.6. BVH motion data defines hierarchical body segments as local translation and rotation information from a root body joint (e.g., a hip). However, the definitions of rotation angles and the coordinate system in BVH motion data are different from the definitions and coordinate system in 3D SSPP™. To address the difference, this study computed the body angles required for 3D SSPP™ based on spatial information (local translations and rotations) in BVH motion data.

First, 3D positions (x-y-z coordinates) of all of the body joints in the BVH motion data are iteratively computed from the root joint using local translations and rotations (i.e., a transformation matrix) based on the predefined hierarchical structure of a human skeleton in the BVH motion data. Then, the joint angles are computed based on the vectors of bones between two connected body joints in a local coordinate system of the body, following the definitions of horizontal, vertical, and rotational angles for each body joint in 3D SSPP^{TM} (Center for Ergonomics, University of Michigan 2011).

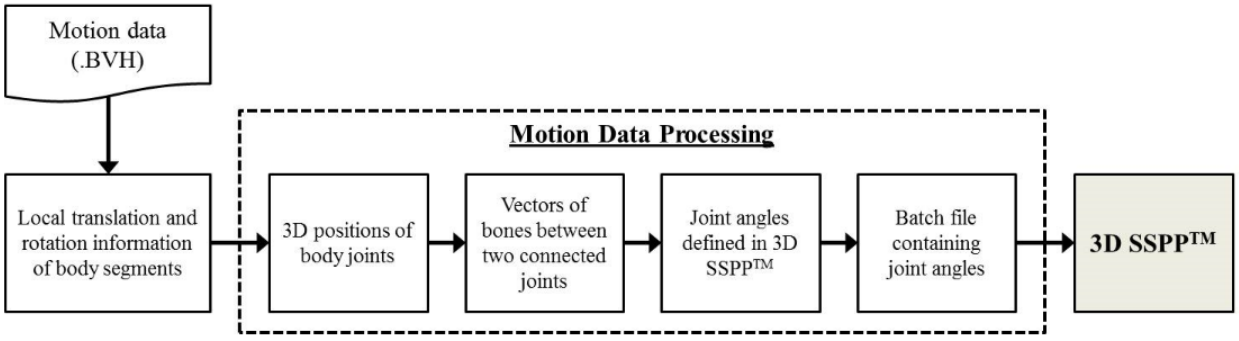

Figure 4.6: Work Flow for Automated Motion Data Processing in 3D SSPP^{TM}

The postural angles calculated from the BVH motion data for each frame are integrated in a batch file that allow automatic analysis of tasks just by importing the batch file into 3D SSPP^{TM} (Center for Ergonomics, University of Michigan 2011). Figure 4.7(a) show an example of a batch file automatically generated, containing information to run a biomechanical analysis in 3D SSPP^{TM}. All lines in the batch file have one command describing relevant data. Types and functions of commands used in a batch file are illustrated in Figure 4.7(b). For example, 'ANTHROPOMETRY', 'HANDLOADS', and 'SEGMENTANGLES' commands are for inputting anthropometry data (gender, height, and weight), hand forces required to perform the tasks, and body angles. Specifically, the values for body angles are computed directly from the BVH motion data. The other commands—such as 'COMMENT', 'DESCRIPTION', 'AUTOEXPORT', 'FRAME', and 'EXPORT'—are used to set configurations of output data (.exp). By running this batch file in 3D SSPP^{TM}, an external text file (.exp) containing the results

(e.g., summary results, joint moments, back compression forces, and strength capabilities) from a biomechanical analysis can be generated.

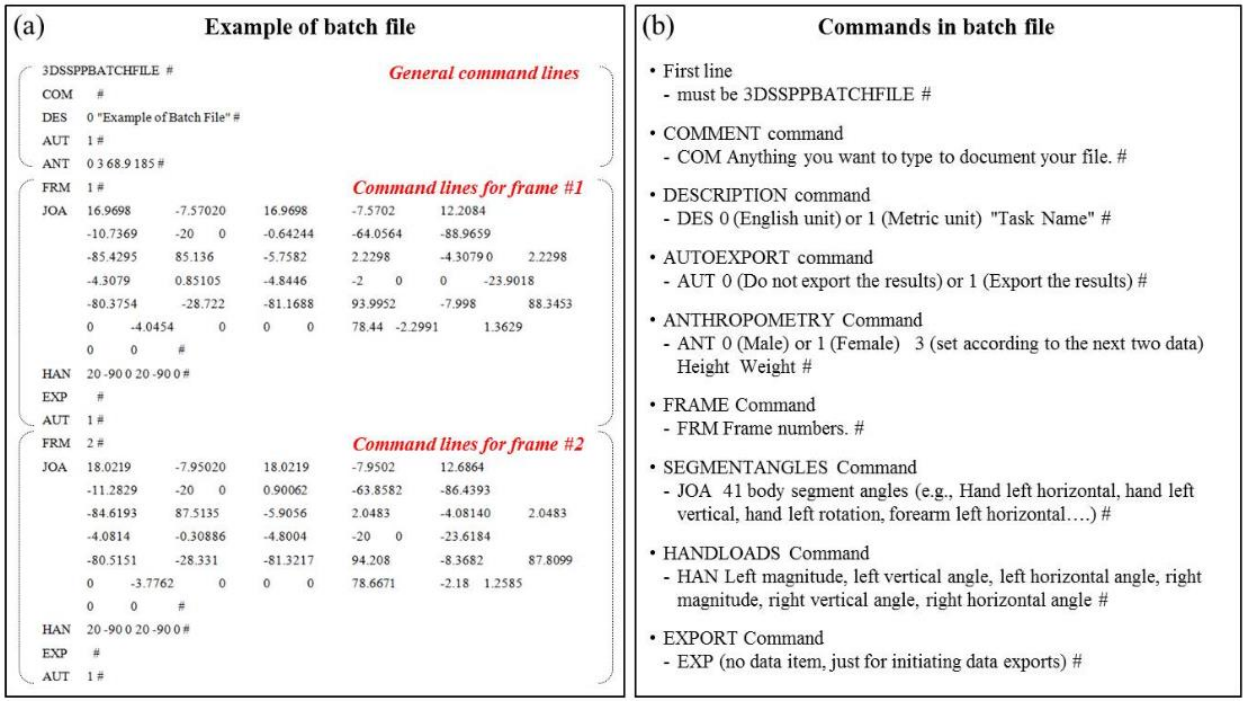

Figure 4.7: Batch File to Run 3D SSPP^{TM}: (a) an Example of a Batch File, (b) Commands in a Batch File

4.3.2 Automated Motion Data Processing for Dynamic Biomechanical Analysis in OpenSim

The procedures required to run OpenSim with marker data (i.e., TRC file) are as follows (Anderson et al. 2012): 1) scaling that adjusts both the mass properties (mass and moment-of-inertia) and the dimensions of the body segment for the subject using locations of markers; 2) inverse kinematics to create motions in the body model by matching experimental markers with virtual markers and to calculate joint angles; 3) inverse dynamics that determines the net forces and torques at each joint that produces movement by solving the equations of motion with the given motion data (joint angles from inverse kinematics) and external force data. For scaling (adjusting anthropometric factors) and inverse kinematics (calculating body angles) processes, marker positions in the TRC marker data are the primary sources; however, such marker

information is not available in the BVH motion data. To enable these two processes to be done with the BVH motion data, this study developed a user-friendly stand-alone system that automatically generates joint moments from motion capture data. This system is based on the OpenSim API to generate a human multibody model (.osim) with anthropometric and physical properties (e.g., body mass, center of mass, and moment of inertia) fitted to the subject, and a motion file (.mot) containing information on joint angles at each body joint from the BVH motion data; Figure 4.8 illustrates the overall workflow.

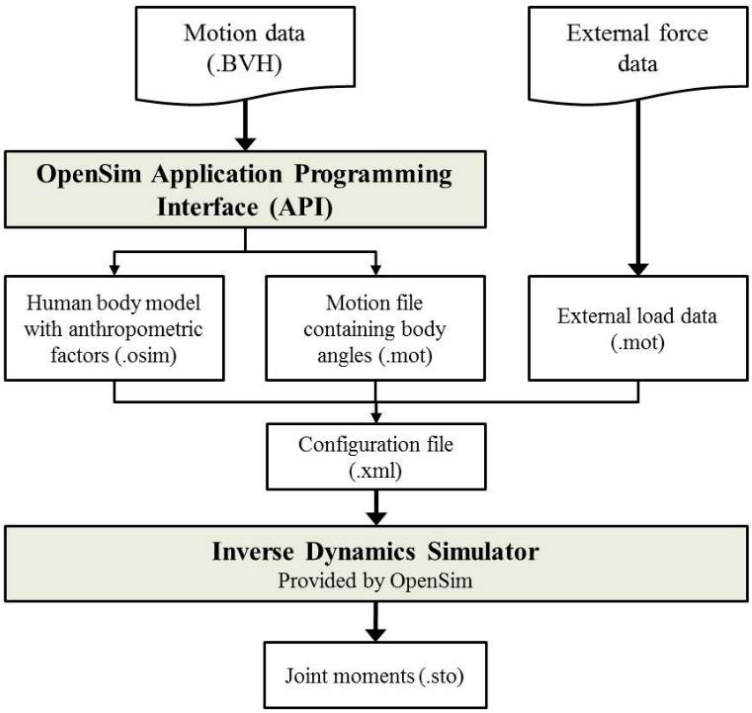

Figure 4.8: Work Flow for Automated Motion Data Processing in OpenSim

First, the proposed system creates a multibody model consisting of body segments and joints based on the hierarchical structures of bones and joints in the BVH motion data (Figure 4.9(a)). In addition, anthropometric parameters of the multibody model—such as mass, length, mass-center location, and moment-of-inertia of each body segment—are determined using a subject's height and weight based on previous studies on these anthropometric parameters (Zatsiorsky et al. 1990; DeLeva 1996). The next step is to generate a motion file (.mot) containing joint angles from the

BVH motion data. Because both the BVH motion data and the motion file (.mot) in OpenSim define motions as joint rotations in degrees relative to the initial position of the joint, geometric information on skeleton structures from the BVH motion data are immediately written to the motion file in OpenSim (.mot). The multibody model that has motion information is shown in Figure 4.9(b).

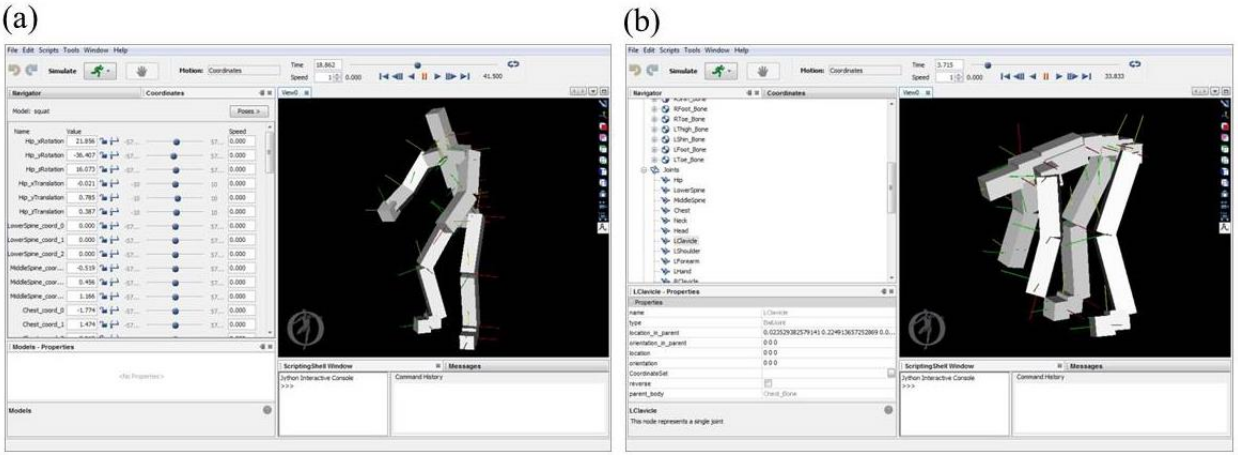

Figure 4.9: Multibody Model from the BVH Motion Data: (a) a Multibody Model with Anthropometric Parameters Fitted to the Subject, (b) Represented Motions in the Multibody Model Based on the BVH Motion Data

Once the OpenSim body model (.osim) and the motion file (.mot) are generated, the system also creates a configuration file (.xml) that will be used by the OpenSim inverse dynamics simulator to integrate the model (.osim), motion (.mot) and external force (.mot) files. The inverse dynamics simulator is an executable module built from the source codes for inverse dynamics from OpenSim, and thus enables us to perform inverse dynamics using the configuration file. The simulator saves the joint moments from dynamic biomechanical analysis to a storage file (.sto). These workflows are automatically processed only by inputting a subject's anthropometric information (height and weight) and the BVH motion data in the stand-alone system.

To verify the proposed approach, motion data during ladder climbing from one male subject was collected by using an optical motion capture system, VICON^{TM}, because climbing activities involve dynamic movements of the whole body. The raw data captured from VICON^{TM} was

converted into the motion data in different file formats: .TRC and .BVH. Then, this study compared anthropometric parameters and joint angles from the proposed approach that uses BVH motion data with the parameters and angles from the existing approach of OpenSim that uses TRC motion data. To measure the differences in anthropometric parameters, the percentage error between the values was used. For joint angles, the normalized root-mean-square errors (NRMSE) between the values from the proposed approach and the ones from the existing approach were calculated during one cycle of climbing (240 frames, 2 seconds). As shown in Table 4.1, the differences in anthropometric parameters except for the radius of gyration of a lower leg were less than 5%. The radius of gyration is determined by the square root of the moment of inertia divided by the mass. Considering that only the dynamic rotational moment is affected by the value of the moment of inertia, the error in the inertial parameters of a lower leg would not significantly affect the joint moments at a knee joint. In addition, NRMSE values for body angles at elbows and knees were 0.079 and 0.081, respectively (Figure 4.10). These results indicate that the proposed approach accurately estimates anthropometric parameters and joint angles based on BVH motion data, compared with the values from the existing approach.

Table 4.1: Comparison of Anthropometric Parameters from OpenSim and the Proposed Approach

	Anthropometric Parameters	**Existing approach**	**Proposed approach**	**% of Error**
Upper arm	Mass (Kg)	1.96	1.97	-0.22%
	Length (m)	0.29	0.30	-5.43%
	Distance from center of mass to proximal joint as % of length	57.37%	57.72%	-0.62%
	Radius of gyration as % of length, transverse	26.73%	26.89%	0.61%
	Radius of gyration as % of length, longitudinal	15.70%	15.80%	0.60%
	Radius of gyration as % of length, frontal	0.28	0.29	0.60%
Lower leg	Mass (Kg)	3.50	3.30	5.71%
	Length (m)	0.43	0.42	2.30%
	Distance from center of mass to proximal joint as % of length	43.42%	44.58%	-2.69%
	Radius of gyration as % of length, transverse	27.11%	25.10%	-7.43%
	Radius of gyration as % of length, longitudinal	8.63%	10.20%	18.26%
	Radius of gyration as % of length, frontal	0.27	0.25	-9.89%

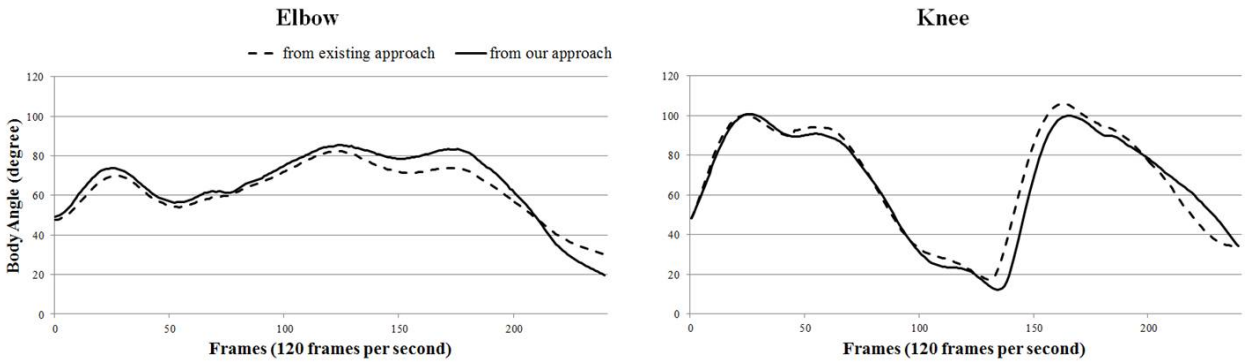

Figure 4.10: Comparison of Body Angles between Existing and Proposed Approaches

4.3.3 A Case Study on Lifting Tasks

The feasibility of the proposed automated motion data processing was tested by conducting a case study on lifting tasks with postural variations. An RGB-D sensor–based motion capture approach was used to collect BVH motion data, and then, both static and dynamic biomechanical analyses were performed in 3D SSPP^{TM} and OpenSim. The results of joint moment estimation by applying the proposed approaches are presented, and then are compared with previous studies that estimated joint moments during lifting tasks using optical motion capture data in this subsection.

4.3.3.1 Motion Data Collection

Motion data during the concrete block lifting was collected by mimicking the tasks in a laboratory as shown in Figure 4.11. A male subject (175 cm, 70kg) was asked to stand in a T-pose, facing the RGB-D sensor, and then repeatedly lift a 20-kg (196-N) concrete block from one side on a floor and move it to the opposite side 10 times. This protocol reflects practices during masonry work in which a worker lifts a block in stock, and puts it on a wall. Then, he was asked to lift a block using the squat technique in which the back remains straight and the knees are bent (Garg and Moore 1992) (Figure 4.11(a)). After taking a break to minimize fatigue, he was asked to apply the stoop technique in which the back is bent to lift a block (Figure 4.11(b)). During the trials, Kinect^{TM} took RGB-D images at a frame rate of 30 Hz, as shown at the top of Figure 4.11, and the images were processed in iPi Desktop Motion Capture to extract BVH motion data, as shown at the bottom of Figure 4.11.

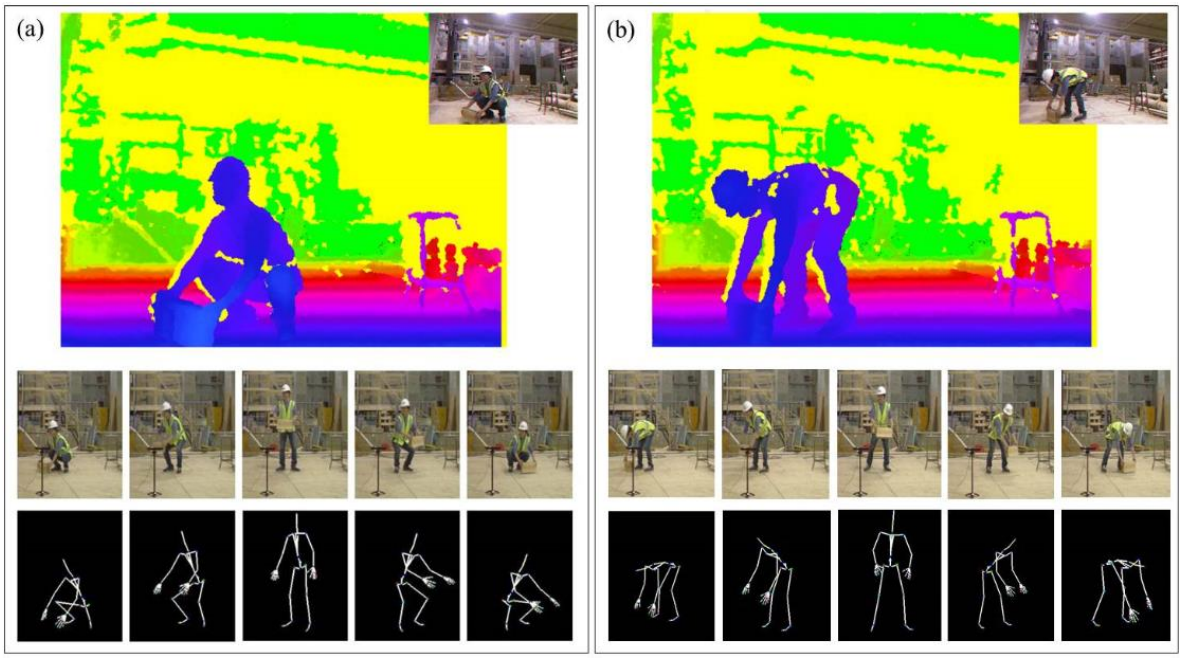

Figure 4.11: Motion Data Collection during Concrete Block Lifting: (a) Squat Lifting, (b) Stoop Lifting

4.3.3.2 Results from Static and Dynamic Biomechanical Analyses

The BVH motion data was post-processed by applying the proposed motion data conversion methods to obtain postural angles for 3D SSPP^{TM} and OpenSim. Anthropometric factors were adjusted based on the subject's height and weight. To determine external forces (e.g., hand and foot forces), it was assumed that the magnitude of external force exerted on each hand was 98 N, and that the direction of the forces was downward. In addition, the foot forces were assumed as a sum of the weight of the subject and a concrete block. Based on these data, static and dynamic biomechanical analyses were conducted to estimate joint moments during squat and stoop lifting.

Figure 4.12 shows joint moments at L5/S1 (i.e., an intervertebral disc between the fifth lumbar and first sacral vertebra), left knee, and left elbow joints during one cycle of squat and stoop lifting (i.e., lift, carry, and put down a concrete block) from the static and dynamic biomechanical analyses. In the graphs, the solid lines indicate joint moments from dynamic biomechanical analysis while the dotted lines indicate joint moments from static biomechanical analysis. Overall, the results show that joint moments from dynamic biomechanical analysis are

higher than those from static analysis. In a dynamic biomechanical model, the moment at a certain body joint is defined as the sum of the static moment and the dynamic inertial forces (i.e., the instantaneous acceleration effect due to the tangential rotation force and the rotational acceleration effect) (Chaffin et al. 2006). According to the study by McGill and Norman (1985), the peak lumbar moment in a static condition was 84% of the peak lumbar moment in a dynamic condition during lifting loads. The results are similar to the results from this study, by showing that the peak static joint moments at the L5/S1 disc are 79% and 73% of the peak dynamic joint moments at the L5/S1 disc during squat and stoop lifting, respectively. One of the reasons why the results showed higher dynamic joint moments compared with static joint moments than the previous study is that the subject lifted a load from waist height in the previous study, while the subject in this case study lifted a concrete block from the floor. The lifting speed when lifting a load (200N) from the floor level could be about 25% higher than the speed during lifting from waist height (Lavender et al. 2003). Thus, differences in lifting heights may contribute to differences in lifting speeds, resulting in higher dynamic joint moments in this case study than the ones from the previous study.

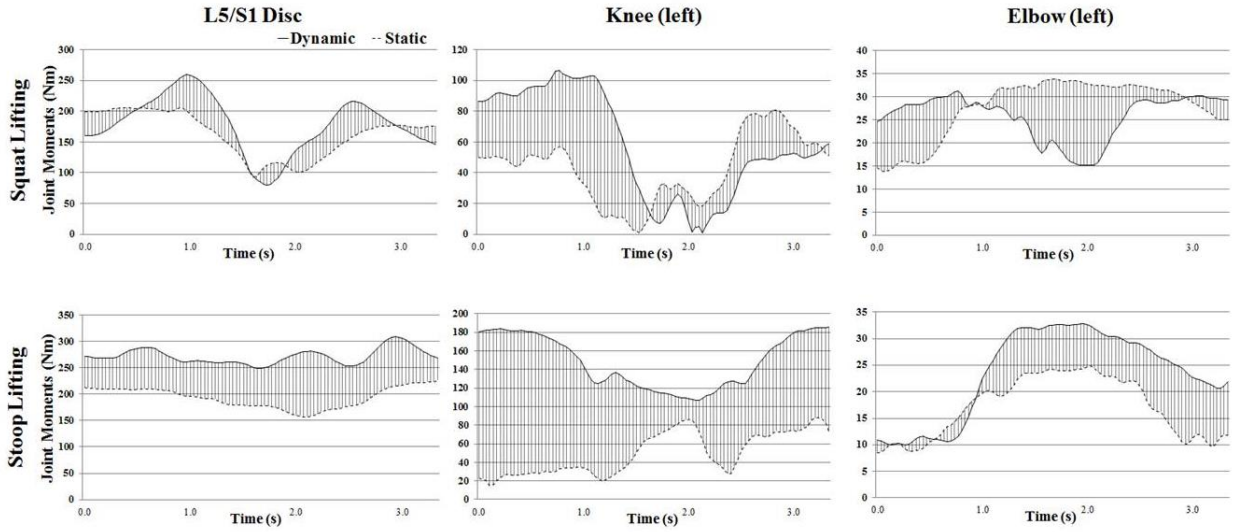

Figure 4.12: Biomechanical Analysis Results during Squat and Stoop Lifting

With regard to lifting techniques, the squat lifting is less stressful to the back from both static and dynamic analyses in this case. This result corresponds to the previous study that the

squat lifting produced fewer maximum lumbar joint moments than the stoop lifting when a subject lifted the heavy object (15kg) (Hwang et al. 2009). However, this result is not always the case because the stoop lifting can maintain the object closer to the torso than squat lifting, resulting in the reduced moment arm of the load (Chaffin et al. 2006). For this reason, previous studies recommended squat lifting only when the subject can put an object between the feet to minimize the moment arm of the load (van Dieën et al. 1999). In addition, the joint moments at a knee during stoop lifting are higher than those during squat lifting, which is similar to the results from the previous study (Hwang et al. 2009). No significant difference in elbow joint moments was observed in the results from a case study because the joint angles between squat and stoop lifting were similar, as shown in Figure 4.12.

4.3.4 Considerations for Motion-data Driven Biomechanical Analysis

This subsection discusses considerations when applying the proposed approaches for on-site biomechanical analysis and when analyzing the results in the context of tasks. The results from the case study imply that the motion data–driven biomechanical analysis provides a robust measure of musculoskeletal stress from both static and dynamic points of view, given motion capture data (e.g., BVH files). In addition, the usability issue of the proposed method is also important from the practical perspective in making the biomechanical models useful when performing ergonomic evaluations during tasks (Chaffin 1997). In this context, it should be clear that the automatic processes of motion data obtained directly from work places enable ergonomists and practitioners to identify a potential risk of WMSDs that exists in certain tasks and work environments by evaluating hazardous internal loading conditions in a timely manner without technical sophistication or skill.

Notably, in-depth understanding of the differences in body configurations between the BVH motion data and the 3D SSPP^{TM} body model may lead to the further improvement on the accuracy of biomechanical analysis. Skeleton structures of the multibody model in OpenSim follow those in the BVH motion data excluding joints in hands, and thus the motions can be exactly simulated according to the motions in the BVH motion data. In the other hand, 3D SSPP^{TM} has its own skeleton structures that are different from those in the BVH motion data, which makes errors when calculating joint angles. For example, in 3D SSPP^{TM}, the trunk flexion angle is defined as an angle between the projection of the trunk-axis (the center of the hips to the center of the shoulders) and

the positive Y-axis as shown at the bottom of Figure 4.13(a). In the top view of the skeleton model in 3D SSPP^{TM} (the top of Figure 4.13(a)), it is found that hips and shoulders are aligned. On the other hand, the hips are located slightly forward in the Y-axis, compared with the shoulders (the top of Figure 4.13(b)). The differences in skeleton structures and joint positions cause errors in the trunk flexion angle that is calculated from the BVH motion data (the bottom of Figure 4.13(b)), resulting in slightly different postures in 3D SSPP^{TM}. Generally, the hierarchical structures of bones and joints in the BVH motion data vary depending on the type of motion capture system and algorithm. For this reason, when applying the BVH motion data to 3D SSPP^{TM}, one should consider the differences in skeleton structures between skeleton models in 3D SSPP^{TM} and motion data, and adjust them if the differences are significant.

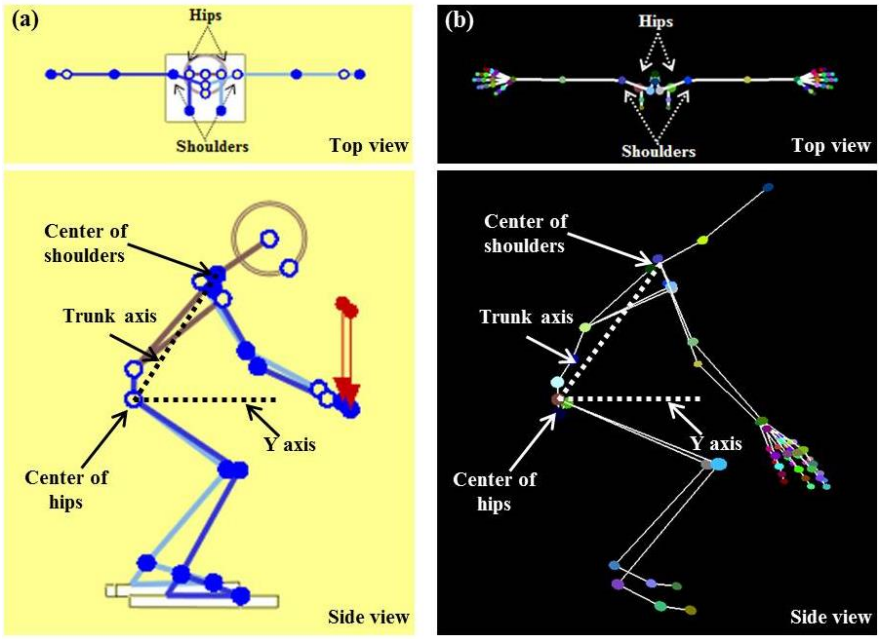

Figure 4.13: Comparison of a Trunk Flexion Angle in (a) 3D SSPP^{TM} and (b) BVH Motion Data

When applying biomechanical analysis on construction tasks, the selection of adequate analysis should be made considering the purpose of the analysis due to differences in tolerance limits under static and dynamic conditions. The results from the case study indicated that acceleration effect could increase joint moments up to 30% in lifting tasks. Therefore, static analysis using 3D SSPP^{TM} is appropriate for tasks involving slow motions where accelerations can

be ignored, while tasks involving jerking motions require dynamic biomechanical analysis in OpenSim. However, it should be noted that there is no available threshold to determine whether the dynamic joint moments are hazardous or not. Tissue injuries occur when the applied musculoskeletal stresses exceed the failure tolerance referring to the strength of the tissue (McGill 1997). Because it is difficult to specify individual differences in joint strength, population-based data is generally used to determine hazardous internal loads. For example, 3D SSPP^{TM} compares the joint moments produced at various body joints during tasks with the static strength moments reported from studies of various populations performing different types of exertions by setting the maximum permissible limit as the joint strength that only 25% of men and 1% of women can exert (Center for Ergonomics, University of Michigan 2011). However, because dynamic strengths are more complex than static strengths, studies on dynamic joint strengths have not yet been fully conducted (Chaffin et al. 2006). This means that joint moments from dynamic biomechanical analysis is hard to be used to determine the degree of risk in a given population of workers, but can only be relatively compared.

4.4 SENSITIVITY ANALYSIS OF MOTION ERRORS ON MUSCULOSKELETAL LOADS

Vision-based motion capture approaches enable us to collect motion data required for biomechanical analysis under real conditions. However, possible errors in vision-based motion data would be detrimental to the reliability of the analysis results. In this section, this study explored the sensitivity of musculoskeletal loads to errors in motion data to empirically examine whether errors in vision-based motion data is acceptable for biomechanical analysis of construction tasks.

4.4.1 Methodology

For the sensitivity analysis, one cycle of motion data (105 frames, 3.5 s) during squat and stoop lifting was selected. As a biomechanical analysis tool, 3D SSPP^{TM} was selected because it provides not only values of musculoskeletal loads (e.g., joint moments, back compression forces), but also ‘Strength Percent Capable’ that helps to identify excessive loads beyond one’s strength.

Chaffin and Erig (1991) have investigated the sensitivity of the Percent Capable according to postural errors by varying angles only on the specific joints (e.g., knees or ankles) with the most limiting Percent Capable. However, motion errors could occur on any joints in the body, and the combination of errors in different body angles may lead to increase or decrease of musculoskeletal loads. To understand how errors on joint angles of a whole body cause variations in musculoskeletal loads, errors of joint angles were randomly created on upper limbs (i.e., horizontal and vertical angles on shoulders and elbows), a torso (i.e., trunk flexion angles), and lower limbs (i.e., horizontal and vertical angles on hips and knees) with the range of ±5°, ±10°, ±15° and ±20°, respectively. During the cycle, the errors were uniformly distributed within each error range. Then, motions with each error range were simulated in 3D SSPP^{TM} to obtain joint moments (Nm) (elbow, shoulder, L5/S1, hip and knee joints), corresponding Percent Capables and back compression forces (L4/L5 disc). As a measure of accuracy in musculoskeletal loads according to motion errors, the Mean Absolute Percentage Error (MAPE) was computed using the following equation:

$$MAPE = \frac{1}{n}\sum_{t=1}^{n}\left|\frac{MSL_{no\ error,t} - MSL_{with\ errors,t}}{MSL_{no\ error,t}}\right| \quad (1)$$

- MAPE: Mean Absolute Percentage Error
- MSL: Musculoskeletal Loads (i.e., joint moments, Percent Capables, and back compression forces)
- t = time frames
- n = total time frames (105)

4.4.2 Results

Figure 4.14 shows musculoskeletal loads on selected joints (e.g., elbows, L4/L5 and knees) according to four different ranges of errors of whole body joint angles during squat and stoop lifting. Variations on joint moments increase as motion errors increase from ±5° to ±20°, but the plots of joint moments and back compression forces for each error range show similar overall patterns. However, the knee joint moments with an error of more than ±10° in body angles showed irregular fluctuations during the cycle of both squat and stoop lifting.

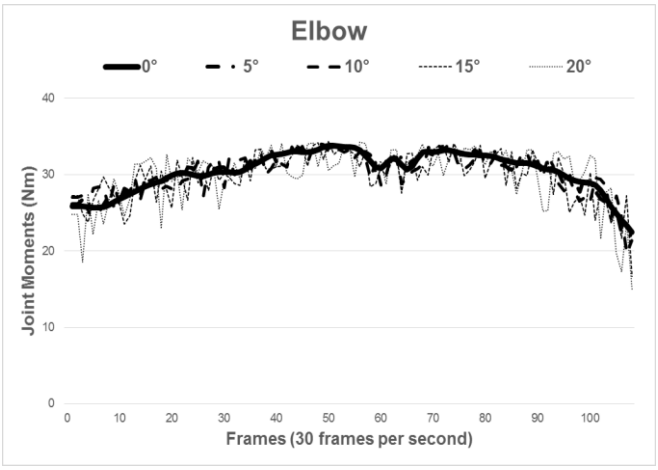

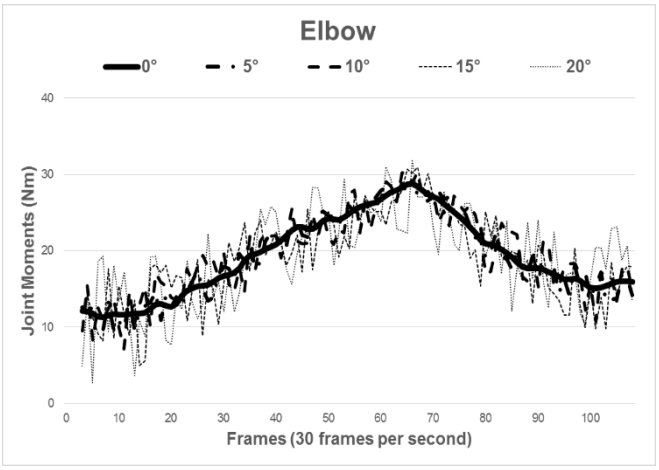

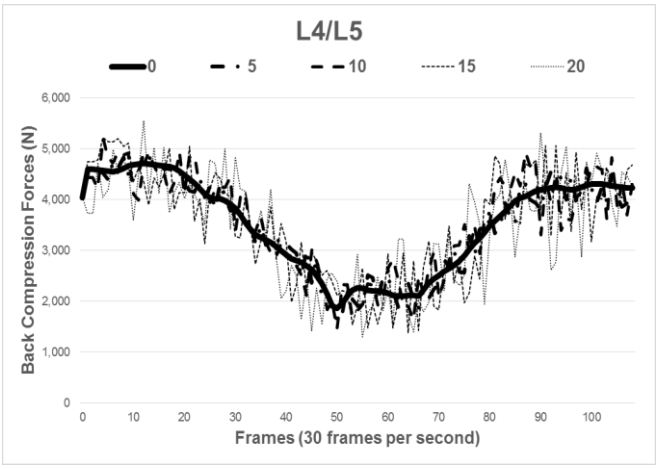

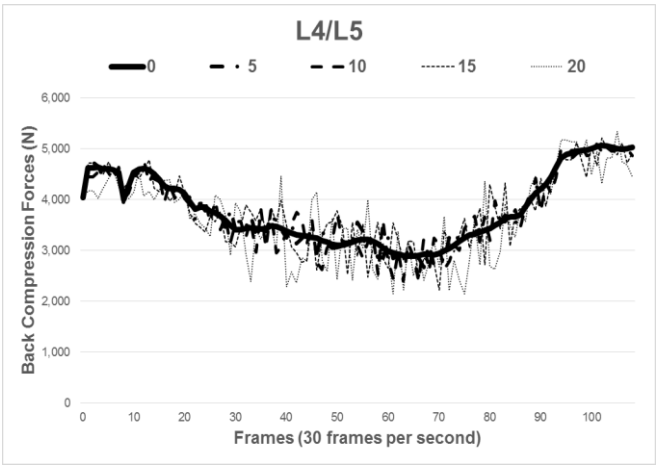

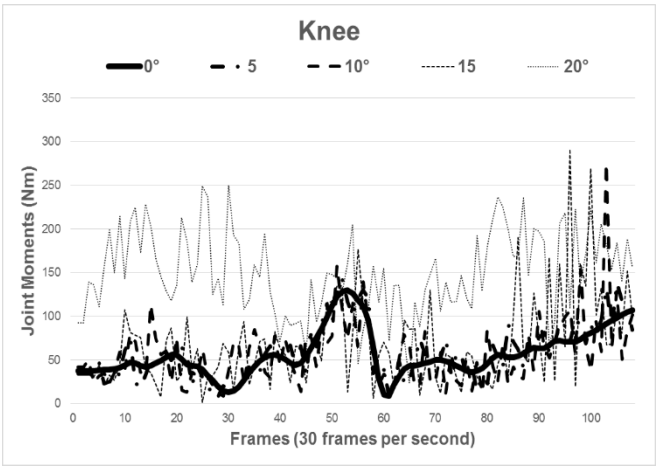

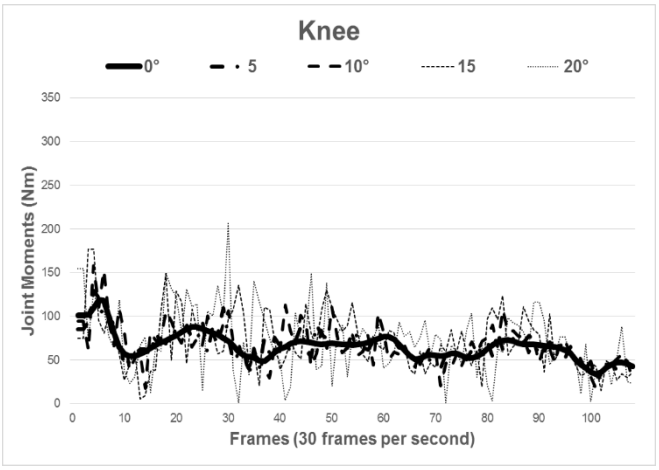

(a) Squat Lifting (b) Stoop Lifting

Figure 4.14: Patterns of Musculoskskletal Loads According to Errors in Joint Angles

Tables 4.3 and 4.4 show MAPEs of joint moments and back compression forces for each error range in body angles during squat and stoop lifting, respectively. A ±10° error produce variations in the loads, ranging from 3.9% and 13.8% during squat lifting, and from 6.0% to 11.6% during stoop lifting according to body joints (except knee joints). When the error range increased to ± 20°, MAPEs of joint moments was almost doubled. Compared with other joints, however, knee joints show higher MAPEs (186.3% for squat lifting, 44.1% for stoop lifting), indicating that knee joint moments are the most sensitive to errors in joint angles. As such, more accurate motion data would be required if reliable joint moments at knees are needed.

Tables 4.5 and 4.6 show MAPEs of 'Strength Percent Capable' at each body joint during squat and stoop lifting, respectively. These results indicate that higher errors in motion data could be acceptable to predict values for 'Strength Percent Capable'. The sensitivity analysis shows that even ± 20° of errors in motion data would create less than 10% of errors in the values of 'Strength Percent Capable' for upper limbs and a back. However, again, more accurate motion data with an error of less than ± 10° would be required if less than 10% of errors for lower limbs such as hips and knees are needed.

Table 4.2: Mean Absolute Percentage Error (MAPE) of Joint Moments (Nm)/Back Compression Forces (N) according to Errors in Body Angles during Squat Lifting

Body Part		Range of Errors in Body Angles			
		± 5°	**± 10°**	**± 15°**	**± 20°**
Upper Limbs	Elbow (Joint Moments)	1.8%	3.9%	5.7%	6.8%
	Shoulder (Joint Moments)	2.9%	6.3%	9.1%	10.1%
Back	L5/S1 (Joint Moments)	8.1%	13.8%	19.7%	20.6%
	L4/L5 (Back Compression Forces)	6.2%	10.0%	14.6%	16.0%
Lower Limbs	Hip (Joint Moments)	6.9%	12.2%	18.7%	22.4%
	Knee (Joint Moments)	26.2%	49.5%	49.6%	186.3%

Table 4.3: Mean Absolute Percentage Error (MAPE) of Joint Moments (Nm)/Back Compression Forces (N) according to Errors in Body Angles during Stoop Lifting

Body Part		Range of Errors in Body Angles			
		± 5°	**± 10°**	**± 15°**	**± 20°**
Upper Limbs	Elbow (Joint Moments)	6.4%	11.6%	15.4%	17.9%
	Shoulder (Joint Moments)	5.9%	10.9%	18.3%	22.1%
Back	L5/S1 (Joint Moments)	2.9%	6.0%	8.8%	12.6%
	L4/L5 (Back Compression Forces)	2.6%	5.6%	7.5%	11.3%
Lower Limbs	Hip (Joint Moments)	5.7%	11.6%	16.4%	21.1%
	Knee (Joint Moments)	11.9%	19.8%	33.7%	44.1%

Table 4.4: Mean Absolute Percentage Error (MAPE) of 'Strength Percent Capables (%)' according to Errors in Body Angles during Squat Lifting

Body Part		**Range of Errors in Body Angles**			
		± 5°	**± 10°**	**± 15°**	**± 20°**
Upper Limbs	Elbow	0.1%	0.1%	0.1%	0.2%
	Shoulder	1.1%	2.3%	3.1%	3.6%
Back	L5/S1	0.7%	1.2%	1.9%	1.8%
Lower Limbs	Hip	2.9%	5.8%	7.7%	9.4%
	Knee	4.5%	8.9%	13.0%	16.0%

Table 4.5: Mean Absolute Percentage Error (MAPE) of 'Strength Percent Capables (%)' according to Errors in Body Angles during Stoop Lifting

Body Part		**Range of Errors in Body Angles**			
		± 5°	**± 10°**	**± 15°**	**± 20°**
Upper Limbs	Elbow	0.0%	0.1%	0.1%	0.1%
	Shoulder	0.2%	0.3%	0.6%	1.0%
Back	L5/S1	1.1%	2.3%	5.0%	5.5%
Lower Limbs	Hip	4.3%	8.5%	10.8%	13.8%
	Knee	2.2%	3.8%	7.2%	8.0%

4.4.3 Considerations for Interpreting Results from Motion-data Driven Biomechanical Analysis

The reliability and practicability of the proposed on-site biomechanical analysis during construction tasks relies on not only automated motion data processing, but also on the accuracy of motion data collected at site. As described in Chapter 3, vision-based motion data showed a different range of errors on joint angles according to body parts, which may lead to inaccuracies when analyzing musculoskeletal stresses using biomechanical analysis. In particular, upper limb motions showed larger errors than lower limb motions.

The sensitivity analysis in the previous subsection revealed that it is important to obtain accurate motion data with an error of less than ± 10° in body angles for reliable biomechanical analysis (less than 10 % of errors in musculoskeletal stresses). Even though further improvement of accuracy are required in vision-based motion data that has more than 10° of errors in body angles according the body parts, the use of vision-based motion data for biomechanical analysis is promising from a practical perspective.

First, as inaccurate motion data would not significantly affect the musculoskeletal load patterns during a cycle of tasks, detecting postures with relatively higher musculoskeletal stresses is possible. For example, during lifting tasks, a back is a potentially problematic body region at the beginning and end of the lifting cycle as workers are exposed to the highest back compression forces as shown in Figure 4.14. Instead, upper limbs (e.g., elbows) should exert the highest joint loads at the middle of the cycle. Despite variations in musculoskeletal loads due to motion errors, these trends are not changed, making it possible to understand specific moments and corresponding postures with relatively high musculoskeletal loads.

More importantly, Percent Capables in 3D SSPP^{TM} would not be significantly affected by errors in body angles. By comparing the Percent Capables with the limits provided by NIOSH, 3D SSPP^{TM} detects excessive physical demands beyond one's strength capability that may lead to WMSDs. As a result, the Percent Capable is a more intuitive measure of the risks of WMSDs than a joint moment. Vision-based motion capture approaches can provide motion data with an error of less than 20° in joint angles, and except knee joints, this range of errors would create only about 5% of errors in the Percent Capables.

4.5 CONCLUSIONS

This study proposed motion data–driven biomechanical analysis during construction tasks using motion data obtained from vision-based motion capture approaches. Body angles required for 3D SSPP^{TM} are computed directly from positions of body joints generated from BVH motion data. For OpenSim, this study created a multibody model with anthropometric parameters adjusted for a subject based on the hierarchical structures of bones and joints in the BVH motion data, and computed joint angles based on joint rotations in degrees that are available in the BVH motion data. The proposed motion data processing for OpenSim was verified by comparing anthropometric parameters and joint angles from the proposed approach with those from the existing approach in OpenSim. In addition, this study conducted a case study on lifting tasks to test the feasibility of the proposed motion data processing for both static and dynamic biomechanical analyses. The results showed that the proposed approaches for motion data processing were successfully used to perform static and dynamic biomechanical analyses by showing similar results from previous studies.

Using the motion data during lifting tasks, this study also conducted the sensitivity analysis of motion data errors to estimated musculoskeletal loads on selected body joints. From this analysis, less than ± 10° of errors in motion data (i.e., body angles) are required for reliable biomechanical analysis. However, the use of vision-based motion data with more than ± 10° of errors would not significantly affect biomechanical analysis results from the practical perspectives because of non-significant variations in load patterns and less-sensitivity of motion errors to the 'Percent Capables'.

Combined with vision-based motion capture, the proposed motion data-driven biomechanical analysis is promising in quantifying internal loads (e.g., musculoskeletal stresses) and identifying risky tasks under real conditions. In construction where laboratory-based biomechanical studies are not feasible, on-site biomechanical analysis has great potential to provide in-depth analysis of physical demands from construction tasks, which other ergonomic evaluation methods (e.g., self-reports, observational methods, and direct measurements) cannot provide. Ultimately, the continuous monitoring of musculoskeletal stresses during construction tasks using the proposed approach will enhance the understanding of the gap between physical work demands and workers' capability, and offer a firm foundation for the improvement of workers' health (e.g., reducing WMSDs), as well as productivity in construction.

CHAPTER 5

SIMULATION-BASED ASSESSMENT OF WORKERS' MUSCLE FATIGUE AND ITS IMPACT ON CONSTRUCTION OPERATIONS[2]

5.1 INTRODUCTION

As presented in the previous chapter, on-site biomechanical analysis at construction sites can be very useful to quantify physical demands on the human musculoskeletal system, and detect specific moments when physical demands (e.g., joint moments) exceed one's capability (e.g., joint strength). However, even during a submaximal force exertion, one could experience excessive physical demands beyond one's strength because muscle strength decreases as an adaptation of the neuro-muscular system to prevent serious damage to muscles (Chaffin et al. 2006). This adaptation process can be defined as 'muscle fatigue,' which refers to "any exercise-induced reduction in the capacity to generate force or power output" (Chalder et al. 1993; Vøllestad 1997). When workers are exposed to excessive physical demands without proper rest time, they suffer from a significant level of localized muscle fatigue that could generate diverse detrimental impacts on the project performance. A systematic understanding and management of workers' fatigue in planned operations of which activities and resources are determined prior to work can greatly contribute to workers' productivity, safety, and health—all by taking proper actions before severe fatigue takes place.

Metabolic demands in different muscle groups and corresponding localized muscle fatigue not only limit the acceptable workloads for manual handling tasks that are performed for short and

[2] This chapter is adapted from Seo, J., Lee, S., and Seo, J. (2016) "Simulation-based Assessment of Workers' Muscle Fatigue and Its Impact on Construction Operations" *Journal of Construction Engineering and Management*, ASCE (Accepted).

intensive periods (Bhattacharya and McGlothlin 1996), but also contribute to cardio-respiratory (i.e., oxygen consumption) or –vascular (i.e., heart rate) responses, resulting in whole-body fatigue (Chaffin 1973). To manage workers' fatigue, evaluating the muscle fatigue from planned operations should take precedence. Previous research efforts to evaluate muscle fatigue during occupational tasks have focused on identification of potential health issues due to excessive physical demands by estimating muscle fatigue from given workloads. For example, one of the widely used methods to predict muscle fatigue is fatigue models that mathematically represent physiological or mechanical mechanisms of fatigue (Liu et al. 2002; Xia and Frey Law 2008; Ma et al. 2009). These approaches aim to detect ergonomic risks due to muscle fatigue that may contribute to the development of WMSDs (Vøllestad 1997; Perez et al. 2014). Manifestations of muscle fatigue during occupational tasks are also associated with work performance contributing to costs associated lost productivity. However, understanding the direct impact of muscle fatigue on time and cost performance is challenging due to the lack of a tool for modeling interactions between human aspects (i.e., muscle fatigue) and construction operations prior to work (Seo et al. 2015b).

To address these issues, this study proposes a simulation-based framework to estimate physical demands and corresponding muscle fatigue from the planned operation, and then evaluate the impact of muscle fatigue on construction operations. Specifically, this study combine a Discrete Event Simulation (DES) model with biomechanical and fatigue models to capture the interactive effects between muscle fatigue and planned operations. The planned construction operation is modeled at the work element level (e.g., placing concrete blocks, lifting drywall etc.) in DES that represents a breakdown of construction work into the fundamental segments of work involving different levels of physical demands. The physical demands from each work element are then estimated using a biomechanical model, simulating varying physical demands from tasks over time. The fatigue models estimate time-varying changes of muscle fatigue under estimated physical demands from the biomechanical model, which, in turn, affects construction operations in DES. Such a comprehensive and cyclic representation of muscle fatigue and corresponding operational behaviors over time allows us to see the impact of muscle fatigue on construction operations and vice versa, thereby enabling a better understanding of muscle fatigue resulting from construction operations prior to work. In addition, a case study on masonry work is conducted to demonstrate how the proposed framework can be applied to the actual construction operation.

Based on the case study, the benefits of the proposed approach for understanding how workers' fatigue under given workloads affect construction operations is discussed.

5.2 MUSCLE FATIGUE AND ITS IMPACT ON OCCUPATIONAL TASKS

Fatigue has been defined as "the decline in the ability of an individual to maintain a level of performance", but the issue of fatigue is complex due to the various physiological and psychological phenomena which contribute to it (De Luca 1983). During physical activities, fatigue is largely associated with muscle fatigue, measured as a loss of muscle performance during repeated or continuous activation (Chalder et al. 1993; Helbostad et al. 2007). Muscle fatigue induces discomfort and pain, and in the long term, is believed to contribute to WMSDs (Armstrong et al. 1993; Chaffin et al. 2006). As a result, for risk reduction associated with muscle fatigue, it may be necessary for managers to adjust work design by providing appropriate rest breaks or reducing workloads (Gerard et al. 2002).

While performing physical tasks, it is hard to maintain muscular strength (i.e., maximum force-producing capacity) because sustained force exertions without sufficient recovery generate muscle fatigue that causes the decline in muscle power output (Chaffin et al. 2006). Figure 5.1 adapted from McGill (1997) illustrates the relationship between force exertions (i.e., physical demands) and reduction in muscular strength (i.e., muscle fatigue). To perform a physical task (e.g., lifting heavy objects), one needs to exert forces on muscles. The required forces should be less than a worker's physical capacity (i.e., muscular strength). However, as one performs the task repeatedly over time, muscles become fatigued, resulting in the reduction of muscle strength due to accumulation of fatigue substances on muscle fibers (dashed line in Figure 5.1). If appropriate recovery time (e.g., rest time) is not provided, the forces required to perform the task become higher than the decreased muscle strength at some point. This is called 'fatigue failure' (McGill 1997), and the time to fatigue failure refers to the endurance time (Chaffin et al. 2006).

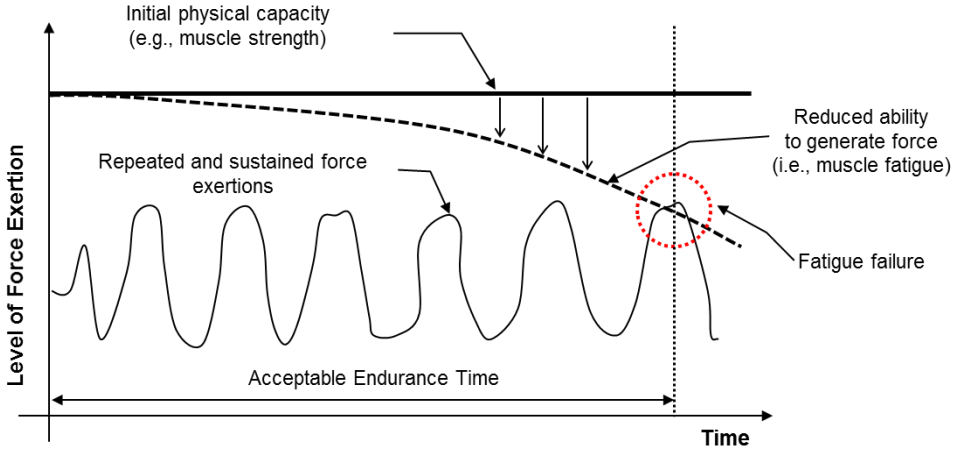

Figure 5.1: Relationship between Physical Demands and Muscle Fatigue

Fatigue failure indicates that forceful exertions beyond one's muscle capacity can result in significant detrimental effects on both workers' health and work performance (e.g., productivity). Repeated over-exertion beyond one's muscular capacity may cause mechanical degradation of the tissues such as muscle damage (i.e., acute injuries). In the long term, muscle fatigue without sufficient recovery reduces the tissues' stress-bearing capacity as a result of an outcome of cellular changes, and thus may result in chronic conditions such as WMSDs (Kumar 2001). In addition, work performance (e.g., productivity) may also be affected by muscle fatigue, which can then cause a decrease in Margin of Manoeuver (MM) (Durand et al. 2009). MM is an ergonomic concept that is defined as the possibility or freedom a worker has to develop different ways of working in order to meet production targets, without having adverse effects on his or her health (Durand et al. 2009). The level of MM can be determined by working conditions (e.g., production or quality target, work flexibility) and personal parameters (e.g., the person's physical capacity). Reduction of workers' capacity due to excessive physical demands (i.e., muscle fatigue) would decrease the MM at work, which, in turn, may jeopardize the balance between attaining production targets and preserving workers' health conditions (Durand et al., 2011). Accordingly, when workers recognize muscle fatigue (physical demands beyond muscular capacity), workers will apply appropriate work adjustment strategies (i.e., taking voluntary pauses or slowing down work pace) to cope with manifestation of muscular fatigue, which results in delay of work by sacrificing production targets.

Unlike machine-paced work such as manufacturing, construction tasks are self-paced, allowing workers a degree of autonomy in determining their optimal work pace or rest strategy (Xiang et al. 2014). As a result, a conflict between attaining production targets and preserving workers' health frequently occurs during construction operations as workers continuously try to adjust their work activity to match variations in their personal (e.g., fatigue, pain) and working conditions (e.g., available work time, MM) (Durand et al. 2009). Determining optimal operational designs to minimize this conflict is of importance for achieving performance goals, and thus requires comprehensive understanding of the effect of excessive physical demands (i.e., muscle fatigue) on planned construction operations not only to prevent health issues, but also to minimize unexpected productivity loss.

5.3 PREVIOUS RESEARCH EFFORTS ON ASSESSING PHYSICAL DEMANDS AND MUSCLE FATIGUE

There have been several research efforts to measure physical demands and muscle fatigue during occupational tasks. Direct measurements during performing tasks or subjective evaluations after performing tasks are commonly used to quantify workers' physical demands from work and the degree of muscle fatigue (Vøllestad 1997; Abdelhamid and Everett 2002; Mitropoulos and Memarian 2012). However, estimating physical demands and muscle fatigue prior to work is challenging because there are no observable operations involved yet prior to work (Perez et al. 2014). In this section, a review on simulation- or model-based approaches to estimate physical demands and muscle fatigue prior to work will be presented.

5.3.1 Methods to Assess Physical Demands Prior to Work

To estimate and evaluate physical demands prior to work, laboratory-based or virtual task simulation has been commonly used in ergonomic studies (Badler et al. 1993; Chaffin 2005; Reed et al. 2006; Nussbaum et al. 2009; Salvendy 2012). Laboratory-based simulation aims to evaluate ergonomic risks of occupational tasks at the stages of planning, scheduling and designing, performing simulated tasks by subjects at the laboratory (Stanton 2006; Nussbaum et al. 2009; Salvendy 2012). While simulating the task, a set of measures (e.g., anthropometric, kinematic, kinetic and electromyography etc.) are collected to estimate physical demands and corresponding

ergonomic risks using physiological or biomechanical ergonomic assessment methods (Nussbaum et al. 2009). Recently, virtual visualization and simulation using Digital Human Modeling (DHM) have provided proactive solutions for workplace ergonomic considerations, such as the ergonomic analysis of human posture and workplace design (Shaikh et al. 2004). This approach creates an avatar (i.e., virtual human), and inserts it into 3D graphic renderings of workplaces, enabling a designer or engineer to investigate different design options of a product or a workplace in the early stages of the design (Reed et al. 2006; Chang and Wang 2007; Demirel and Duffy 2007). However, because developing laboratory-based or virtual simulations is time-consuming, these approaches focus on specific tasks with higher ergonomic risks at the workstation level that are feasible for experimental settings (Czaja and Sharit 2003; Chaffin 2005).

To understand physical demands at the system level in the early design phase, previous research efforts have used DES from an ergonomic perspective (Keller 2002; Neumann and Kazmierczak 2005; Kazmierczak et al. 2007; Neumann and Medbo 2009; Perez et al. 2014). DES has been recognized as a useful technique for analyzing operational design alternatives or optimizing resources with many applications in diverse industries including construction (Martinez and Ioannou 1999; AbouRizk 2010). DES is the representation of a system (e.g., sequence and times of the process) in which the state of resources (e.g., materials, equipment and workers) change at discrete points in time (Banks et al. 2005). Generally, the state of labor resources is modeled as a queuing system to determine the availability of resources, and occupied or waiting times for events as DES focuses on the optimization of resources or cost evaluation (Fishman 2013). However, combined with ergonomic methods to measure physical demands (e.g., subjective rating, biomechanical analysis), DES enables us to analyze cumulative physical demands from the planned operations. For example, Keller (2002) estimated cumulative workloads by determining the workload of each task through subjective rating by experts, and then adding up the workloads according to task scenarios from DES. Neumann and Kazmierczak (2005) suggested DES combined with biomechanical analysis that estimates musculoskeletal loads on a back and shoulders based on representative postures. Cumulative loads can be calculated by multiplying each task's load by its duration and summing up cumulative loads for tasks based on simulation results of DES (Neumann and Kazmierczak 2005). This approach, which has been applied and tested for manufacturing assembly systems, demonstrates great potential for the assessment of physical demands of alternative system configurations during a design phase (Kazmierczak et al.

2007; Neumann and Medbo 2009; Perez et al. 2014). Once cumulative physical demands from the planned operation are estimated, an analyst needs to determine whether the demands are excessive or not. This judgement generally relies on expert judgement (Keller 2002) or qualitative comparison of physical demands from diverse operational options (Kazmierczak et al. 2007). However, for objective evaluation, specific criteria are needed to determine if there could be potential health or performance issues due to excessive physical demands from the operations.

5.3.2 Methods to Estimate Muscle Fatigue Prior to Work

As muscle fatigue is developed gradually in sustained force exertions and is associated with an ability to continue the task (Enoka and Duchateau 2008), it has been used as a measure of cumulative workload (Village et al. 2005). Muscle fatigue has been studied using a wide variety of models, protocols and assessment methods (Vøllestad 1997). Electromyography is most often used to assess the level of muscle fatigue during or after task performance (Sommerich et al. 1993). In case of fatigue measurement prior to work, however, model-based measurement has been widely used (Vøllestad 1997; Perez et al. 2014). Most of exiting muscle fatigue models is based on the quantitative relationships between static (i.e., constant) workloads and Maximum Endurance Time (MET) (e.g., time to fatigue) that are empirically derived from laboratory experiments (Hagberg 1981; Sato et al. 1984; Manenica 1986; Rohmert et al. 1986; Rose et al. 1992; Rose et al. 2000). However, due to the assumption of constant force exertions to estimate MET, these models are not suitable for evaluating fatigue during construction tasks that involve time-varying force exertions and irregular pauses (e.g., short breaks). To address this issue, dynamic fatigue models have been introduced to estimate the level of fatigue as a function of varying force exertions over time. For example, Liu et al. (2002) proposed a set of dynamic equations to describe the effect of muscle fatigue and recovery as a function of the number of Motor Units (MUs) being activated by the voluntary drive. Despite the ability to reflect varying voluntary efforts (i.e., force exertions), the application of this model is limited to theoretical studies on muscle physiology, neural control mechanisms, and clinical applications because it is difficult to specify the number of motor units during specific occupational tasks. Based on Liu et al. (2000)'s approach, Xia and Frey Law (2008) developed a mathematical muscle fatigue model that can predict muscle fatigue for complex tasks with varying intensities. This approach, however, has to specify diverse model parameters (e.g., the number of MUs to exert a certain level of forces,

muscle compositions of body segments etc.) and inputs (e.g., angular velocity and joint angles for performing a task), and thus it is too complex to be used for occupational tasks. Compared with these models (Liu et al. 2000; Xia and Frey Law 2008), the dynamic fatigue model proposed by Ma et al. (2009) is more suitable for evaluating muscle fatigue during occupational tasks due to its applicability to any types of force exertions (e.g., both static and dynamic exertions) on specific body parts (e.g., upper limbs, back or lower limbs) and simplicity of input data (i.e., muscle force). By defining muscle fatigue as a reduction of the maximum exertable force capacity of muscle, this model estimates the reduced capacity of muscle based on muscle force history on specific body parts (i.e., accumulated physical demands), and thus can detect fatigue failure described in Figure 5.1. However, this model does not take into account fatigue recovery, which makes it difficult to be used to understand fatigue resulting from construction tasks. There is a significant amount of irregular pauses and short breaks in construction tasks, which can account for up to 31% of the total working time (Serpell et al. 1995).

For the use of fatigue models prior to work, estimation of physical demands from the planned operation is required. As described earlier, DES combined with biomechanical analysis can be a promising tool for estimating cumulative physical demands on specific body parts during the whole operation, and thus can provide input for fatigue models to investigate the level of muscle fatigue during the planned operation. For example, Perez et al. (2014) proposed combination of DES, biomechanical analysis and static fatigue models to estimate physical demands and then to calculate corresponding 'fatigue rate' that refers to the relative degree of muscle fatigue levels for manufacturing assembly tasks. However, as this approach focused on detection of potential ergonomic risks due to muscle fatigue from diverse operational scenarios, it can't capture the interaction between production system design and muscle fatigue. As described earlier, manifestation of muscle fatigue during work can result in delay of work to be recovered from fatigue that may affect the work performance of workers. Modeling of this interaction is not reflected in Perez et al. (2014)'s work, which makes it difficult to understand how excessive physical demands would affect operation performance, and how to optimize operational designs to achieve production targets without sacrificing workers' health. In addition, this approach estimated muscle fatigue under static conditions where the level of force exertions during each activity is constant, which may not be suitable for construction activities involving dynamic force exertions.

5.4 METHOS

This study proposes a simulation-based framework for systematically assessing muscle fatigue and its impact on construction operations. This framework is intended to depict the relationship between cumulative physical demands and corresponding muscle fatigue as shown in Figure 5.1, aiming to detect fatigue failures that result from excessive demands during the planned operation. One of the novel features of this framework is that the impact of excessive physical demands on construction operations can be simulated by modeling workers' behaviors to cope with muscle fatigue such as voluntary rests. In addition, both fatigue generation and recovery processes are reflected in this framework, capturing the dynamics of muscle fatigue in construction that involves time-varying force exertions and irregular idling. Figure 5.2 shows the overview of the proposed framework which integrates DES, biomechanical and fatigue models to represent interactions between human aspects (i.e., muscle fatigue) and construction operations prior to work.

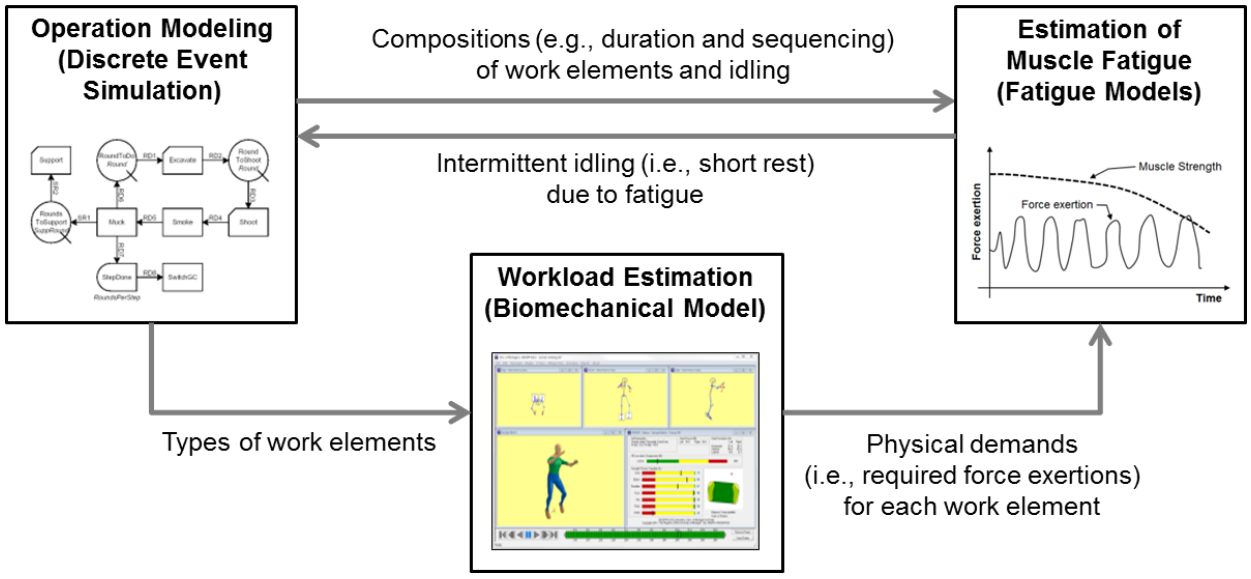

Figure 5.2: Overview of Proposed Framework

5.4.1 Modeling of Construction Operations Using DES

The first step of the framework needs to model the construction operation in DES. Different types of simulation modeling approaches have been used to understand the real system, and these

include but not limited to DES, System Dynamics (SD), and Agent-Based Modeling (ABM). Among them, DES is the most widely used modeling approach due to its process-centric approach that enables the quantitative analysis of operations and processes (Martinez 2009; Zankoul et al. 2015). By using DES as a simulation platform for modeling construction operations and workers' behaviors, the proposed framework helps to quantify the effect of fatigue on construction performance. However, one of the limitations of DES is that entities' behaviors at the individual level are pre-determined while workers' behaviors should be dynamically determined by the current fatigue level in this framework. To address this issue, workers' physical demands and corresponding level of fatigue are externally modeled using biomechanical and fatigue models. Then, the strategy to mitigate muscle fatigue (i.e., tacking a rest to be recovered from fatigue) is combined into the DES by holding workers in queues such as idling when workers are in fatiguing conditions. These will be described in more detail in the following sections.

The basic modeling element of the DES model is a 'work element'. Construction operations are defined by collections of work tasks that can be further divided into work elements (Halpin 1992). For example, one of the examples of physically demanding construction operations, masonry work consists of several work tasks such as scaffolding, material preparation, and brick (or block) laying. The task, brick (or block) laying can be decomposed in to work elements (i.e., basic tasks) such as lifting drywalls or placing bricks (or blocks) (Everett and Slocum 1994). As each work element generally involves different levels of physical demands, modeling the operation at the work element level is helpful to capture dynamic changes of physical demands through biomechanical analysis in the next step.

To determine model behaviors, the work elements' attributes such as the duration or priority of a work element and the amount of resource that flows from one element to another should be further defined based on prior knowledge on the operation. Especially, the durations of defined work elements can be empirically determined through time-motion studies on existing operations (e.g. direct and continuous observation of construction operations) (AbouRizk and Halpin 1992). By simulating the DES model, the states of workers (e.g., types of work elements including idling the workers are involved at specific moments) throughout the operation can be predicted.

5.4.2 Estimation of Workloads of Given Operations through Biomechanical Analysis

Once a DES model for the operation is developed, physical demands from each work element are estimated using a biomechanical model. Biomechanical modeling and analysis aims to estimate musculoskeletal stresses (e.g., muscle forces) required to perform a task as a function of postures, external loads and anthropometric data (Chaffin et al. 2006). It provides an effective means to understand physical demands on the musculoskeletal system of human body during construction tasks (Seo et al. 2014).

This study applied 3DSSPP^{TM} that is a computerized biomechanical analysis tool to estimate physical demands from each work element (Chaffin et al. 2006). Using 3DSSPP^{TM}, physical demands from work (i.e., required forces to perform tasks) can be estimated as a percentage of Maximum Voluntary Contraction (%MVC: level of muscle forces compared to an individual's maximum muscle strength) that can be a direct input for the dynamic fatigue models. As muscle forces to be exerted on a group of muscles vary depending on postures, a collection of representative working postures is required to obtain reliable %MVC for specific work elements. Laboratory-based simulations of tasks and motion measurement using motion capture devices (e.g., marker-based or Inertial Measurement Unit (IMU)-based) can be used to collect data of working postures during occupational tasks. Physical demands from each work element are then added up according to the states of workers (i.e., working or idling) obtained from the DES, generating physical demands during the entire operation over time.

5.4.3 Estimation of Muscle Fatigue Using Dynamic Fatigue Models

Dynamic fatigue models aim to estimate muscle fatigue at a group of muscle level at specific body parts (e.g., shoulders, knees or a back) as a function of estimated physical demands from the previous step. The dynamic fatigue models consist of a fatigue generation model to estimate the reduction of muscle strength due to continuous physical demands (e.g., %MVC) and a fatigue recovery model to predict how much muscle fatigue (i.e., reduced muscle strength) can be recovered during non-working time (e.g., rest or idle time).

The mathematical model developed by Ma et al. (2009) is used for the fatigue generation model in this study (See Eq. (1)). The model is based on the motor unit activation pattern on muscles of which force and movement are produced by contraction of muscle fibers, representing

the process of fatigue generation in mathematics. This model was validated with 24 existing static models that estimate METs under isometric exertions by comparing the calculated METs, and qualitatively or quantitatively validated with three existing dynamic models by comparing specific model parameters (Ma et al. 2009). Eq. (1) can be explained as follows:

$$\frac{F_{cem}(t)}{MVC} = e^{\int_0^t -\frac{F_{load}(u)}{MVC} du} \quad (1)$$

- MVC : Maximum voluntary contraction (maximum capacity of muscle)
- $F_{cem}(t)$: Current exertable maximum force (current muscle strength)
- $F_{load}(t)$: Forces required for the task (e.g., workloads)
- t: current time (seconds)

$F_{cem}(t)$ describes the capacity of the muscle group (i.e., current muscle strength) while $F_{load}(t)$ means the forces which the muscle needs to produce to perform tasks at a time instant t. By dividing $F_{cem}(t)$ and $F_{load}(t)$ by MVC that is a measure of force that can be exerted maximally by one's muscle group, both the current muscle strength and physical demands can be expressed proportional to one's MVC (%MVC), reflecting individual's difference in muscle strength. As a result, the equation indicates that the current capacity of muscle strength can be determined by the negative exponential function of cumulative physical demands from work.

However, one of the critical limitations of this model is that this model does not reflect the recovery from fatigue during non-working time (e.g., rest or idle time), which is essential to measure the impact of fatigue on work performance. To address this issue, a recovery model based on the physiological recovery rate on muscle groups is proposed as shown in Eq. (2). Empirical studies on recovery from muscle fatigue found that reduced muscle strength after fatiguing exertions can be recovered quickly in 5-10 minutes up to about 90%MVC while more than 30 minutes are additionally required to be fully recovered (Lind 1959; Mills 1982; Kuorinka 1988; Bogdanis et al. 1995; Fulco et al. 1999; Shin and Kim 2007). This is due an exponential relationship between recovery time and levels of fatigue recovered (Lin et al. 2009). Especially,

Mills (1982)'s experiments on the recovery time for the hand and forearm showed it took about 10 minutes to be recovered from 40%MVC to 90%MVC. Based on this study (50%MVC recovery in 10 minutes), this study assumed 5% of average recovery rate per one minute for the recovery of up to 90%MVC. In addition, as 30 minutes are additionally required to be fully recovered from 90%MVC (10%MVC recovery in 30 minutes), this study assumed 0.3% of recovery rate for the recovery from 90%MVC to 100%MVC. As a result, the proposed fatigue recovery model reflects the exponential behavior of fatigue recovery that show a fast recovery rate at the beginning of recovery and a relatively slow recovery rate at the end of recovery.

$$F_{cem}(t_b) = (1 + recovery\ rate \times\ (b - a))\ F_{cem}(t_a) \qquad (2)$$

- $F_{cem}(t_a)$: Current exertable maximum force at start time a of non-working time
- $F_{load}(t_b)$: Current exertable maximum force at finish time b of non-working time

As a result, the fatigue models quantify the current muscle strength as a function of time-varying values of physical demands. By comparing the current muscle strength with the physical demands from the operation, fatigue failure (i.e., physical demands beyond the current muscle strength) can be detected.

5.4.4 Modelling of Interactions between Muscle Fatigue and Operations

Once fatigue failure is detected, workers may want to adjust work to mitigate muscle fatigue. For example, they may want to slow down work pace or change postures to reduce muscle forces exerted at fatiguing body parts. However, these strategies still expose workers to the certain level of physical demands, and changing postures may lead to even higher risk of injury due to reduced postural stability (Kumar 2001). This research adapted voluntary rests as a fatigue mitigation strategy by workers to be recovered from muscle fatigue. Specifically, when fatigue failure occurs, these voluntary rests are added in the DES model by hindering the onset of the following work element, and thus making workers stay at the queue. This model behavior results in the delay of work, increasing both total duration and cost. As a result, this framework can evaluate the impact

of muscle fatigue on time and cost performance due to excessive physical demands during the planned construction operation.

The duration of voluntary rests that workers would take could vary depending on their level of muscle fatigue. Bonen and Belcastro (1975) found that subjects would choose optimal recovery time that allows them to be recovered from fatigue at the fastest rate when they can determine the duration of rests during intensive exercise. Seiler and Hetlelid (2005) also found that self-selected recovery duration is subjectively determined to maintain expected performance level during interval training. Based on these findings, it was assumed that the duration of voluntary rests are determined by the gap between the current level of muscle strength after finishing the preceding work element and the desired level of muscle strength by workers. For example, as a worker can perceive the level of muscle fatigue, he or she may want to take a rest until the muscle strength is recovered sufficiently enough to exert forces for the next task (at least 10%MVC higher than the following physical demand).

5.5 CASE STUDY ON MASONRY WORK

The proposed framework is applied to a case study to demonstrate the usefulness of evaluating muscle fatigue and its impact on construction operations. The operation for the case study is masonry work for building a three-story research complex, located at the north campus of the University of Michigan. Site conditions obtained from this project served as basic conditions for developing a DES model for masonry work. As shown in Figure 5.3, the masonry work was to build a concrete block wall with 7 courses and 24 concrete blocks (6 inches (width) × 8 inches (height) × 16 inches (length)) per course. A crew for this operation consisted of three masons and one laborer. The masons took a major role in masonry work such as cutting and laying blocks, or installing rebar if needed while the laborer performed supportive tasks, mainly material handling tasks (e.g., preparation and distribution of material (e.g., block, mortar)). Total work duration for building the concrete block wall was about 54 minutes including about 4 minutes of idle time (e.g., chatting with co-workers).

This case study focused on evaluation of muscle fatigue on upper limbs, especially shoulders that are one of the most demanding body parts during masonry work that involve frequent heavy

lifting tasks. In construction workers, low back and shoulder pain are the most frequent self-reported musculoskeletal disorders (Faber et al. 2009). Especially, Yates et al. (1980) found that upper body strength could be the most limiting factor in lifting task instead of back strength during lifting tasks.

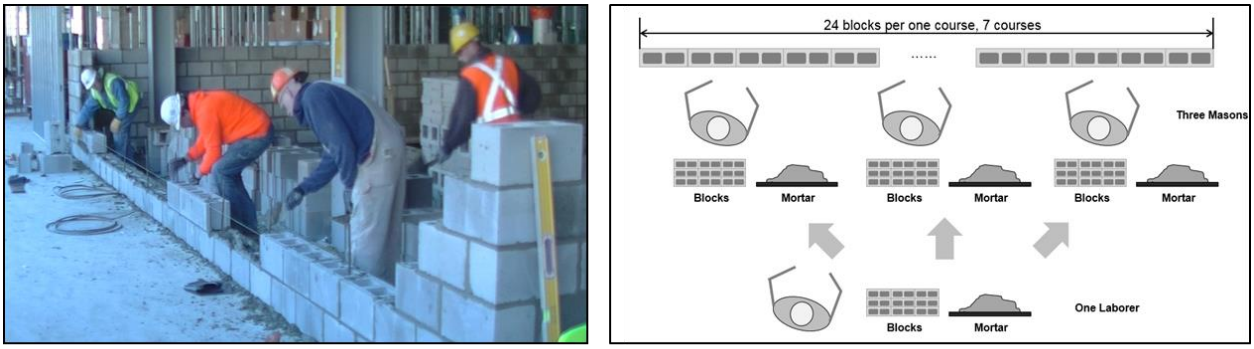

A. Site Photo B. Site Layout

Figure 5.3: Site Conditions

The case study examines how different operational plans affect workers' muscle fatigue on shoulders, and in turn, time and cost performance of the masonry work. First, by changing crew composition (i.e., the number of masons and laborers), the optimized resource plan (i.e., crew composition) was selected to minimize time and cost without consideration of muscle fatigue as the typical DES analysis does. Then, the operation was simulated using the crew composition that is optimized only for time and cost by considering fatigue effects on the operation simulation. Through comparison between simulation results without and with consideration of muscle fatigue, potential conflicts between achieving performance targets and preserving workers' health are described. Specifically, this study focuses on muscle fatigue on shoulders because shoulder pain is one of the frequently reported musculoskeletal disorders by masonry workers due to heavy lifting, working above shoulder level and repetitive movements (Goldsheyder et al. 2004; Faber et al. 2009).

5.5.1 DES Model Development

To develop a DES model for this masonry work, tasks by masons and laborers are divided into work elements based on observations as shown in Table 5.1. While masons perform the work elements, M1, M2 and M6 once for each course, M3 to M5 are repeated for the next blocks to

complete the full course of concrete blocks. Material handling tasks by laborers are to deliver mortar (L1) and concrete blocks (L2) to masons. It was assumed that there are enough materials prepared, and thus the laborers just deliver materials to masons who have the least amount of material first not to make them idle due to lack of materials during this operation. The duration of each work element was determined based on time-motion analysis of the observed operation.

Table 5.1: Work Elements and Durations for Masonry Work

Crew	Work Elements	Durations (seconds)
Mason	M1. Setting up (e.g., setting a string for reference)	40.0
	M2. Spreading two parallel lines of mortar using a trowel	92.0
	M3. Lifting and laying a concrete block onto the mortar lines	4.6
	M4. Tapping the top of the block to level it & collecting the excessive mortar mix that squeezes out from under the block	19.3
	M5. Spreading mortar at the side of the block just laid on	6.0
	M6. Rechecking each block for level and alignment when the course has been completed.	47.0
Laborer	L1. Delivering mortar	10.0
	L2. Delivering concrete blocks	10.0

Based on these assumptions and descriptions on the masonry work operation, a DES model for this masonry work operation was constructed in STROBOSCOPE (State and Resource Based Simulation of Construction Processes) (Martinez 1996) as shown in Figure 5.4. STROBOSCOPE is a programmable and extensible simulation system designed for modeling complex construction operations in detail and for the development of special-purpose simulation tools (Martinez and Ioannou 1999). Work elements by masons and laborers are modeled independently, but resources such as concrete blocks and mortar are shared by both masons for resource consumption and laborers for resource production. The total simulation time to build the wall with the same crew composition (i.e., three masons and one laborer) of this case operation was 48 minutes while the actual duration was 54 minutes from the field observation. However, about 4 minutes of idle time such as chatting with co-workers that was not associated with the operation were found from the observation, which was not considered in the model. If this idling is excluded, the model performed well to represent this masonry work, showing 4% of the difference in working time (48 minutes vs. 50 minutes). Though it is only one instance, it can be a good reality check of the developed DES model.

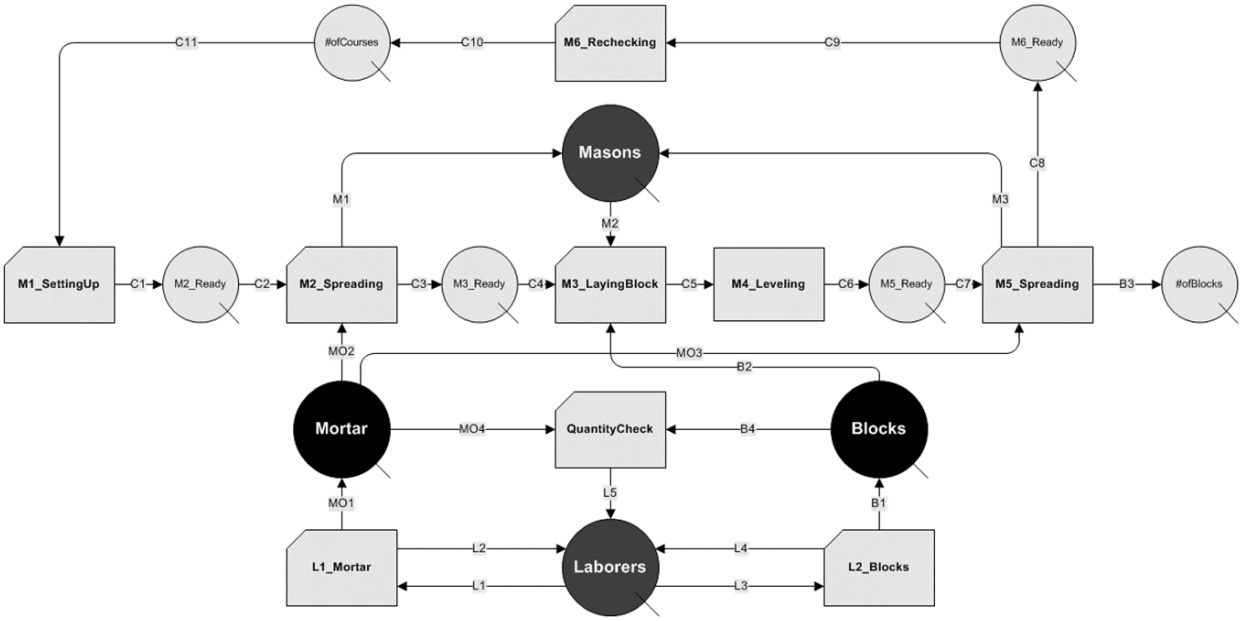

Figure 5.4: DES Model for Masonry Work

To identify the optimal design for this operation without considering the effect of muscle fatigue, the model was simulated by varying crew compositions. Table 5.2 shows time and cost performance (e.g., total duration, labor productivity and cost rate) by varying the numbers of masons and laborers. The results imply that adding an additional laborer would not reduce total duration in this operation as work progress is determined by masons, and material supply by one laborer is sufficient not to delay the work progress by masons. As a result, a crew with two masons and one laborer is recommended for this operation because this crew shows the highest productivity and the lowest cost rate (hourly labor costs for masons and laborers are obtained from RS Means (2015)). However, if the objective is to choose the fastest completion, a crew with three masons and one laborer can be chosen.

Table 5.2: Simulation Results According to Different Crew Compositions

Crew Combination		Simulation Results		
# of masons	# of laborer	Total duration (hr)	Labor productivity (blocks/hr/person)	Cost rate (labor cost) ($/block)
1	1	1.74	48.2	0.81
2	1	1.05	53.6	0.75
3	1	0.81	51.7	0.80
1	2	1.74	32.1	1.17
2	2	1.05	40.2	0.97
3	2	0.81	41.3	0.96

5.5.2 Biomechanical Analyses on Work Elements

Biomechanical analyses were performed to estimate physical demands on shoulders from each work element using in 3DSSPP^{TM}. To collect working postures required to perform biomechanical analyses on work elements, laboratory experiments were conducted in a controlled environment. Five experienced masons were recruited to examine postural variations of their working techniques, and were asked to perform laying block tasks with a comfortable pace. Masons' motions were collected using an Inertial Measurement Unit (IMU)-based motion capture system. Working techniques for each work element were similar except lifting technique. In some cases, masons lifted and laid a concrete block with one hand while they typically used both hands. This study assumed two-hand lifting as a representative lifting technique because it is recommended to reduce ergonomic risks during lifting tasks (Cheung et al. 2007). Hand loads were estimated based on what types of objects (e.g., blocks, mortar, a trowel and a shovel) workers were handling.

Table 5.3 shows average physical demands on shoulders as %MVC to perform work elements from biomechanical analyses based on collected motion data and estimated hand loads. To compute %MVC, this study assumed 50th percentile of workers for anthropometry (e.g., height and weight) and muscle strength. For example, for laying a concrete block (M3) that is the most physically demanding work element performed by masons, a mason has to exert muscle forces on shoulders up to 35% of one's maximum muscle strength. The other work elements required force exertions less than 10%MVC. Work elements by laborers are more physically demands than the ones by masons because delivering mortar (L1) and concrete blocks (L2) involve heavy material lifting, showing 35%MVC and 40%MVC, respectively. Based on the physical demands for each

work element from biomechanical analyses and duration and sequencing of work elements from DES, total physical demands by both masons and laborers during this operation were obtained.

Table 5.3: Average Physical Demands (%MVC) from Work Elements

Work Elements		Physical Demands (%MVC)
Masons	M1	5%
	M2	10%
	M3	35%
	M4	5%
	M5	10%
	M6	10%
Laborers	L1	35%
	L2	40%

5.5.3 Evaluation of Muscle Fatigue for Different Crew Compositions

To examine how muscle fatigue due to excessive physical demands affects the operation of masonry work, the level of muscle fatigue by workers (i.e., a mason and a laborer) was evaluated for different crew compositions using the proposed dynamic fatigue models. Figure 5.5 shows physical demands and corresponding muscle fatigue for a mason and a laborer according to different crew compositions when voluntary rests to be recovered from fatigue are not considered. The red line indicates 'current exertable maximum forces (%MVC)' that refers current muscle strength while the blue line means 'forces required for the tasks (%MVC)' that refers physical demands from the operation. Based on the previous simulation results from the DES model that did not take into account muscle fatigue impact (e.g., Table 5.2), it was found that the crew with two masons and one laborer or with three masons and one laborer was recommended to achieve the best performance in terms of time or cost. However, when muscle fatigue is taken into consideration, the laborer could experience 'fatigue failure' in both crew compositions due to excessive physical demands from work elements (e.g., delivering mortar and concrete blocks) while the masons would not become fatigued before finishing the operation. As mentioned above,

‘forces required for the tasks (%MVC)’ beyond ‘current exertable maximum forces (%MVC)’ indicates fatigue failure that may result in health issues such as WMSDs.

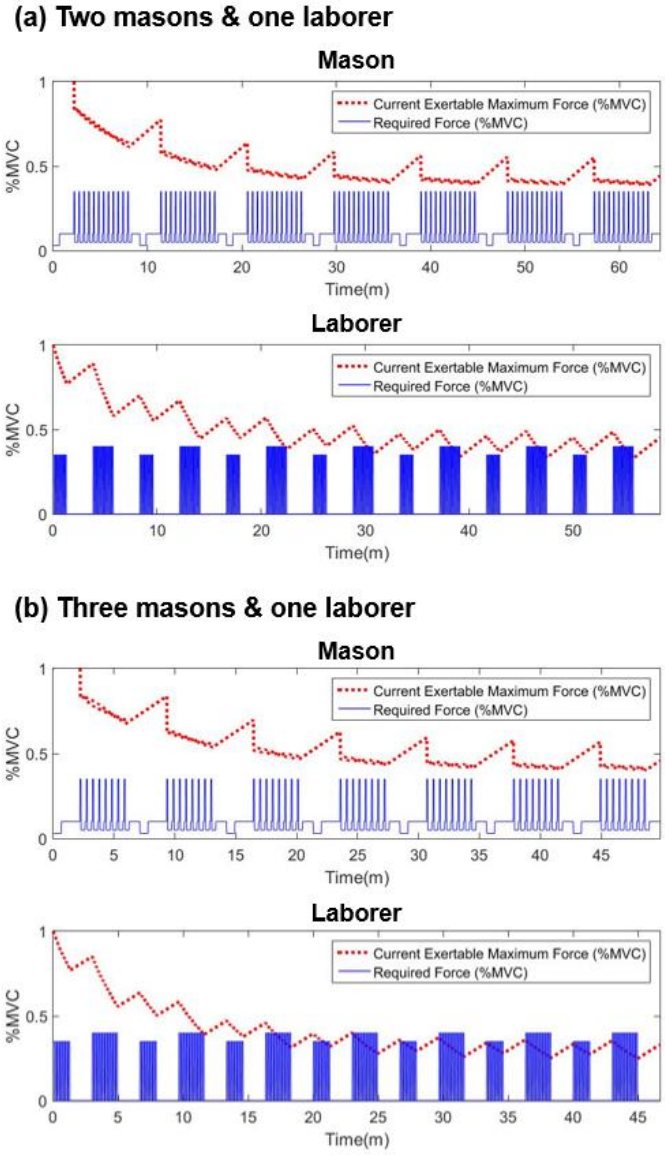

Figure 5.5: Fatigue Evaluation for Masonry Work with Different Crew Compositions

Figure 5.6 shows how muscle fatigue can affect work performance during masonry work with a crew composition of three masons and one laborer. As described above, the laborer could experience fatigue failures due to excessive physical demands at the beginning of the operation (about 11.6 minutes) (Figure 5.6A). Whenever fatigue failures occur, the laborer may want to take voluntary rests to be recovered from muscle fatigue, which can decrease work performance of the

operation (Figure 5.6B). Unexpected idling due to the laborer's muscle fatigue results in the increase of total duration from 48 minutes to 54 minutes because the masons also have to wait until materials are provided by the laborer. As a result, due to the impact of muscle fatigue by the laborer, work progress can be delayed about 12.5%, resulting in reduction of labor productivity (9.7%) and increase of cost rate (10%).

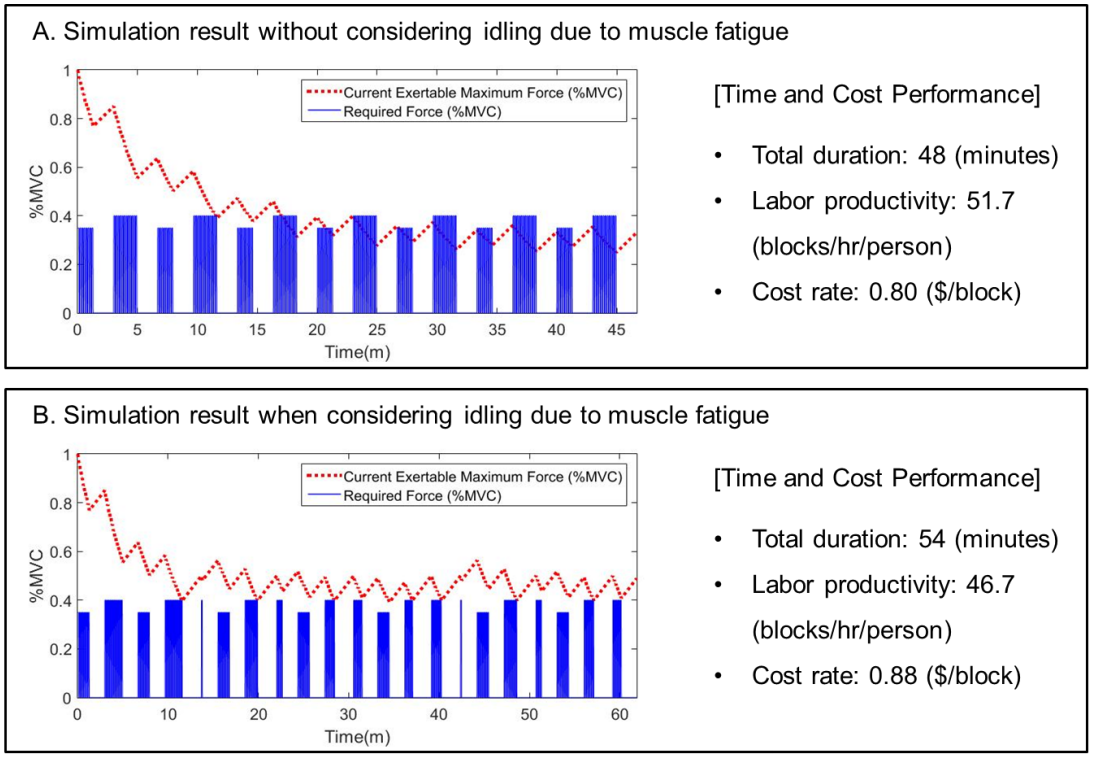

Figure 5.6: Impact of Muscle Fatigue on Work Performance (Crew Composition: Three Masons and One Laborer)

5.6 DISCUSSION

The case study on masonry work demonstrates how the proposed framework can be applied to actual construction operations. As found in the case study, excessive physical demands beyond one' physical capacity may result in both health and performance issues even during a short-term operation (i.e., less than an hour). However, masons and laborers are generally exposed to more workloads than the ones handled in the case study (i.e., 56 blocks per mason) during a whole day

(a typical production rate per mason is 150 blocks per day (RS Means 2015)). Thus, more severe adversary effects on performance and ergonomic risk caused by excessive physical demands are expected when the analysis is expended to a longer operation (e.g., days and weeks).

As this study primarily focuses on the methodological development and demonstration of the proposed framework, testing the accuracy of the fatigue recovery equation (Eq. (2)) and its impact on time and cost performance is beyond the scope of the research. This framework goes beyond Neumann and Kazmierczak (2005)'s or Perez et al. (2014)'s approaches from a methodological perspective, enabling us to estimate varying physical demands and corresponding muscle fatigue generation and recovery using comparable measures (i.e., %MVC), and thus to identify potential impact of muscle fatigue on construction operations. This novelty of the proposed framework is of importance for construction tasks involving different levels of physical demands (e.g., work intensity and duration) and irregular rest/pause.

Evaluation of muscle fatigue in early stages of the design of the construction operations is important because it can provide a great opportunity to mitigate occupational health risks such as WMSDs (Nussbaum et al. 2009). When the planned construction operation is expected to have fatigue failures, a manager may want to redesign work places and tasks. Considering limited resources for redesigning, it is important to set a priority of work elements to be redesigned. Estimating physical demands (%MVC multiplied by duration) from work elements using the proposed framework can provide criteria to determine the target work element for intervention. In the case study on masonry work, it was found that delivering concrete blocks by laborers is the most physically demand work element. In terms of design of workplaces, reducing the distance between a pile of concrete blocks and the wall, if site conditions allow, can reduce the duration for material delivering, contributing to decrease physical demands. In addition, providing appropriate guideline or training on working techniques can also help workers minimize physical demands from work. For example, asymmetric load carrying such as one-hand carrying may have a greater injury potential compared to symmetric carrying techniques, especially when transporting loads of 20% of bodyweight or more (Devita et al. 1991). Laborers who carry heavy materials such as mortar and concrete blocks are recommended to distribute hand loads symmetrically or to carry them interchangeably on the left and right arms (Drury et al. 1989; Devita et al. 1991). As described

above, understanding of potential ergonomic issues due to muscle fatigue from the planned construction operations helps to develop ideas for effective ergonomic interventions prior to work.

The proposed framework can also serve as a tool for optimization of construction operations considering workers' physical capacity. DES has been a useful technique for construction operation modeling to develop better project plans, optimize resource usage, reduce costs and duration, or improve overall project performance in construction (Martinez and Ioannou 1999; AbouRizk 2010). For building accurate models which represent construction operations, modeling of resources and their state is one of the important elements because operations can be sensitive to resource properties (e.g., size, weight and cost) that are allocated to specific activities (Martinez and Ioannou 1999). Resources in construction generally refer to materials, equipment and labor, all of which has a set of constant attributes in DES, for example, an amount of materials required for one cycle of an activity, working capacity of equipment or labor. However, unlike other resources, there is significant variability in human capacities which are affected by physical demands from work (Chaffin et al. 2006). However, consideration of human aspects such as fatigue has been seen as the 'missing link' in discrete event simulation (Baines et al., 2004). As the case study found, selection of optimized operational scenarios in terms of time and cost are not necessarily optimal decision making when considering limited human capacity. Given constraints regarding human aspects, specifically limited physical capacity, the DES that considers reduced physical capacity of workers during construction operations enables managers to experiment with diverse alternatives for resource allocation (e.g., the number of workers and crew compositions) to prevent unexpected performance loss due to excessive physical demands. For example, in the case study above, the operational scenario with the crew of three masons and one laborer may result in unexpected delay of work (e.g., 12.5% of increased total duration) due to muscle fatigue by the laborer, showing the cost rate of 0.88 $/block (Figure 5.6B). To prevent the unexpected delay by the laborer, adding one more laborer (e.g., three masons and two laborers) is recommended, even though the cost rate could be slightly increased up to 0.96 $/block (Figure 5.7). As described in this example, understanding of muscle fatigue and its impact on work performance can support decision making when designing construction operations.

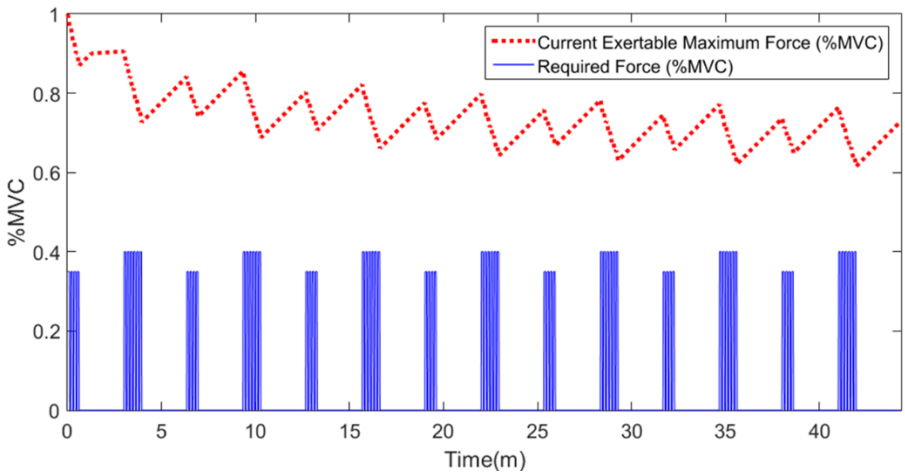

Figure 5.7: Simulation Result When Adding One More Laborer (Three Masons and Two Laborers)]

If an additional resource like one more laborer is not available, the detection of fatigue failures during construction operations can be still useful by pursuing the optimal work-rest schedule that provides appropriate duration of rests in a timely manner (Kopardekar and Mital 1994). In construction, work-rest schedules are generally determined just based on working time without considering variations of physical demands according to types of operations. Using the proposed framework, fatigue failures due to excessive demands can be detected, which provide the right timing of rests for workers. In addition, simulating diverse scenarios of the duration and frequency of rest breaks in the DES model, the optimal work-rest schedule that permits a recovery from muscle fatigue without jeopardizing the work progress can be determined.

The proposed framework aims to understand localized muscle fatigue at specific body parts in the perspective of biomechanical demands (e.g., muscle forces) from work. However, contractile process to exert forces in muscle also requires a lot of energy that refers to metabolic demands (i.e., energy demands) (Sahlin et al. 1998). When the metabolic demands from prolonged physical activities exceed human's capacity to produce energy, workers could experience whole body fatigue that also significantly affects work performance (Walters et al. 1993). Especially, in construction where long work hours are common, accumulative effects of metabolic demands such as energy depletion could be also critical to work performance (Hallowell 2010). Alvanchi et al. (2011) investigated the impact of working hours and overtime on workers' performance on the

basis of human energy consumption, and found that almost 20% of productivity loss could exist depending on the amount of metabolic demands. Further studies are needed to reflect workers' fatigue at the whole body level in the proposed framework.

5.7 CONCLUSIONS

This research introduces a new approach for modeling interactions between human aspects (i.e., muscle fatigue) and construction operations. The proposed framework estimates physical workloads by combining DES and biomechanical analysis, predicts the level of fatigue under estimated workloads using dynamic fatigue models, and then evaluates the impact of muscle fatigue on the planned operation. The case study on masonry work was performed to demonstrate the usefulness of the proposed framework. Specifically, the results from the case study indicate that the optimized operational scenario only for time and cost performances may expose workers excessive physical demands, and thus an unexpected delay of the operation due to workers' muscle fatigue could be observed. This implies that incorporating muscle fatigue into the operational design phase provides systematic understanding of the trade-off between time and cost performances and ergonomic risks. As a result, this approach has great potential as an effective means to design optimized operations considering limited human capacity, as well as to assess potential ergonomic risks due to excessive physical demands.

As this framework is built on validated models (e.g., DES, biomechanical and fatigue models), it is not the scope of this research to validate each step in the framework. However, this framework requires integration of different models that may result in unexpected model behaviors. A validation for fully integrated models will be further needed to identify potential issues due to interacted model behaviors. Even though several limitations and research challenges remain, they do not negate the potential application of this framework. If workers' fatigue due to excessive physical demands from operations could be evaluated in the early design stages, it would open the door to not only more pro-active management of ergonomic aspects in the design of construction operation, but also optimization of construction operations considering workers' physical capacity. Ultimately, the proposed framework provides opportunities to take into account both workers' health and work performance in early design stages.

CHAPTER 6

CONCLUSIONS AND RECOMMENDATIONS

6.1 SUMMARY OF RESEARCH

This research effort started with the following overarching research goals: 1) to enable practitioners to evaluate construction workers' physical demands on sites in a timely manner without technical sophistication or skill; and 2) to enhance our understanding of the impact of excessive physical demands on construction operations. Considering these goals, the research had these four more specific research objectives: 1) to enable an automated initial assessment of postural stresses to compare different jobs or tasks within a job to determine a prioritization of ergonomics efforts; 2) to non-invasively and accurately collect kinematics data required for in-depth analysis of physical demands at construction sites; 3) to test the feasibility of on-site biomechanical analysis using the kinematics data obtained from sites for quantifying musculoskeletal stresses on different body parts; and 4) to develop a means to model interactions between human aspects (i.e., muscle fatigue) and tasks and to evaluate the impact of excessive physical demands on construction operations.

To achieve these research objectives, four inter-related studies were conducted. A summary of these studies' results and implications are as follows.

1. Automated Postural Ergonomic Risk Assessment Using Vision-based Posture Classification: This study proposed vision-based posture classification algorithms using virtual training image datasets and silhouette-based image features. From laboratory tests, it was found that the proposed approach can achieve about 90% of classification accuracy for four representative working postures (e.g., standing, arm-raising, back-bending and knee-bending).

This result supports the potential of virtual training datasets for posture classification from real-world images that have variations in viewpoints and workers' anthropometry. Also, it was found that selection of optimal training images that reflects actual views and workers' anthropometry is an important factor to achieve better performance, which can be addressed by using virtual training images without significant efforts to extensive training images from a real world.

2. Three Dimensional Body Kinematics Measurement Using Vision-based Motion Capture Approaches: This study evaluated the accuracy of motion data from three vision-based motion capture approaches (e.g., RGB-D sensor-based, stereovision camera-based and multiple camera-based approaches) through an experimental study. The results showed that vision-based motion data can measure body kinematics with about 10 degrees of errors in body angles. Based on specification and performance comparison of these approaches, it was concluded that multiple camera- and stereovision camera-based motion capture approaches have great potential as in-field motion data collection methods from a practical perspective. Also, it was found that given inaccuracies in motion data vision-based approaches can be used for diverse in-depth analysis without sacrificing its reliability to better understand workers' physical demands during occupational tasks including construction.

3. Motion Data-Driven Biomechanical Analysis Using Vision-based Motion Capture Approaches: This study tested the feasibility of on-site biomechanical analysis using the vision-based motion data by proposing automated motion data processing. The results from the experiment showed that the proposed approaches for motion data processing were successfully used to perform static and dynamic biomechanical analyses by showing similar results from previous studies. Also, the sensitivity analysis of motion data errors to estimated musculoskeletal loads revealed that the use of vision-based motion data with more than ± 10° of errors would not significantly affect biomechanical analysis results from the practical perspectives because of non-significant variations in load patterns and less-sensitivity of motion errors to the 'Percent Capable' that is an indicator of excessive physical demands.

4. Simulation-based Assessment of Workers' Muscle Fatigue and Its Impact on Construction Operations: This study proposed a simulation-based framework to estimate physical demands and corresponding muscle fatigue from the planned operation, and then evaluate the impact of muscle fatigue on construction operations. The results from the case study on masonry

work indicate that the optimized operational scenario only for time and cost performances may expose workers excessive physical demands, and thus an unexpected delay of the operation due to workers' muscle fatigue could be observed. Specifically, during masonry work, this delay could result in 12.5% of increased total duration. This implies that incorporating muscle fatigue into the operational design phase provides systematic understanding of the trade-off between time and cost performances and ergonomic risks. If workers' fatigue due to excessive physical demands from operations could be evaluated in the early design stages, it would open the door to not only more pro-active management of ergonomic aspects in the design of construction operation, but also optimization of construction operations considering workers' physical capacity.

6.2 FUTURE RESEARCH

While this work has expanded our understanding of construction workers' physical demands and their impact on construction operations, many methodological and technical challenges remain which still warrant further attention in future research efforts. A few such questions follow.

1. Whether vision-based posture classification can be applied to more complex postures involving combinations of different postures according to body parts? Further, is the proposed algorithm robust to environmental noise that exists at actual construction sites?

2. How accurate are vision-based motion capture approaches when they are applied to real-world scenes? How can vision-based motion capture approaches be further refined and improved to obtain more accurate and reliable motion data?

3. Is there a possibility that errors in vision-based motion data may lead to significant bias for estimating musculoskeletal stresses at construction sites? Further, how can practitioners use biomechanical analysis results to improve both productivity and health issues?

4. Are combined models for evaluating the impact of muscle fatigue on construction operations generalized enough to reflect diverse conditions at construction sites? Is muscle fatigue on a specific body part dominant for a worker to decide to take a rest?

BIBLIOGRAPHY

[1] Abdelhamid, T. S., and Everett, J. G. (2002). "Physiological demands during construction work." *Journal of Construction Engineering and Management*, 128(5), 427-437.

[2] AbouRizk, S. (2010). "Role of simulation in construction engineering and management." *Journal of Construction Engineering and Management*, 136(10), 1140-1153.

[3] AbouRizk, S. M., and Halpin, D. W. (1992). "Statistical properties of construction duration data." *Journal of Construction Engineering and Management*, 118(3), 525-544.

[4] Al-Eisawi, K. W., Kerk, C. J., Congleton, J. J., Amendola, A. A., Jenkins, O. C., and Gaines, W. G. (1999). "The effect of handle height and cart load on the initial hand forces in cart pushing and pulling." *Ergonomics*, 42(8), 1099-1113.

[5] Alvanchi, A., Lee, S., and AbouRizk, S. (2011). "Dynamics of working hours in construction." *Journal of Construction Engineering and Management*, 138(1), 66-77.

[6] Aminian, K., and Najafi, B. (2004). "Capturing human motion using body-fixed sensors: outdoor measurement and clinical applications." *Computer Animation and Virtual Worlds*, 15(2), 79-94.

[7] Anderson, F. C., Delp, S., DeMers, M., Guendelman, E., Habib, A., Hamner, S., ... and Sherman, M. (2012). *OpenSim User's Guide*. <https://opensim.stanford.edu>

[8] Ardiny, H., Witwicki, S., and Mondada, F. (2015). "Are autonomous mobile robots able to take over construction? A review." *International Journal of Robotics, Theory and Applications*, 4(3), 10-21.

[9] Armstrong, T. J., Buckle, P., Fine, L. J., Hagberg, M., Jonsson, B., Kilbom, A., ... and Viikari-Juntura, E. R. (1993). "A conceptual model for work-related neck and upper-limb musculoskeletal disorders." *Scandinavian Journal of Work, Environment & Health*, 19(2), 73-84.

[10] Armstrong, T. J., Franzblau, A., Haig, A., Keyserling, W. M., Levine, S., Streilein, K., ... and Werner, R. (2001). "Developing ergonomic solutions for prevention of musculoskeletal disorder disability." *Assistive Technology*, 13(2), 78-87.

[11] Armstrong, T.J., Ashton-Miller, J., Wooley, C., Kemp, J., Young, J., and Kim, H. (2008). *Development of Design Interventions for Preventing Falls from Fixed Ladders*, CPWR Technical Report

[12] Badler, N.I., Phillips, G.B., and Webber, B.L. (1993). *Simulating Humans: Computer Graphics Animation and Control*. Oxford University Press, USA.

[13] Baines, T., Mason, S., Siebers, P.O., and Ladbrook, J. (2004). "Humans: the missing link in manufacturing simulations?" *Simulation Modelling Practice and Theory*, 12(7), 515-526.

[14] Barnich, O., and Van Droogenbroeck, M. (2011). "ViBe: A universal background subtraction algorithm for video sequences." *Image Processing, IEEE Transactions on*, 20(6), 1709-1724.

[15] Bay, H., Tuytelaars, T., and van Gool, L. (2008), "SURF: Speeded up robust features", *Computer Vision and Image Understanding*, 110(3), 346-359.

[16] Bernold, L. E., and AbouRizk, S. M. (2010). *Managing Performance in Construction*. John Wiley & Sons, New Jersey.

[17] Bhattacharya, A., and McGlothlin, J. D. (1996). *Occupational Ergonomics: Theory and Applications (No. 27)*. CRC Press, Boca Raton, Florida

[18] Bogdanis, G. C., Nevill, M. E., Boobis, L. H., Lakomy, H. K., and Nevill, A. M. (1995). "Recovery of power output and muscle metabolites following 30 s of maximal sprint cycling in man." *Journal of Physiology*, 482(2), 467-480.

[19] Bonen, A., and Belcastro, A. N. (1975). "Comparison of self-selected recovery methods on lactic acid removal rates." *Medicine and Science in Sports*, 8(3), 176-178.

[20] Borg, G. A. (1982). "Psychophysical bases of perceived exertion." *Medicine and Science in Sports and Exercise*, 14(5), 377-381.

[21] Boschman, J. S., van der Molen, H. F., Sluiter, J. K., and Frings-Dresen, M. H. (2012). "Musculoskeletal disorders among construction workers: a one-year follow-up study." *BMC musculoskeletal disorders*, 13(1), 196.

[22] Buchholz, B., Paquet, V., Punnett, L., Lee, D., and Moir, S. (1996). "PATH: a work sampling-based approach to ergonomic job analysis for construction and other non-

repetitive work." *Applied Ergonomics*, 27(3), 177-187.

[23] Bureau of Labor Statistics (BLS) (2015a). *National Census of Fatal Occupational Injuries in 2014.* < http://www.bls.gov/news.release/pdf/cfoi.pdf>

[24] Bureau of Labor Statistics (BLS) (2015b). *Nonfatal Occupational Injuries and Illnesses Requiring Days Away from Work, 2014.* <http://www.bls.gov/news.release/pdf/osh2.pdf>

[25] Burt, S., and Punnett, L. (1999). "Evaluation of interrater reliability for posture observations in a field study." *Applied Ergonomics*, 30(2), 121-135.

[26] CDC (Centers for Disease Control and Prevention) (2012). *Anthropometric Reference Data for Children and Adults: United States, 2007–2010* <http://www.cdc.gov/nchs/data/series/sr_11/sr11_252.pdf>

[27] Center for Ergonomics, University of Michigan (2011). *3D Static Strength Prediction Program: User's Manual.* University of Michigan, MI.

[28] Chaffin, D. B. (1973). "Localized muscle fatigue-definition and measurement." *Journal of Occupational and Environmental Medicine,* 15(4), 346-354.

[29] Chaffin, D. B. (1997). "Development of computerized human static strength simulation model for job design." *Human Factors and Ergonomics in Manufacturing*, 7(4), 305-322

[30] Chaffin, D. B. (2005). "Improving digital human modelling for proactive ergonomics in design." *Ergonomics*, 48(5), 478-491.

[31] Chaffin, D. B., and Erig, M. (1991). "Three-dimensional biomechanical static strength prediction model sensitivity to postural and anthropometric inaccuracies." *IIE Transactions*, 23(3), 215-227.

[32] Chaffin, D. B., Andersson, G., and Martin, B. J. (2006). *Occupational Biomechanics (4th edition).* Wiley, New York.

[33] Chalamala, S. R., and ALP, P. K. (2016). "A probabilistic approach for human action recognition using motion trajectories." *7th International Conference on Intelligent Systems, Modelling and Simulation*, Washington, DC.

[34] Chalder, T., Berelowitz, G., Pawlikowska, T., Watts, L., Wessely, S., Wright, D., and Wallace, E. P. (1993). "Development of a fatigue scale." *Journal of Psychosomatic Research*, 37(2), 147-153.

[35] Chang, S. W., and Wang, M. J. J. (2007). "Digital human modeling and workplace evaluation: Using an automobile assembly task as an example." *Human Factors and*

Ergonomics in Manufacturing & Service Industries, 17(5), 445-455.

[36] Cheung, Z., Height, R., Jackson, K., Patel, J., and Wagner, F. (2008). *Ergonomic Guidelines for Manual Material Handling.* DHHS Publication 2007-131, National Institute for Occupational Safety and Health.

[37] Cooper, R., Kuh, D., and Hardy, R. (2010). "Objectively measured physical capability levels and mortality: systematic review and meta-analysis." BMJ, 341, c4467.

[38] Corazza, S., Mündermann, L., Chaudhari, A. M., Demattio, T., Cobelli, C., and Andriacchi, T. P. (2006). "A markerless motion capture system to study musculoskeletal biomechanics: Visual hull and simulated annealing approach." *Annals of Biomedical Engineering*, 34(6), 1019-1029.

[39] Corlett, E. N., and Bishop, R. P. (1976). "A technique for assessing postural discomfort." *Ergonomics*, 19(2), 175-182.

[40] Corlett, E. N., Madeley, S., and Manenica, I. (1979). "Posture targeting: a technique for recording working postures." *Ergonomics*, 22(3), 357-366.

[41] Czaja, S. J., and Sharit, J. (2003). "Practically relevant research: Capturing real world tasks, environments, and outcomes." *The Gerontologist*, 43(1), 9-18.

[42] David, G. C. (2005). "Ergonomic methods for assessing exposure to risk factors for work-related musculoskeletal disorders." Occupational medicine, 55(3), 190-199.

[43] De Looze, M. P., Van Greuningen, K., Rebel, J., Kingma, I., and Kuijer, P. P. F. M. (2000). "Force direction and physical load in dynamic pushing and pulling." *Ergonomics*, 43(3), 377-390.

[44] DeLeva, P. (1996). "Adjustments to Zatsiorsky-Seluyanov's segment inertia parameters." *Journal of Biomechanics*, 29 (9), 1223-1230.

[45] Delp, S. L., Anderson, F. C., Arnold, A. S., Loan, P., Habib, A., John, C. T., and Thelen, D. G. (2007). "OpenSim: open-source software to create and analyze dynamic simulations of movement. Biomedical Engineering." *Biomedical Engineering*, 54(11), 1940-1950.

[46] De Luca, C. J. (1983). "Myoelectrical manifestations of localized muscular fatigue in humans." *Critical Reviews in Biomedical Engineering*, 11(4), 251-279.

[47] Demirel, H. O. and Duffy, V. G. (2007). "Applications of digital human modeling in industry." *Digital Human Modeling*, 4561, 824-832.

[48] DeVita, P., Hong, D., and Hamill, J. (1991). "Effects of asymmetric load carrying on the

biomechanics of walking." *Journal of Biomechanics*, 24(12), 1119-1129.

[49] Dong, Y., and Xu, S. (2007). "A new directional weighted median filter for removal of random-valued impulse noise." *Signal Processing Letters, IEEE*, 14(3), 193-196.

[50] Drury, C. G., Deeb, J. M., Hartman, B., Woolley, S., Drury, C. E., and Gallagher, S. (1989). "Symmetric and asymmetric manual materials handling Part 1: physiology and psychophysics." *Ergonomics*, 32(5), 467-489.

[51] Durand, M. J., Vézina, N., Baril, R., Loisel, P., Richard, M. C., and Ngomo, S. (2011). "Relationship between the margin of manoeuvre and the return to work after a long-term absence due to a musculoskeletal disorder: an exploratory study." *Disability and Rehabilitation*, 33(13-14), 1245-1252.

[52] Durand, M. J., Vézina, N., Baril, R., Loisel, P., Richard, M. C., and Ngomo, S. (2009). "Margin of manoeuvre indicators in the workplace during the rehabilitation process: a qualitative analysis." *Journal of Occupational Rehabilitation*, 19(2), 194-202.

[53] Elgammal, A., Harwood, D., and Davis, L. (2000). "Non-parametric model for background subtraction." In Computer Vision—ECCV 2000 (pp. 751-767). *Springer Berlin Heidelberg*.

[54] Enoka, R. M., and Duchateau, J. (2008). "Muscle fatigue: what, why and how it influences muscle function." *Journal of Physiology*, 586(1), 11-23.

[55] Esser, P., Dawes, H., Collett, J., and Howells, K. (2009). "IMU: inertial sensing of vertical CoM movement." *Journal of Biomechanics*, 42(10), 1578-1581.

[56] Everett, J. G. (1999). "Overexertion injuries in construction." *Journal of Construction Engineering and Management*, 125(2), 109-114.

[57] Everett, J. G., and Slocum, A. H. (1994). "Automation and robotics opportunities: construction versus manufacturing." *Journal of Construction Engineering and Management*, 120(2), 443-452.

[58] Faber, G. S., Kingma, I., Kuijer, P. P. F. M., Van der Molen, H. F., Hoozemans, M. J. M., Frings-Dresen, M. H. W., and Van Dieen, J. H. (2009). "Working height, block mass and one-vs. two-handed block handling: the contribution to low back and shoulder loading during masonry work." *Ergonomics*, 52(9), 1104-1118.

[59] Fishman, G. (2013). *Discrete-Event Simulation: Modeling, Programming, and Analysis.* Springer Science & Business Media, New York.

[60] Flegal, K. M., Carroll, M. D., Kit, B. K., and Ogden, C. L. (2012). "Prevalence of obesity

and trends in the distribution of body mass index among US adults, 1999-2010." *Journal of the American Medical Association*, 307(5), 491-497.

[61] Frings-Dresen, M. H., Windhorst, J., Hoozemans, M. J., van der Beek, A. J., and van der Molen, H. F. (2000). "Push and pull forces in the building and Construction Industry." *Human Factors and Ergonomics Society Annual Meeting*, Santa Monica, California.

[62] Fulco, C. S., Rock, P. B., Muza, S. R., Lammi, E., Cymerman, A., Butterfield, G., ... and Lewis, S. F. (1999). "Slower fatigue and faster recovery of the adductor pollicis muscle in women matched for strength with men." *Acta Physiologica Scandinavica*, 167(3), 233-240.

[63] Garg, A. R. U. N., and Moore, J. S. (1992). "Prevention strategies and the low back in industry." *Occupational Medicine*, 7(4), 629.

[64] Gerard, M. J., Armstrong, T. J., Martin, B. J., & Rempel, D. A. (2002). "The effects of work pace on within-participant and between-participant keying force, electromyography, and fatigue." *Human Factors: The Journal of the Human Factors and Ergonomics Society*, 44(1), 51-61.

[65] Golabchi, A., Han, S., Seo, J., Han, S., Lee, S., and Al-Hussein, M. (2015). "An automated biomechanical simulation approach to ergonomic job analysis for workplace design." *Journal of Construction Engineering and Management*, 141(8), 04015020.

[66] Goldsheyder, D., Weiner, S. S., Nordin, M., and Hiebert, R. (2004). "Musculoskeletal symptom survey among cement and concrete workers." *Work: A Journal of Prevention, Assessment and Rehabilitation*, 23(2), 111-121.

[67] Golparvar-Fard, M., Heydarian, A., and Niebles, J. C. (2013). "Vision-based action recognition of earthmoving equipment using spatio-temporal features and support vector machine classifiers." *Advanced Engineering Informatics*, 27(4), 652-663.

[68] Gong, J., Caldas, C. H., and Gordon, C. (2011). "Learning and classifying actions of construction workers and equipment using Bag-of-Video-Feature-Words and Bayesian network models" *Advanced Engineering Informatics*, 25(4), 771-782.

[69] Grandjean, E. (1989). *Fitting the Task To The Human: A Textbook Of Occupational Ergonomics (5th Edition).* CRC Press, New York.

[70] Hagberg, M. (1981). "Muscular endurance and surface electromyogram in isometric and dynamic exercise." *Journal of Applied Physiology*, 51(1), 1–7.

[71] Halpin, D. W. (1992). *Planning and Analysis of Construction Operations*. John Wiley &

Sons, New Jersey.

[72] Han, S., and Lee, S. (2013). "A vision-based motion capture and recognition framework for behavior-based safety management." *Automation in Construction*, 35, 131-141.

[73] Han, S., Achar, M., Lee, S., and Peña-Mora, F. (2013a). "Empirical assessment of a RGB-D sensor on motion capture and action recognition for construction worker monitoring." *Visualization in Engineering*, 1(1), 1-13.

[74] Han, S., Lee, S., and Armstrong, T. (2013b). "Automated 3D skeleton extraction from multiple videos for biomechanical analysis on Sites." *Proceedings of the 8th International Conference on Prevention of Work-related Musculoskeletal Disorders (PREMUS)*, Busan, Korea.

[75] Han, S., Lee, S., and Peña-Mora, F. (2012). "Vision-based motion detection for safety behavior analysis in construction." *Proceeding of the 2012 Construction Research Congress (CRC)*, West Lafayette, Illinois.

[76] Hanna, A. S. (2001). *Quantifying the impact of change orders on electrical and mechanical labor productivity.* Research Rep. No. 158-11, Construction Industry Institute, Austin, Tex.

[77] Hartley, R., and Zisserman, A. (2003). *Multiple View Geometry in Computer Vision*. Cambridge University Press. Cambridge, United Kingdom.

[78] Haslegrave, C. M. (1994). "What do we mean by a 'working posture'?" *Ergonomics*, 37(4), 781-799.

[79] Helbostad, J. L., Leirfall, S., Moe-Nilssen, R., & Sletvold, O. (2007). "Physical fatigue affects gait characteristics in older persons." *The Journals of Gerontology Series A: Biological Sciences and Medical Sciences*, 62(9), 1010-1015.

[80] Hignett, S., and McAtamney, L. (2000). "Rapid entire body assessment (REBA)." *Applied Ergonomics*, 31(2), 201-205.

[81] Hoozemans, M.J.M. Van der Beek, A.J. Frings-Dresen, M.H.W., and Van der Molen, H.F. (2001). "Evaluation of methods to assess push/pull forces in a construction task." *Applied Ergonomics*. 32(5), 509-516.

[82] Hsiao, H., and Stanevich, R. L. (1996). "Biomechanical evaluation of scaffolding tasks." *International Journal of Industrial Ergonomics*, 18(5), 407-415.

[83] Hsu, C. W., and Lin, C. J. (2002). "A comparison of methods for multiclass support vector machines." *Neural Networks, IEEE Transactions on*, 13(2), 415-425.

[84] Hwang, S., Kim, Y., and Kim, Y. (2009). "Lower extremity joint kinetics and lumbar curvature during squat and stoop lifting." *BMC Musculoskeletal Disorders*, 10(1).

[85] Jacobs, D. A., and Ferris, D. P. (2015). "Estimation of ground reaction forces and ankle moment with multiple, low-cost sensors." *Journal of Neuroengineering and Rehabilitation*, 12(1).

[86] Jäger, M., and Luttmann, A. (1999). "Critical survey on the biomechanical criterion in the NIOSH method for the design and evaluation of manual lifting tasks." *International Journal of Industrial Ergonomics*, 23(4), 331–337.

[87] Janowitz, I. L., Gillen, M., Ryan, G., Rempel, D., Trupin, L., Swig, L., ... and Blanc, P. D. (2006). "Measuring the physical demands of work in hospital settings: Design and implementation of an ergonomics assessment." *Applied Ergonomics*, 37(5), 641-658.

[88] Janowitz, I. L., Gillen, M., Ryan, G., Rempel, D., Trupin, L., Swig, L., ... and Blanc, P. D. (2006). "Measuring the physical demands of work in hospital settings: Design and implementation of an ergonomics assessment." *Applied Ergonomics*, 37(5), 641-658.

[89] Jin, S., Cho, J., Pham, X. D., Lee, K. M., Park, S. K., Kim, M., and Jeon, J. W. (2010). "FPGA design and implementation of a real-time stereo vision system." *Circuits and Systems for Video Technology, IEEE Transactions on*, 20(1), 15-26.

[90] Karhu, O., Härkönen, R., Sorvali, P., and Vepsäläinen, P. (1981). "Observing working postures in industry: Examples of OWAS application." *Applied Ergonomics*, 12(1), 13-17.

[91] Karhu, O., Kansi, P., and Kuorinka, I. (1977). "Correcting working postures in industry: a practical method for analysis." *Applied Ergonomics*, 8(4), 199-201.

[92] Karwowski, W. (2001). *International Encyclopedia of Ergonomics and Human Factors*, Taylor & Francis, London.

[93] Karwowski, W., and Marras, W. S. (1998). *The Occupational Ergonomics Handbook*. CRC Press, New York.

[94] Kazmierczak, K., Neumann, W. P., and Winkel, J. (2007). "A case study of serial-flow car disassembly: Ergonomics, productivity and potential system performance." *Human Factors and Ergonomics in Manufacturing & Service Industries*, 17(4), 331-351.

[95] Kee, D., and Karwowski, W. (2007). "A comparison of three observational techniques for assessing postural loads in industry." *International Journal of Occupational Safety and Ergonomics*, 13(1), 3-14.

[96] Keller, J. (2002). "Human performance modeling for discrete-event simulation: workload." *In Simulation Conference, 2002. Proceedings of the Winter*, IEEE, 1, 157-162.

[97] Khoshnevis, B. (2004). "Automated construction by contour crafting—related robotics and information technologies." *Automation in Construction*, 13(1), 5-19.

[98] Kilbom, Å. (1994). "Repetitive work of the upper extremity: part II—the scientific basis (knowledge base) for the guide." *International Journal of Industrial Ergonomics*, 14(1), 59-86.

[99] Kilbom, Å., and Persson, J. (1987). "Work technique and its consequences for musculoskeletal disorders." *Ergonomics*, 30(2), 273-279.

[100] Kim, M. Y., Ayaz, S. M., Park, J., and Roh, Y. (2014). "Adaptive 3D sensing system based on variable magnification using stereo vision and structured light." O*ptics and Lasers in Engineering*, 55, 113-127.

[101] Kim, S., Nussbaum, M. A., and Jia, B. (2011). "Low back injury risks during construction with prefabricated (panelised) walls: effects of task and design factors." *Ergonomics*, 54(1), 60-71.

[102] Kivi, P., and Mattila, M. (1991). "Analysis and improvement of work postures in the building industry: application of the computerised OWAS method." *Applied ergonomics*, 22(1), 43-48.

[103] Kopardekar, P., and Mital, A. (1994). "The effect of different work-rest schedules on fatigue and performance of a simulated directory assistance operator's task." *Ergonomics*, 37(10), 1697-1707.

[104] Kreßel, U. (1999) "Pairwise classification and support vector machines," *in Advances in Kernel Methods—Support Vector Learning*, B. Schölkopf, C. J. C. Burges, and A. J. Smola, Eds. MIT Press, Cambridge, MA, 255-268.

[105] Kumar, S. (2001). "Theories of musculoskeletal injury causation." *Ergonomics*, 44(1), 17-47.

[106] Kuorinka, I. (1988). "Restitution of EMG spectrum after muscular fatigue." *European Journal of Applied Physiology and Occupational Physiology*, 57(3), 311-315.

[107] Laurig, W., Kühn, F. M., and Schoo, K. C. (1985). "An approach to assessing motor workload in assembly tasks by the use of predetermined-motion-time systems." *Applied Ergonomics*, 16(2), 119-125.

[108] Lavender, S. A., Andersson, G. B., Schipplein, O. D., and Fuentes, H. J. (2003). "The effects of initial lifting height, load magnitude, and lifting speed on the peak dynamic L5/S1 moments." *International Journal of Industrial Ergonomics*, 31(1), 51-59.

[109] Lee, M. W., and Cohen, I. (2006). "A model-based approach for estimating human 3D poses in static images." *Pattern Analysis and Machine Intelligence*, 28(6), 905-916.

[110] Lee, Y.H., Cheng, C.K., and Tsuang, Y.H. (1994). "Biomechanical analysis in ladder climbing: the effect of slant angle and climbing speed." *Proceedings of the National Science Council*, 18(4), 170–178.

[111] Li, G., and Buckle, P. (1999). "Current techniques for assessing physical exposure to work-related musculoskeletal risks, with emphasis on posture-based methods." *Ergonomics*, 42(5), 674-695.

[112] Li, K. W., and Lee, C. L. (1999). "Postural analysis of four jobs on two building construction sites: an experience of using the OWAS method in Taiwan." *Journal of Occupational Health*, 41(3), 183-190.

[113] Lin, D., Nussbaum, M. A., Seol, H., Singh, N. B., Madigan, M. L., and Wojcik, L. A. (2009). "Acute effects of localized muscle fatigue on postural control and patterns of recovery during upright stance: influence of fatigue location and age." *European Journal of Applied Physiology*, 106(3), 425-434.

[114] Lind, A. R. (1959). "Muscle fatigue and recovery from fatigue induced by sustained contractions." *Journal of Physiology*, 147(1), 162-171.

[115] Liu, C., Yuen, J., and Torralba, A. (2011), "SIFT flow: Dense correspondence across scenes and its applications." *IEEE Transactions on Pattern Analysis and Machine Intelligence*, 33(5), 978-994.

[116] Liu, J. Z., Brown, R. W., and Yue, G. H. (2002). "A dynamical model of muscle activation, fatigue, and recovery." *Biophysical Journal*, 82(5), 2344-2359.

[117] Liu, M., Han, S., and Lee, S. (2016). "Tracking-based 3D human skeleton extraction from stereo video camera toward an on-site safety and ergonomic analysis." *Construction Innovation, Emerald* (Accepted).

[118] Loosemore, M., Dainty, A., and Lingard, H. (2003). *Human Resource Management in Construction Projects: Strategic and Operational Approaches*. Spon Press, London, United Kingdom

[119] Lowe, B. D. (2004). "Accuracy and validity of observational estimates of wrist and forearm posture." *Ergonomics*, 47(5), 527-554.

[120] Ma, L., Chablat, D., Bennis, F., and Zhang, W. (2009). "A new simple dynamic muscle fatigue model and its validation." *International Journal of Industrial Ergonomics*, 39(1), 211-220.

[121] Manenica, I. (1986). "A technique for postural load assessment." *The Ergonomics of Working Postures*, Taylor & Francis, London, 270–277.

[122] Maragos, P. (2005). "Lattice image processing: a unification of morphological and fuzzy algebraic systems." *Journal of Mathematical Imaging and Vision*, 22(2-3), 333-353.

[123] Marras, W.S., and Radwin, R.G. (2005). "Biomechanical modeling." *Reviews of Human Factors and Ergonomics*, 1(1), 1-88.

[124] Martinez, J. C. (1996). "STROBOSCOPE state and resource based simulation of construction processes," PhD dissertation, Civil and Environmental Engineering. Dept., University of Michigan, Ann Arbor, MI

[125] Martinez, J. C. (2009). "Methodology for conducting discrete-event simulation studies in construction engineering and management." *Journal of Construction Engineering and Management*, 136(1), 3-16.

[126] Martinez, J. C., and Ioannou, P. G. (1999). "General-purpose systems for effective construction simulation." *Journal of Construction Engineering and Management*, 125(4), 265-276.

[127] Mattila, M., Karwowski, W., and Vilkki, M. (1993). "Analysis of working postures in hammering tasks on building construction sites using the computerized OWAS method." *Applied Ergonomics*, 24(6), 405-412.

[128] McAtamney, L., and Corlett, E. N. (1993). "RULA: a survey method for the investigation of work-related upper limb disorders." *Applied Ergonomics*, 24(2), 91-99.

[129] McGill, S. M. (1997). "The biomechanics of low back injury: implications on current practice in industry and the clinic." *Journal of Biomechanics*, 30(5), 465–475.

[130] McGill, S. M., and Norman, R. W. (1985). "Dynamically and statically determined low back moments during lifting." *Journal of Biomechanics*, 18(12), 877–885.

[131] McIntyre, D.R. (1983). "Gait patterns during free choice ladder ascents." *Human Movement Science*, 2(3), 187-195.

[132] Mills, K. R. (1982). "Power spectral analysis of electromyogram and compound muscle action potential during muscle fatigue and recovery." *Journal of Physiology*, 326(1), 401-409.

[133] Mitropoulos, P., and Memarian, B. (2012). "Task demands in masonry work: sources, performance implications, and management strategies." *Journal of Construction Engineering and Management*, 139(5), 581-590.

[134] Mitropoulos, P., Cupido, G., and Namboodiri, M. (2009). "Cognitive approach to construction safety: Task demand-capability model." J*ournal of Construction Engineering and Management*, 135(9), 881-889.

[135] Neumann, W. P., and Kazmierczak, K. (2005). "Integrating flow and human simulation to predict workload in production systems." *Proceedings of 37th Annual Conference of the Nordic Ergonomics Society*, Oslo, Norway.

[136] Neumann, W. P., and Medbo, P. (2009). "Integrating human factors into discrete event simulations of parallel flow strategies." *Production Planning and Control*, 20(1), 3-16.

[137] Nussbaum, M. A., Shewchuk, J. P., Kim, S., Seol, H., and Guo, C. (2009). "Development of a decision support system for residential construction using panellised walls: Approach and preliminary results." *Ergonomics*, 52(1), 87-103.

[138] Ogale, A. S., Karapurkar, A., and Aloimonos, Y. (2007). "View-invariant modeling and recognition of human actions using grammars." in: Revised Papers of the Workshops on Dynamical Vision (WDV'05 and WDV'06), Lecture Notes in Computer Science, Beijing, China, May 2007, 115-126.

[139] Ogale, A., Karapurkar, A., Guerra-Filho, G. and Aloimonos, Y. (2004). "View-invariant identification of pose sequences for action recognition." *In Video Analysis and Content Extraction Workshop (VACE).*

[140] Olendorf, M. R., and Drury, C. G. (2001). "Postural discomfort and perceived exertion in standardized box-holding postures." *Ergonomics*, 44(15), 1341-1367.

[141] Pan, C. S., and Chiou, S. S. (1999). "Analysis of biomechanical stresses during drywall lifting." *International Journal of Industrial Ergonomics*, 23(5), 505-511.

[142] Paquet, V. L., Punnett, L., and Buchholz, B. (2001). "Validity of fixed-interval observations for postural assessment in construction work." *Applied Ergonomics*, 32(3), 215-224.

[143] Perez, J., de Looze, M. P., Bosch, T., and Neumann, W. P. (2014). "Discrete event simulation

as an ergonomic tool to predict workload exposures during systems design." *International Journal of Industrial Ergonomics*, 44(2), 298-306.

[144] Perry, J., and Bekey, G. A. (1980). "EMG-force relationships in skeletal muscle." *Critical Reviews in Biomedical Engineering*, 7(1), 1-22.

[145] Piccardi, M. (2004). "Background subtraction techniques: a review." *In Systems, Man and Cybernetics, 2004 IEEE international conference on*, IEEE, 4, 3099-3104.

[146] Plagemann, C., Ganapathi, V., Koller, D., and Thrun, S. (2010). "Real-time identification and localization of body parts from depth images." *Proceedings of the 2010 IEEE International Conference on Robotics and Automation (ICRA)*, Anchorage, AK, 3108-3113.

[147] Poppe, R. (2010). "A survey on vision-based human action recognition." *Image and Vision Computing*, 28(6), 976-990.

[148] Priel, V. Z. (1974). "A numerical definition of posture." *Journal of the Human Factors and Ergonomics Society*, 16(6), 576-584.

[149] Radwin, R. G., Marras, W. S., and Lavender, S. A. (2001). "Biomechanical aspects of work-related musculoskeletal disorders." *Theoretical Issues in Ergonomics Science*, 2(2), 153-217.

[150] Rafibakhsh, N., Gong, J., Siddiqui, M. K., Gordon, C., and Lee, H. F. (2012). "Analysis of xbox kinect sensor data for use on construction sites: depth accuracy and sensor interference assessment." *In Constitution research congress*, 848-857.

[151] Ray, S. J., and Teizer, J. (2012). "Real-time construction worker posture analysis for ergonomics training," *Advanced Engineering Informatics*, 26(2), 439-455.

[152] Reed, M. P., Faraway, J., Chaffin, D. B., and Martin, B. J. (2006). "The HUMOSIM Ergonomics Framework: A new approach to digital human simulation for ergonomic analysis (No. 2006-01-2365)." SAE Technical Paper.

[153] Rogez, G., Guerrero, J. J., Martínez, J., and Orrite-Urunuela, C. (2006). "Viewpoint independent human motion analysis in man-made environments." *Proceedings of British Machine Vision Conference*, 659-668.

[154] Rohmert, W., Wangenheim, M., Mainzer, J., Zipp, P., and Lesser, W. (1986). "A study stressing the need for a static postural force model for work analysis." *Ergonomics*, 29(10), 1235-1249.

[155] Rojas, E. M., and Aramvareekul, P. (2003). "Is construction labor productivity really

declining?" *Journal of Construction Engineering and Management*, 129(1), 41-46.

[156] Rose, L., Ericson, M. O., Glimskär, B., Nordgren, B., and Örtengren, R. (1992). "Ergo-index. Development of a model to determine pause needs after fatigue and pain reactions during work." *Computer Applications in Ergonomics, Occupational Safety and Health*, 461-468.

[157] Rose, L., Ericson, M., and Ortengren, R. (2000). "Endurance time, pain and resumption in passive loading of the elbow joint." *Ergonomics*, 43(3), 405–420.

[158] RS Means (2015). *Building Construction Cost Data, 2015*. RS Means Company, Kingston, Massachusetts.

[159] Sahlin, K., Tonkonogi, M., and Söderlund, K. (1998). "Energy supply and muscle fatigue in humans." *Acta Physiologica Scandinavica*, 162(3), 261-266.

[160] Salvendy, G. (2012). *Handbook of Human Factors and Ergonomics*. John Wiley & Sons, New Jersey.

[161] Sato, H., Ohashi, J., Iwanaga, K., Yoshitake, R., and Shimada, K. (1984). "Endurance time and fatigue in static contractions." *Journal of Human Ergology*, 13(2), 147–154.

[162] Savitzky, A., and Golay, M. J. (1964). "Smoothing and differentiation of data by simplified least squares procedures." *Analytical Chemistry*, 36(8), 1627-1639.

[163] Seiler, S., and Hetlelid, K. J. (2005). "The impact of rest duration on work intensity and RPE during interval training." *Medicine and Science in Sports and Exercise*, 37(9), 1601-1607.

[164] Seo, J., Han, S., Armstrong, T. J., and Lee, S. (2013). "Force Prediction during Ladder Climbing for Biomechanical Analysis" *Proceedings of the 8th International Conference on Prevention of Work-related Musculoskeletal Disorders*, Busan, Korea.

[165] Seo, J., Han, S., Lee, S. and Kim, H. (2015a). "Computer vision techniques for construction safety and health monitoring." *Advanced Engineering Informatics*, 29(2), 239-251.

[166] Seo, J., Lee, S., and Seo, J. (2016) "Simulation-based Assessment of Workers' Muscle Fatigue and Its Impact on Construction Operations" *Journal of Construction Engineering and Management*, ASCE (Accepted).

[167] Seo, J., Moon, M., and Lee, S. (2015b). "Construction operation simulation reflecting workers' muscle fatigue." *Proc., 2015 International Workshop on Computing in Civil Engineering*, ASCE, Reston, Virginia.

[168] Seo, J., Starbuck, R., Han, S., Lee, S., and Armstrong, T. (2014). "Motion-Data–driven Biomechanical Analysis during Construction Tasks on Sites" *Journal of Computing in Civil*

Engineering, ASCE, 29(4).

[169] Serpell, A., Venturi, A., and Contreras, J. (1995). "Characterization of waste in building construction projects." *3rd Annual Conference International Group for Lean Construction*, 67-78.

[170] Shaikh, I., Jayaram, U., Jayaram, S., and Palmer, C. (2004). "Participatory ergonomics using VR integrated with analysis tools." *Proceedings of the 2004 Winter Simulation Conference, IEEE*, 2, 1746-1754.

[171] Shan, C., Tan, T., and Wei, Y. (2007). "Real-time hand tracking using a mean shift embedded particle filter." *Pattern Recognition*, 40(7), 1958-1970.

[172] Shin, H. J., and Kim, J. Y. (2007). "Measurement of trunk muscle fatigue during dynamic lifting and lowering as recovery time changes." *International Journal of Industrial Ergonomics*, 37(6), 545-551.

[173] Shotton, J., Sharp, T., Kipman, A., Fitzgibbon, A., Finocchio, M., Blake, A., and Moore, R. (2013). "Real-time human pose recognition in parts from single depth images." *Communications of the ACM*, 56(1), 116–124.

[174] Siddiqui, M., and Medioni, G. (2010). "Human pose estimation from a single view point, real-time range sensor." *Proceedings of the 2010 IEEE Computer Society Conference on Computer Vision and Pattern Recognition Workshops (CVPRW)*, San Francisco, California.

[175] Sommerich, C. M., McGlothlin, J. D., and Marras, W. S. (1993). "Occupational risk factors associated with soft tissue disorders of the shoulder: a review of recent investigations in the literature." *Ergonomics*, 36(6), 697-717.

[176] Spielholz, P., Silverstein, B., Morgan, M., Checkoway, H., and Kaufman, J. (2001). "Comparison of self-report, video observation and direct measurement methods for upper extremity musculoskeletal disorder physical risk factors." *Ergonomics*, 44(6), 588-613.

[177] Stanton, N. A. (2006). "Hierarchical task analysis: Developments, applications, and extensions." *Applied Ergonomics*, 37(1), 55-79.

[178] Starbuck, R., Seo, J., Han, S., and Lee, S. (2014). "A stereo vision-based approach to marker-less motion capture for on-site kinematic modeling of construction worker tasks." *Proceedings of the 15th International Conference on Computing in Civil and Building Engineering (ICCCBE)*, Reston, Virginia.

[179] Symeonidis, I., Kavadarli, G., Schuller, E., and Peldschus, S. (2010). "Simulation of

biomechanical experiments in OpenSim." *Proceedings of the 12th Mediterranean Conference on Medical and Biological Engineering and Computing (MEDICON*), Chalkidiki, Greece.

[180] Tran, D., and Sorokin, A. (2008). "Human activity recognition with metric learning." *In Computer Vision–ECCV*, Springer Berlin Heidelberg, 548-561.

[181] U.S. Census Bureau (2012). *Construction: Summary Series: General Summary: Detailed Statistics by Subsectors and Industries for U.S., Regions, and States: 2012*. < http://factfinder.census.gov/faces/tableservices/jsf/pages/productview.xhtml?pid=ECN_2012_US_23SG01&prodType=table>

[182] Uijlings, J.R.R., Smeulders, A.W.M. and Scha, R.J.H. (2010). "Real-time visual concept classification." *IEEE Transactions on Multimedia*, 12(7), 665-681.

[183] Vailaya, A., Zhang, H., Yang, C., Liu, F. I., and Jain, A. K. (2002). "Automatic image orientation detection." *Image Processing, IEEE Transactions on*, 11(7), 746-755.

[184] van Dieën, J. H., Hoozemans, M. J., and Toussaint, H. M. (1999). "Stoop or squat: a review of biomechanical studies on lifting technique." *Clinical Biomechanics*, 14(10), 685–696.

[185] Village, J., Frazer, M., Cohen, M., Leyland, A., Park, I., and Yassi, A. (2005). "Electromyography as a measure of peak and cumulative workload in intermediate care and its relationship to musculoskeletal injury: an exploratory ergonomic study." *Applied Ergonomics*, 36(5), 609-618.

[186] Vøllestad, N. K. (1997). "Measurement of human muscle fatigue." *Journal of Neuroscience Methods*, 74(2), 219-227.

[187] Waters, T. R., Putz-Anderson, V., Garg, A., and Fine, L. J. (1993). "Revised NIOSH equation for the design and evaluation of manual lifting tasks." *Ergonomics*, 36(7), 749-776.

[188] Weinland, D., Ronfard, R., and Boyer, E. (2011). "A survey of vision-based methods for action representation, segmentation and recognition." *Computer Vision and Image Understanding*, 115(2), 224-241.

[189] Weir, P. L., Andrews, D. M., van Wyk, P. M., and Callaghan, J. P. (2011). "The influence of training on decision times and errors associated with classifying trunk postures using video-based posture assessment methods." *Ergonomics*, 54(2), 197-205.

[190] Woodfill, J. I., Gordon, G., and Buck, R. (2004). "Tyzx deepsea high speed stereo vision system." *In Computer Vision and Pattern Recognition Workshop*, IEEE.

[191] Xia, T., and Frey Law, L. A. F. (2008). "A theoretical approach for modeling peripheral muscle fatigue and recovery." *Journal of Biomechanics*, 41(14), 3046-3052.

[192] Xiang, J., Peng, B. I., Pisaniello, D., and Hansen, A. (2014). "Health impacts of workplace heat exposure: an epidemiological review." *Industrial Health*, 52(2), 91-101.

[193] Yates, J. W., Kamon, E., Rodgers, S. H., and Company, P. C. (1980). "Static lifting strength and maximal isometric voluntary contractions of back, arm and shoulder muscles." *Ergonomics*, 23(1), 37-47.

[194] Zankoul, E., Khoury, H., and Awwad, R. (2015). "Evaluation of agent-based and discrete-event simulation for modeling construction earthmoving operations." *The 32nd International Symposium on Automation and Robotics in Construction and Mining (ISARC 2015).*

[195] Zatsiorski, V. M. (2002). *Kinematics of human motion*. Human Kinetics, Champaign, Illinois.

[196] Zatsiorsky, V. M., Seluyanov, V. N., and Chugunova, L. G. (1990). "Methods of determining mass-inertial characteristics of human body segments." *In G.G. Chernyi & S.A. Regirer, Contemporary Problems of Biomechanics*, CRC Press.

[197] Zhang, Z. (2000). "A flexible new technique for camera calibration." *Pattern Analysis and Machine Intelligence, IEEE Transactions on*, 22(11), 1330-1334

[198] Zhang, Z. (2012). "Microsoft kinect sensor and its effect." *MultiMedia, IEEE*, 19(2), 4-10.